A Model for Nonlinear Diffusion in Polymers

Thesis by

David A. Edwards

in Partial Fulfillment of the Requirements

for the Degree of Doctor of Philosophy

California Institute of Technology

Pasadena, California

1994

(submitted March 29, 1994)

Acknowledgments

No man is an island; I certainly could not have completed this dissertation without a great deal of help from people in many different areas. Educationally, I am indebted to those people who decide it is as important to pass along knowledge as it is to gain it. From them I learned much more than course material; I learned a moral lesson. This dissertation is certainly the culmination of a long journey, and I thank those who took the time to help me along it: Loretta Hansen, who first placed my feet on this path; my high school teachers, who guided my dawdling steps; and my college professors, who taught me how to stride. Of course, the final steps of this journey were by far the most treacherous and the most important; without the guidance of my advisor, Prof. Donald S. Cohen, there would be no dissertation.

Beyond the academic guidance I have received from my advisor, there are several other important contributors I wish to acknowledge. I have learned an immense amount about chemical engineering in general and polymer physics in particular from Prof. Christopher Durning of Columbia University. Tom Witelski, another graduate student in Prof. Cohen's group here at Caltech, has also provided valuable input and insight throughout the creative process.

Of course, there would also be no dissertation without financial support, and I am very grateful to the following organizations who contributed to support my graduate study: the United States Army Research Office (Durham, contract DAAL03-89-K-0014), the National Science Foundation (grant DMS-9024963 and an NSF Graduate Fellowship), the Air Force Office of Scientific Research (grant AFOSR-

91-0045), and the John and Fannie Hertz Foundation.

Though it may have seemed like it at times, this journey did not take place in a vacuum. For every hour I spent at work there was another hour I spent elsewhere. The sum total of my life has always been much greater than the quest for this dissertation; I have always striven to enrich and be enriched by the lives around me. If I tried to write down the names of all the people who touched my life, the acknowledgments would be longer than the dissertation and I still would have forgotten someone. Suffice to say that I am deeply grateful to everyone who supported me, critiqued me, laughed with me, or troubled me. Those who do not kill me make me stronger.

A few people, though, deserve special mention. My family has always been there to lend a word of encouragement when I thought I would never make it through this process. My officemate Beth Wedeman and my *amiga* Darna Gongora have endured four years of my almost constant complaining, and have done so with a sense of humor that lasts until this day. Most especially, I wish to acknowledge my fiancée, Jacqueline M. Holmes. Without her daily support and encouragement, I most assuredly would either have abandoned this pursuit long before it was completed or cracked under the strain of this monumental task. I am honored to know her, and I am honored that she has chosen to continue this task of love and support for the rest of her life.

Lastly, this dissertation is lovingly dedicated to my father, Leonard C. Edwards, who over the course of the last year has shown me the true meaning of courage. I sincerely hope that I have many more opportunities to learn from him.

Abstract

In certain polymer-penetrant sytems, the effects of Fickian diffusion are augmented by nonlinear viscoelastic behavior. Consequently, such systems often exhibit concentration fronts unlike those seen in classical Fickian systems. These fronts not only are sharper than in standard systems, but also they propagate at speeds other than that typical of Fickian diffusion. A model is presented which replicates such behavior. This model is reduced to a moving boundary-value problem where the boundary separates the polymer into two distinct states: glassy and rubbery, in each of which different physical processes dominate. An unusual condition at the moving interface, which arises from the inclusion of a viscoelastic memory term, is not solvable by similarity solutions, but can be solved by integral equation techniques. Perturbation methods are used to obtain asymptotic solutions for differing strengths of molecular diffusion and viscoelastic stress. These solutions are characterized by sharp fronts which move with constant speed; the asymptotic solutions mimic those found experimentally in polymer-penetrant systems.

Table of Contents

Nomenclature

Variables and Parameters

Units are listed in terms of length (L), mass (M), moles (N), or time (T). If the same letter appears both with and without tildes, the letter with a tilde has dimensions, while the letter without a tilde is nondimensionalized. The equation number where a particular quantity first appears is listed, if applicable.

$\tilde{a}$: coefficient in flux-front speed relationship (2.8), units N/L^3.

A: constant, variously defined.

B: the Bromwich contour for inverting a Laplace transform.

c: stationary point for Laplace's method (8.20).

$\tilde{C}(\cdot, \tilde{t})$: concentration of penetrant or diluent at position $\cdot$ and time $\tilde{t}$, units N/L^3.

$D(\tilde{C})$: binary diffusion coefficient for system, units L^2/T.

$E(\tilde{C})$: coefficient preceding the stress term in the modified diffusion equation, units NT/M (2.2b).

$f(\cdot)$: arbitrary function, variously defined.

$F(\cdot)$: arbitrary integral, variously defined.

$\mathcal{F}_n[\tilde{C}]$: nonlinear differential operator on $\tilde{C}$ (1.1).

$\mathcal{G}_n[\cdot]$: hereditary kernel (1.1).

$H(\cdot)$: Heaviside step function, defined as 0 for negative argument and 1 for pos-

itive argument (2.2a).

$I_j(\cdot)$: the jth modified Bessel function (7.19).

$\tilde{\mathbf{J}}(\cdot, \tilde{t})$: flux at position $\cdot$ and time $\tilde{t}$, units N/L^2T.

$\mathcal{J}[\tilde{C}]$: jump operator (3.9b).

m: exponent for width of boundary layer (8.5a).

n: indexing variable (1.1) or variable exponent in expansions (5.1).

p: variable in Laplace transform space (4.21).

r: dimensionless parameter in dissolution problem (8.1).

$\tilde{\mathbf{s}}(\tilde{t})$: position of phase transition front, units L (2.6).

$\bar{s}(\tilde{x})$: the inverse function of $\tilde{s}(\tilde{t})$, written as $\tilde{t} = \bar{s}(\tilde{x})$ (3.7b).

$\tilde{t}$: time from imposition of external concentration, units T (1.1).

$\tilde{t}_0$: time from which the polymer has a memory, units T (2.2a).

T: imbedding of C from one region to the fully semi-infinite region (4.11a).

$\tilde{\mathcal{U}}$: internal energy density of the system, units N^2/LT.

$\tilde{\mathbf{x}}$: three-dimensional distance coordinate, units L.

y: dummy integration variable.

z: dummy integration variable.

$\mathcal{Z}$: the integers.

α: nondimensional parameter.

$\beta(\tilde{C})$: inverse of the relaxation time, units T^{-1} (2.2b).

γ: nondimensional parameter (4.7a).

δ_{1n}: the Kronecker delta function.

$\delta(\cdot)$: the Dirac delta function.

ϵ: perturbation expansion parameter, value β_g/β_r (4.1a).

ζ: dimensionless boundary layer variable, value $[x - s(t)]/\epsilon^m$ (8.5a).

η: coefficient of concentration in stress evolution kernel (3.12), units ML^2/NT^3.

κ: nondimensional parameter (7.5a).

$\tilde{\mu}$: chemical potential, units N/LT.

ν: coefficient of $\tilde{C}_{\tilde{t}}$ in stress evolution kernel (3.12), units ML^2/NT^2.

$\tilde{\sigma}(\cdot, \tilde{t})$: stress in polymer at position $\cdot$ and time $\tilde{t}$, units M/LT^2 (2.3b).

τ: dimensionless boundary layer variable, value t (8.5a).

Ω: region occupied by the polymer (1.1).

Other Notation

b: as a sub- or superscript, used to indicate a quantity at the boundary of the polymer (2.1b).

c: as a subscript, used to indicate the characteristic value of a quantity (3.23); as a superscript, used to indicate concentration (7.9).

d: as a sub- or superscript, used to indicate a quantity related to the Neumann fictitious problem (7.23).

F: as a subscript, used to indicate a quantity arising from Fick's law.

g: as a sub- or superscript, used to indicate the glassy state (3.5b).

i: as a sub- or superscript, used to indicate a quantity at $\tilde{t} = 0$ (2.1b).

$j \in \mathcal{Z}$: as a sub- or superscript, used to indicate a term in an expansion.

k: as a subscript, used to indicate a quantity solvable from explicitly known quantities.

r: as a sub- or superscript, used to indicate the rubbery state (3.5b).

R: as a subscript, used to indicate a quantity arising from relaxation effects.

u: as a sub- or superscript, used to indicate a quantity related to the Dirichlet fictitious problem (7.9).

σ: as a superscript, used to indicate stress (7.9).

$*$: as a subscript, used to indicate at the transition value between the glassy and rubbery states (2.7).

∞: as subscript, used to indicate a term in an expansion in t or x.

$+$: as a superscript on a dependent variable, used to indicate a boundary-layer expansion in the glassy region (8.5b).

$-$: as a superscript on a dependent variable, used to indicate a boundary-layer expansion in the rubbery region (8.13).

$\dot{}$: used to indicate differentiation with respect to t (3.26) or τ.

$\hat{}$: used to indicate a quantity in Laplace transform space (4.21).

$'$: on an independent variable, indicates a dummy integration variable (1.1); on a dependent variable, used to indicate differentiation other than with respect to t or τ (3.8).

$[\cdot]_{\tilde{\mathbf{s}}}$: jump across the front $\tilde{\mathbf{s}}$, defined as $\cdot^g(\tilde{\mathbf{s}}^+(\tilde{t}),\tilde{t}) - \cdot^r(\tilde{\mathbf{s}}^-(\tilde{t}),\tilde{t})$ (2.6).

Part One:

Preliminaries

Chapter I: Introduction

In recent years, engineers and scientists have found a panoply of uses for polymers and other synthetic materials. These new materials promise to revolutionize entire industries and create new ones. The sudden explosion in the development of these materials has thrust materials science to the forefront of mathematical applications, especially since there is so little mathematical modeling of the dynamics of synthetic materials. Mathematicians are handicapped by the uncertainties among chemical engineers and materials scientists as to the exact physical mechanisms involved. However, all agree that the unusual behavior exhibited by these new materials indicates that the standard Fickian flux $\tilde{\mathbf{J}} = -D(\tilde{C})\nabla\tilde{C}$, where $\tilde{C}$ is the concentration and $D(\tilde{C})$ is the second-order diffusion tensor, is not general enough to model the desired behavior accurately. It is also a growing consensus that some sort of viscoelastic effect plays a major role in diffusion in many of these materials, sharing dominance with molecular diffusion.

The promise that these new types of materials hold is astounding. New types of adhesives will adhere more while weighing less [1], [2]. "Smart" polymer gels and synthetic polymers will forever change how doctors administer medicine, as they abandon standard global delivery methods in favor of internal or external on-site administrations [3]-[6]. Microlithographic patterning using polymer substrates has emerged as a major technology [7]. Polymer films have great value in protective clothing, equipment, or sealants [8].

Polymer-penetrant systems are particularly interesting since much of the ob-

served behavior is inconsistent with a purely Fickian diffusion model. In particular, unless pathological conditions are met, moving Fickian fronts always proceed with speed proportional to $\tilde{t}^{-1/2}$. However, in so-called case II diffusion in polymers, concentration fronts propagate with constant speed [3], [9]. These fronts are usually sharp, and often the concentration flux into the phase change boundary is *less* than the concentration flux out! All of these characteristics are inconsistent with those of the Fickian diffusion model. Though the concentration fronts are sharp, there is no discontinuity in $\tilde{C}$ as has been observed in other, more standard chemical systems [10].

The type of polymers which we wish to study can occupy one of two phases: *glassy* or *rubbery*. In the glassy state, the polymer has a finite *relaxation time* associated with the length of the polymer in relation to the entanglement network. This nonlocal effect implies that in any effective model there will be a hereditary integral term associated with the "memory" of the polymer with respect to its concentration history. In the rubbery state, the polymer swells, making the relaxation time almost instantaneous. Hence, the "memory" of the polymer in the rubbery state is very faint. In addition, in some cases, there is a great increase in the diffusion coefficient as the polymer changes from the glassy to rubbery state.

In order to incorporate this more complicated behavior into the model, Cohen and Edwards have proposed [11] the following much more general model for the flux:

$$\tilde{\mathbf{J}} = -\sum_{n=1}^{\infty} D_n(\tilde{C})\nabla \int_{\Omega}\int_{-\infty}^{\tilde{t}} \mathcal{F}_n[\tilde{C}(\tilde{\mathbf{x}}',\tilde{t}')]\mathcal{G}_n[\tilde{\mathbf{x}}-\tilde{\mathbf{x}}',\tilde{t}-\tilde{t}',\tilde{C}(\tilde{\mathbf{x}}',\tilde{t}')]\,d\tilde{t}'\,d\tilde{\mathbf{x}}', \quad (1.1)$$

where the D_n are second-order tensors, the $\mathcal{F}_n$ are general differential operators on

$\tilde{C}$ which model the dependency of $\tilde{\mathbf{J}}$ on different dynamical processes, and the $\mathcal{G}_n$ are general nonlinear hereditary kernels. Each term in the expansion represents a flux contribution from a different source, such as molecular diffusion or viscoelastic effects. This form for the flux is general enough to model accurately many more types of anomalous diffusive behavior than simply those associated with polymer-penetrant systems. Furthermore, note that if we let $\mathcal{F}_n = \delta_{1n}\tilde{C}(\tilde{\mathbf{x}}', \tilde{t}')$ and $\mathcal{G}_n = \delta_{1n}\delta(\tilde{\mathbf{x}} - \tilde{\mathbf{x}}', \tilde{t} - \tilde{t}')$ we obtain the Fickian diffusion flux.

Cohen and his colleagues have used various simplified forms of (1.1) to examine many types of polymer-penetrant systems where viscoelastic diffusion plays a role [11]-[18]. Further discussion of their contributions will appear in Chapter II. The main purpose of this thesis is to formulate and discuss several classes of non-Fickian problems involving moving boundaries. In the next section we will specialize $\mathcal{F}_n$ and $\mathcal{G}_n$ to the particular set of viscoelastic effects we wish to consider and consider the extra complication of dynamics at a moving boundary.

Chapter II: Governing Equations

1. Transport and Stress Equations

Consider a domain Ω which is divided into two connected disjoint subdomains Ω_1 and Ω_2. Ω_1 is the region in which the polymer is in the glassy state, while Ω_2 is the region in which the polymer is in the rubbery state. We specify the value of the concentration in the interior of Ω at time $\tilde{t} = 0$ and on the boundary $\partial\Omega$ for all time. We could just have easily specified the flux on the boundary, though in the systems we wish to study the concentration is usually specified. In addition, the standard diffusion equation $\tilde{C}_{\tilde{t}} = -\nabla \cdot \tilde{\mathbf{J}}$ holds for the concentration in both domains, though the flux $\tilde{\mathbf{J}}$ may be different in each region. Specifically, we are considering the following system of equations:

$$\tilde{C}_{\tilde{t}} = -\nabla \cdot \tilde{\mathbf{J}}_1, \quad \tilde{\mathbf{x}} \in \Omega_1; \qquad \tilde{C}_{\tilde{t}} = -\nabla \cdot \tilde{\mathbf{J}}_2, \quad \tilde{\mathbf{x}} \in \Omega_2; \tag{2.1a}$$

$$\tilde{C}(\tilde{\mathbf{x}}, \tilde{t}) = C_b(\tilde{t}), \quad \tilde{\mathbf{x}} \in \partial\Omega; \qquad \tilde{C}(\tilde{\mathbf{x}}, 0) = \tilde{C}_i(\tilde{\mathbf{x}}), \quad \tilde{\mathbf{x}} \in \Omega. \tag{2.1b}$$

Experimentalists note several important properties in the polymer-penetrant systems which we are trying to study. First, there is a finite relaxation time [19] when the polymer is in the glassy state. This indicates the presence of a viscoelastic memory term in our flux. The polymer is affected by past values of the concentration

and its time derivative [9], [20], [21], so we make the following definitions in (1.1):

$$\mathcal{F}_1 = \tilde{C}, \quad \mathcal{F}_2 = H(\tilde{t}' - \tilde{t}_0) f(\tilde{C}, \tilde{C}_{\tilde{t}}), \quad \mathcal{F}_n = 0, \quad n > 2; \qquad \mathcal{G}_1 = \delta(\tilde{\mathbf{x}} - \tilde{\mathbf{x}}', \tilde{t} - t'), \tag{2.2a}$$

$$\mathcal{G}_2 = \exp\left[- \int_{\tilde{t}'}^{\tilde{t}} \beta(\tilde{C}(\tilde{\mathbf{x}}, z))\, dz \right]; \qquad D_1(\tilde{C}) = D(\tilde{C}), \quad D_2(\tilde{C}) = E(\tilde{C}). \tag{2.2b}$$

Here $H(\tilde{t}' - \tilde{t}_0)$ is the Heaviside step function, f is some general scalar function, $\beta(\tilde{C})$ is the inverse of the relaxation time for the polymer, and $E(\tilde{C})$ is a tensor. Specific forms for f, β, and E will be chosen later. Hence we may write the flux (1.1) as

$$\tilde{\mathbf{J}} = -D(\tilde{C}) \nabla \tilde{C} - E(\tilde{C}) \nabla \tilde{\sigma}, \text{ where} \tag{2.3a}$$

$$\tilde{\sigma} = \int_{\tilde{t}_0}^{\tilde{t}} \left[f\left(\tilde{C}(\tilde{\mathbf{x}}, \tilde{t}'), \tilde{C}_{\tilde{t}}(\tilde{\mathbf{x}}, \tilde{t}') \right) \right] \exp\left[- \int_{\tilde{t}'}^{\tilde{t}} \beta(\tilde{C}(\tilde{\mathbf{x}}, z))\, dz \right] d\tilde{t}'. \tag{2.3b}$$

The constant $\tilde{t}_0$ in (2.3b) determines whether the memory is state-dependent. If the memory of the material is dependent on other properties of the system (temperature, density, pressure, etc.), we set $\tilde{t}_0$ to a finite value (in this thesis chosen to be 0) corresponding to the time at which the system is first in the *memory state.* If the polymer always has a memory, which we denote as the *state-independent* case, then we take the limit $\tilde{t}_0 \to -\infty$.

An alternative derivation of equations (2.3) is given in Cohen *et al.* [18]. We outline the derivation here since it is instructive to note that equations (2.3) may also be derived directly from thermodynamic first principles from an augmented chemical potential. We would like to use equations (2.3) even when significant deformation and shear of the polymer occur. Therefore, if $\tilde{\mathcal{U}}$ is, in some sense,

the internal energy density of the system, then a chemical potential $\tilde{\mu}_F$ for Fickian diffusion is given by

$$\tilde{\mu}_F = \frac{\delta \tilde{\mathcal{U}}}{\delta \tilde{C}}.$$

The flux is related to the gradient of the potential $\tilde{\mu}_F$ in the following way:

$$\begin{aligned} \tilde{\mathbf{J}} &= -E(\tilde{C})\nabla\tilde{\mu}_F \\ &= -D(\tilde{C})\nabla\tilde{C}, \end{aligned} \tag{2.4}$$

where $E(\tilde{C})$ is some arbitrary tensor, and $D(\tilde{C}) = E(\tilde{C})\tilde{\mu}'_F(\tilde{C})$. Note that since $E(\tilde{C})$ need not be isotropic, $D(\tilde{C})$ need not be isotropic.

Now we postulate that relaxation is also an important part of the system and contributes to the dynamics in a fundamental way. Then we may augment the potential by a term

$$\tilde{\mu}_R = \int_{\tilde{t}_0}^{\tilde{t}} \left[f\left(\tilde{C}(\tilde{\mathbf{x}}, \tilde{t}'), \tilde{C}_{\tilde{t}}(\tilde{\mathbf{x}}, \tilde{t}')\right)\right] \exp\left[-\int_{\tilde{t}'}^{\tilde{t}} \beta(\tilde{C}(\tilde{\mathbf{x}}, z))\, dz \right] d\tilde{t}'.$$

Letting $\tilde{\mu} = \tilde{\mu}_F + \tilde{\mu}_R$ and following the same analysis as in (2.4), we obtain equations (2.3). We note that if $D(\tilde{C})$ and $E(\tilde{C})$ are anistropic, their anisotropies must be of the same form since they differ only by a scalar quantity. The above argument can be generalized to any number of other contributions to the chemical potential, and hence (1.1) is obtained.

Using equations (2.3) in (2.1a) and making $\tilde{\sigma}$ another dependent variable, we have the following system of partial differential equations:

$$\tilde{C}_{\tilde{t}} = \nabla \cdot \left(D(\tilde{C})\nabla\tilde{C} + E(\tilde{C})\nabla\tilde{\sigma} \right), \tag{2.5a}$$

$$\tilde{\sigma}_{\tilde{t}} + \beta(\tilde{C})\tilde{\sigma} = f(\tilde{C}, \tilde{C}_{\tilde{t}}). \tag{2.5b}$$

Equations (2.5) have been studied in great detail by Cohen and his colleagues.

Cohen and White [12], [13] examine simplified forms of (2.5). In particular, their relaxation time is chosen to be a smoothly varying function of $\tilde{C}$, thus eliminating the phase transition model. In addition, they eliminate the dependence of f on $\tilde{C}_{\tilde{t}}$. They perform steady-state analyses on a finite domain and trace the position and stability of a moving front.

Cox [14] and Cox and Cohen [15] performed asymptotic analyses of simplified forms of (2.5), as well as numerical simulations of equations (2.5) where some of the variable parameters were held fixed. The problem was solved on a finite domain and did not involve a phase transition or a moving boundary-value problem. Fickian profiles were obtained for long time. In addition, convective terms were added to (2.5a) and phase plane analysis was used to find traveling wave solutions.

Hayes [16] and Hayes and Cohen [17] added a bimolecular reaction term to (2.5a). They made some of the variable parameters in (2.5) constant and allowed others to vary in such a way that a strict phase transition problem was avoided. They translated their equations to a moving frame and solved for traveling wave solutions. In addition, they solved equations (2.5) numerically and using perturbation methods on a finite-domain problem. In some of these solutions they found shocks in the solution profiles.

Cohen *et al.* [18] extend the work of Cohen and White to multiple dimensions. A multivalued solution which satisfies an ordinary differential equation formulation is presented; in addition, a rule is stated which allows one to determine the position of a shock in the multivalued solution.

In contrast to the work cited above, we will allow discontinuities in $\beta(\tilde{C})$, $D(\tilde{C})$, $E(\tilde{C})$, and f across the front, indicating distinct values in the glassy and rubbery regions. This is more in keeping with our phase transition model.

In equations (2.5), $\tilde{\sigma}$ is simply a mathematical artifice introduced to simplify what would be a highly nonlinear partial differential equation into two coupled partial differential equations. However, note that equation (2.5b) is in the form of an evolution equation for viscoelastic stress. In addition, the additional "forces" on the system that are caused by a term of the form of $\tilde{\sigma}$ can be thought of as analogous to those caused by the trace of an actual mechanical stress tensor. Therefore, for purposes of analogy and heuristic physical interpretation *only*, we will refer to $\tilde{\sigma}$ as a "stress" throughout this thesis.

In order to solve (2.5b), an initial condition is needed for $\tilde{\sigma}$, which we give as the following:

$$\tilde{\sigma}(\tilde{\mathbf{x}}, 0) = \tilde{\sigma}_i(\tilde{\mathbf{x}}). \tag{2.6}$$

In order to allow equation (2.6) to be totally general, we will need to make slight modifications to (2.3b) on occasion. Such modifications will be discussed in greater detail when they are made.

2. Front Conditions

In our problem will be using piecewise continuous functions to model our material coefficients. Hence, our problem will involve matching the solutions in the two regions where the polymer is in the glassy and rubbery states. (Note that the discontinuity is in the *dependent* variable.) Thus, it is necessary to impose conditions

at the moving boundary $\tilde{\mathbf{s}}(\tilde{t})$ between the two regions. In a moving boundary-value problem, several conditions need to be imposed at the moving front $\tilde{\mathbf{x}} = \tilde{\mathbf{s}}(\tilde{t})$. One of these conditions involves a relationship between the flux $\tilde{\mathbf{J}}$ at the front and the speed at which the front travels. There are two main candidates for such a condition, the first of which is used extensively in diffusion theory [22]:

$$\tilde{\mathbf{J}}_2(\tilde{\mathbf{s}}(\tilde{t}),\tilde{t})\cdot\mathbf{n} - \tilde{\mathbf{J}}_1(\tilde{\mathbf{s}}(\tilde{t}),\tilde{t})\cdot\mathbf{n} \equiv -\left[\tilde{\mathbf{J}}\cdot\mathbf{n}\right]_{\tilde{\mathbf{s}}} = [\tilde{C}]_{\tilde{\mathbf{s}}}\frac{d\tilde{\mathbf{s}}}{d\tilde{t}}\cdot\mathbf{n}, \quad \tilde{\mathbf{x}}\in\tilde{\mathbf{s}}(\tilde{t}). \tag{2.7}$$

However, in polymer-penetrant systems, one does not see a *jump* in concentration, but rather a *sharp rise* in concentration over a width of several nanometers [20], [21]. Hence, we see that in our model there should be no jump in concentration at the front. In addition, in a standard diffusion problem (2.7) is a mass balance which does not include the possibility that some of the flux might be used up in the phase transition. This is the case we wish to consider, so for both reasons listed we reject (2.7).

Our above assumption of continuity of concentration at a specified transition value $\tilde{C}_*$ can be written as

$$\tilde{C} = \tilde{C}_*, \quad \tilde{C}_{\tilde{t}} > 0, \qquad \tilde{\mathbf{x}} = \tilde{\mathbf{s}}(\tilde{t}). \tag{2.8}$$

We include the derivative in (2.8) since we now mathematically define the glassy region as the region where $\tilde{C} \leq \tilde{C}_*$ and the rubbery region as the region where $\tilde{C} > \tilde{C}_*$. Note also that the relatively large width of the front, when compared with molecular length scales, also assures us that the continuum model we use is still valid.

At the moving boundary $\tilde{\mathbf{s}}(\tilde{t})$ between the two regions a phase change takes place. Therefore, the more reasonable candidate for a flux condition is one used

extensively in phase transition problems. While the same physical processes do not occur here, it is instructive to recall the boundary condition used in the classical Stefan problem [10], where a change of phase takes place between ice and water. In that problem, the following condition holds:

$$\left[\tilde{\mathbf{J}} \cdot \mathbf{n}\right]_{\tilde{\mathbf{s}}} = -\tilde{a}\frac{d\tilde{\mathbf{s}}}{d\tilde{t}} \cdot \mathbf{n}, \quad \tilde{\mathbf{x}} \in \tilde{\mathbf{s}}(\tilde{t}), \tag{2.9}$$

where $\tilde{a}$ is a constant.

Here $\tilde{a}$ is the *phase change parameter.* Equation (2.9) states that the difference between the flux into and out of the front is used up in the phase transition. In a standard problem, the constant $\tilde{a}$ is related to the latent heat of melting of the substance. Here we are assuming that there is a fundamental change that takes place in the polymer as we go from the glassy to the rubbery state; this change can be described as a "phase transition" in the polymer. Experimentally, this has been shown to be related to a stretching of the polymer entanglement network. The flux used up by the polymer in this stretching is directly analogous to the energy used up in melting in a standard two-phase heat conduction problem. However, the direct physical interpretation of $\tilde{a}$ is rather tricky and will be discussed in greater detail later.

Now using equation (2.3a) in our flux condition (2.9), we have the following:

$$\left[D(\tilde{C}_*)\nabla\tilde{C} + E(\tilde{C}_*)\nabla\tilde{\sigma}\right]_{\tilde{\mathbf{s}}} \cdot \mathbf{n} = \tilde{a}\frac{d\tilde{\mathbf{s}}}{d\tilde{t}} \cdot \mathbf{n}. \tag{2.10}$$

This is the condition at the moving boundary which replaces the standard Stefan flux condition; it is clearly more complicated than the standard Stefan condition, and the interesting details of these complications will be explored in the next section.

Lastly, we need a condition for the stress at the front. We follow the work of Knauss and Kenner [23], where the derivative of stress with respect to a state variable has a jump in slope at the phase transition, but the actual stress is continuous:

$$\tilde{\sigma}\left(\tilde{\mathbf{s}}^{-}(\tilde{t}),\tilde{t}\right)=\tilde{\sigma}\left(\tilde{\mathbf{s}}^{+}(\tilde{t}),\tilde{t}\right). \tag{2.11}$$

This choice is consistent with our reasoning that though our relevant dependent variables may change quickly near the front, they are still continuous.

Now we have all the equations necessary to facilitate a further consideration of our problem.

Chapter III: Simplifications

1. The Reduced Flux Condition

For analytical tractability, we first consider a one-dimensional problem on a semi-infinite domain. By choosing a semi-infinite interval, we have eliminated complications that occur due to the swelling of the polymer entanglement network in the rubbery region. We now denote the glassy region (the region ahead of the front) with a superscript g and the rubbery region (the region behind the front) with a superscript r. In this case, equations (2.5), (2.10), (2.1b), (2.6), (2.8), and (2.11) become

$$\tilde{C}_{\tilde{t}} = \left(D(\tilde{C})\tilde{C}_{\tilde{x}} + E(\tilde{C})\tilde{\sigma}_{\tilde{x}} \right)_{\tilde{x}}, \quad \tilde{x} > 0; \tag{3.1a}$$

$$\tilde{\sigma}_{\tilde{t}} + \beta(\tilde{C})\tilde{\sigma} = f\left(\tilde{C}, \tilde{C}_{\tilde{t}}\right), \quad \tilde{t} > 0; \tag{3.1b}$$

$$\left[D(\tilde{C}_*)\tilde{C}_{\tilde{x}} + E(\tilde{C}_*)\tilde{\sigma}_{\tilde{x}} \right]_{\tilde{s}} = \tilde{a}\frac{d\tilde{s}}{d\tilde{t}}; \tag{3.2}$$

$$\tilde{C}(\tilde{x}, 0) = \tilde{C}_i(\tilde{x}), \quad \tilde{C}_i(\tilde{x}) < \tilde{C}_* \text{ for all } \tilde{x} > 0; \tag{3.3a}$$

$$\tilde{C}(0, \tilde{t}) = \tilde{C}_b(\tilde{t}), \quad \tilde{C}_b'(\tilde{t}) > 0, \quad \tilde{C}_b(\tilde{t}) > C_* \text{ for all } \tilde{t} > 0; \tag{3.3b}$$

$$\tilde{\sigma}(\tilde{x}, 0) = \tilde{\sigma}_i(\tilde{x}); \tag{3.4}$$

$$\tilde{C}(\tilde{s}(\tilde{t}), \tilde{t}) = \tilde{C}_*, \qquad \tilde{C}_{\tilde{t}}(\tilde{s}(\tilde{t}), \tilde{t}) > 0; \tag{3.5a}$$

$$\tilde{\sigma}^r\left(\tilde{s}(\tilde{t}), \tilde{t}\right) = \tilde{\sigma}^g\left(\tilde{s}(\tilde{t}), \tilde{t}\right). \tag{3.5b}$$

We take $E(\tilde{C})$ and $D(\tilde{C})$ to be scalar non-negative strictly increasing functions of $\tilde{C}$, reflecting the situation typically encountered in controlled-release pharmaceuticals [3]-[5]. Note that in one dimension $\tilde{\sigma}$ can be interpreted as being analogous to stress. The conditions in (3.3) guarantee that the polymer is initially in the glassy state, and that the boundary is always in the rubbery region. This phase discontinuity between boundary and polymer at time $\tilde{t} = 0$ implies that our phase transition front $\tilde{s}(\tilde{t})$ must initially be at the boundary:

$$\tilde{s}(0) = 0. \tag{3.6}$$

We begin by exmaining equation (3.2) to determine its meaning. First consider the case where the stress is negligible. This corresponds to the moving boundary condition in a standard Stefan problem. Since now the flux is proportional only to the concentration gradient, and a flux in larger than a flux out should force the front in a positive direction, it is clear that we should take $\tilde{a} > 0$. A sketch of a concentration profile corresponding to such a solution is shown in Figure 3a.

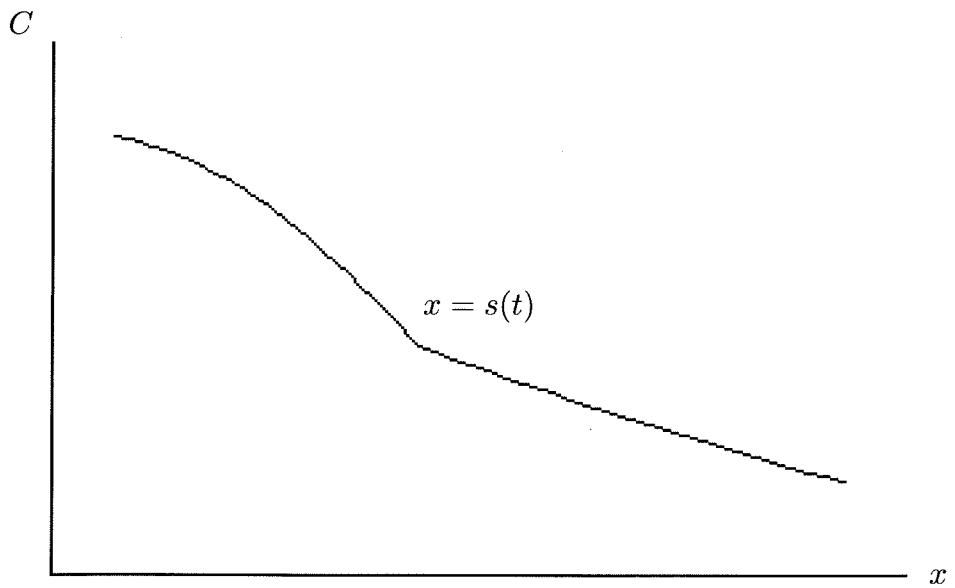

Figure 3a. Concentration profile for standard moving boundary-value problem.

However, it has been experimentally demonstrated that in Case II diffusion quite different front profiles appear. In fact, it commonly happens that $[\tilde{C}_{\tilde{x}}]_{\tilde{s}} < 0$. A sketch of such a profile is shown in Figure 3b.

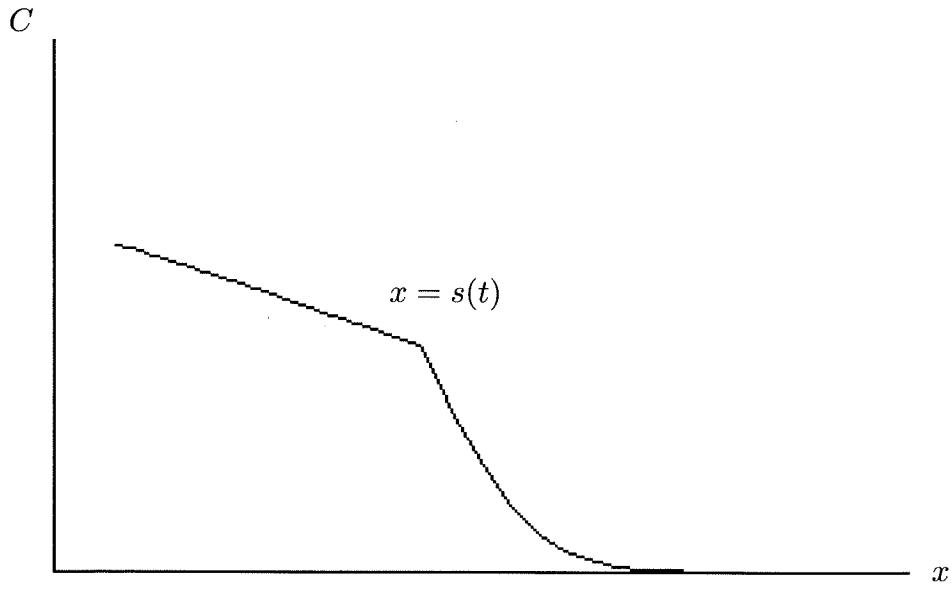

Figure 3b. Concentration profile for Case II diffusion.

In this case, the stress is non-negligible and has a maximum at the front, as shown in figure 3c.

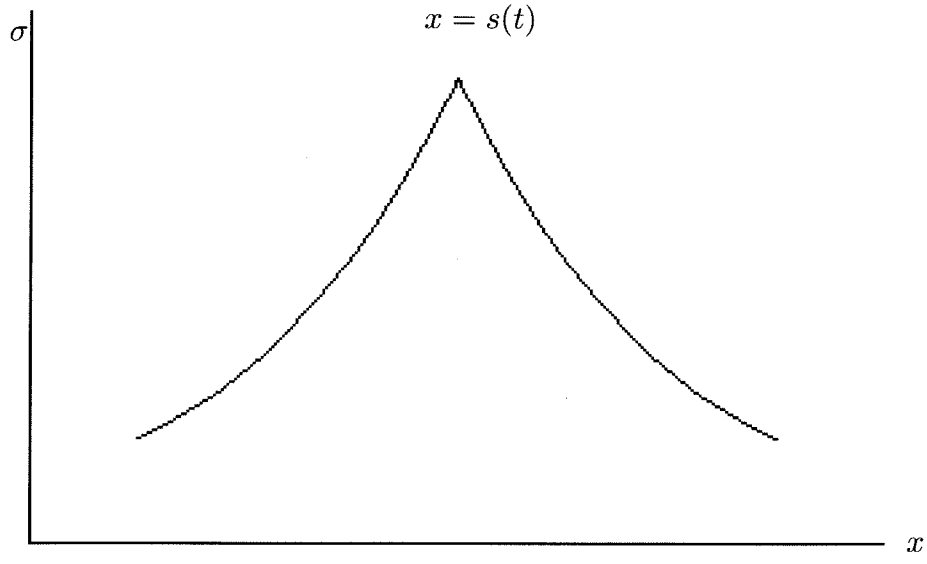

Figure 3c. Stress profile for Case II diffusion.

Hence, we see from equation (3.2) that in this case we must select $\tilde{a} < 0$. In fact, in Case II diffusion, a decrease in the concentration gradient will *slow* the front. This is also consistent with taking $\tilde{a} < 0$. Like the latent heat in a Stefan problem, $\tilde{a}$ must be known in order to solve the problem. The dilemma of selecting the correct parameter range for $\tilde{a}$ for each phenomenon will recur throughout this work. However, there are experiments which can be performed to determine $\tilde{a}$ just as there are experiments which can be performed to determine the latent heat of a substance. One such experiment is outlined in Chapter VIII.

At first, we wish to simplify equation (3.2) somewhat. In so doing, we will discover some interesting aspects of our moving boundary-value problem. Since we expect our front $\tilde{x} = \tilde{s}(\tilde{t})$ to be monotonically increasing in $\tilde{t}$, we may invert to write the front as $\tilde{t} = \bar{s}(\tilde{x})$. We then solve equation (3.1b) subject to (3.4) and (3.5b) to yield

$$\tilde{\sigma}^g(\tilde{x},\tilde{t}) = \tilde{\sigma}_i(\tilde{x}) + \int_0^{\tilde{t}} \left[f\left(\tilde{C}(\tilde{x},\tilde{t}'), \tilde{C}_{\tilde{t}}(\tilde{x},\tilde{t}')\right)\right] \exp\left[-\int_{\tilde{t}'}^{\tilde{t}} \beta(\tilde{C}(\tilde{x},z))\, dz \right] d\tilde{t}', \quad (3.7a)$$

$$\begin{aligned}\tilde{\sigma}^r(\tilde{x},\tilde{t}) = \tilde{\sigma}_i(\tilde{x}) &+ \int_0^{\bar{s}} \left[f(\tilde{C}(\tilde{x},\tilde{t}'), \tilde{C}_{\tilde{t}}(\tilde{x},\tilde{t}'))\right] \times \\ &\exp\left[-\int_{\tilde{t}'}^{\bar{s}} \beta(\tilde{C}(\tilde{x},z))\, dz - \int_{\bar{s}}^{\tilde{t}} \beta(C(\tilde{x},z))\, dz \right] d\tilde{t}' \\ &+ \int_{\bar{s}}^{\tilde{t}} \left[f(\tilde{C}(\tilde{x},\tilde{t}'), \tilde{C}_{\tilde{t}}(\tilde{x},\tilde{t}'))\right] \exp\left[-\int_{\tilde{t}'}^{\tilde{t}} \beta(\tilde{C}(\tilde{x},z))\, dz \right] d\tilde{t}'. \quad (3.7b)\end{aligned}$$

We have expanded the argument of the exponential in the first term of $\tilde{\sigma}^r$ since we expect the relaxation time to undergo a discontinuous jump at $\tilde{C} = \tilde{C}_*$ in agreement with experiments [20].

In general, if we have functions

$$f^g(\tilde{x},\tilde{t}) = \int_0^{\tilde{t}} f^{(1)}(\tilde{x},\tilde{t}';\tilde{t})\,d\tilde{t}',$$

$$f^r(\tilde{x},\tilde{t}) = \int_0^{\bar{s}(\tilde{x})} f^{(3)}(\tilde{x},\tilde{t}';\tilde{t})\,d\tilde{t}' + \int_{\bar{s}(\tilde{x})}^{\tilde{t}} f^{(2)}(\tilde{x},\tilde{t}';\tilde{t})\,d\tilde{t}',$$

then Liebniz's rule for differentiation states that

$$[f_{\tilde{x}}]_{\bar{s}} = \int_0^{\bar{s}} \left[f^{(1)} - f^{(3)}\right]_{\tilde{x}} (\tilde{x},\tilde{t}';\bar{s})\,d\tilde{t}' + \bar{s}'\left[f^{(2)}(\tilde{x},\bar{s};\bar{s}) - f^{(3)}(\tilde{x},\bar{s};\bar{s})\right]. \tag{3.8}$$

Here the prime indicates differentiation with respect to $\tilde{x}$. Note that since we have changed variables, $[f_{\tilde{x}}]_{\bar{s}} = f^g_{\tilde{x}}(\tilde{x},\bar{s}^-(\tilde{x})) - f^r_{\tilde{x}}(\tilde{x},\bar{s}^+(\tilde{x}))$.

Now using equations (3.7) in (3.8), we have the following:

$$\left[E(\tilde{C}_*)\tilde{\sigma}_{\tilde{x}}\right]_{\bar{s}} = \int_0^{\bar{s}} \left\{\mathcal{J}[\tilde{C}] + \bar{s}'[E(\tilde{C}_*)\beta(\tilde{C}_*)]_{\bar{s}}\right\} \exp\left[-\int_{\tilde{t}'}^{\bar{s}} \beta(\tilde{C}(\tilde{x},z))\,dz\right] d\tilde{t}'$$

$$- E(\tilde{C}_*^+)\bar{s}'\left[f(\tilde{C}_*,\tilde{C}_{\tilde{t}})\right]_{\bar{s}}, \text{ where} \tag{3.9a}$$

$$\mathcal{J}[\tilde{C}] = \left[E(\tilde{C}_*)\right]_{\bar{s}} \left[f_{\tilde{x}}\left(\tilde{C}(\tilde{x},\tilde{t}'),\tilde{C}_{\tilde{t}}(\tilde{x},\tilde{t}')\right) - \int_{\tilde{t}'}^{\bar{s}} \beta'\left(\tilde{C}(\tilde{x},z)\right)\tilde{C}_{\tilde{x}}(\tilde{x},z)\,dz\right]. \tag{3.9b}$$

Simplifying and transforming to our original variables where possible, we have

$$\left[E(\tilde{C}_*)\tilde{\sigma}_{\tilde{x}}\right]_{\bar{s}} = \int_0^{\bar{s}} \mathcal{J}[\tilde{C}] \exp\left[-\int_{\tilde{t}'}^{\bar{s}} \beta(\tilde{C}(\tilde{x},z))\,dz\right] d\tilde{t}'$$

$$+ \frac{[E(\tilde{C}_*)\beta(\tilde{C}_*)]_{\tilde{s}}\tilde{\sigma}(\tilde{s}(\tilde{t}),\tilde{t})}{\tilde{s}'(\tilde{t})} - \frac{E(\tilde{C}_*^+)\left[f(\tilde{C}_*,\tilde{C}_{\tilde{t}})\right]_{\tilde{s}}}{\tilde{s}'(\tilde{t})}, \tag{3.10}$$

which makes our flux condition (3.2)

$$\left[D(\tilde{C}_*)\tilde{C}_{\tilde{x}}\right]_{\tilde{s}} + \int_0^{\bar{s}} \mathcal{J}[\tilde{C}] \exp\left[-\int_{\tilde{t}'}^{\bar{s}} \beta(\tilde{C}(\tilde{x},z))\,dz\right] d\tilde{t}'$$

$$+ \frac{[E(\tilde{C}_*)\beta(\tilde{C}_*)]_{\tilde{s}}\tilde{\sigma}(\tilde{s}(\tilde{t}),\tilde{t})}{\tilde{s}'(\tilde{t})} - \frac{E(\tilde{C}_*^+)\left[f(\tilde{C}_*,\tilde{C}_{\tilde{t}})\right]_{\tilde{s}}}{\tilde{s}'(\tilde{t})} = \tilde{a}\tilde{s}'(\tilde{t}). \quad (3.11)$$

There are several interesting things to note in equation (3.11). First, it may seem that we have not simplified matters much, since $\tilde{\sigma}$ still appears in our flux condition. However, in practice it is much easier to determine $\tilde{\sigma}$ than $\tilde{\sigma}_{\tilde{x}}$. Note also that we have a negative contribution to the left-hand side, so we cannot be assured that $\tilde{a}$ is positive, as was always true in the latent heat formulation.

More interesting is the appearance of $\tilde{s}'$ in the denominator of some of our flux terms. This condition is highly unusual and leads to non-standard front motion, especially when one considers the fact that $\tilde{s}'$ may also appear in the expressions for the concentration and the flux. In general, the behavior is highly complicated. In the next section we will specialize our problem further, thereby making it possible to find analytical solutions.

2. A Tractable Problem

The first simplification we choose to make is to postulate the simplest form for f:

$$f(\tilde{C},\tilde{C}_{\tilde{t}}) = \eta\tilde{C} + \nu\tilde{C}_{\tilde{t}}, \quad (3.12)$$

where η and ν are positive constants. Though at first glance this may seem overly simplistic, it will become obvious later that this simple form does indeed produce

the desired behavior. We choose this form because it is simple to analyze and accurately captures the dominant physical processes in the system [12].

Then equations (3.1b) and (3.11) become

$$\tilde{\sigma}_{\tilde{t}} + \beta(\tilde{C})\tilde{\sigma} = \eta\tilde{C} + \nu\tilde{C}_{\tilde{t}}, \tag{3.13}$$

$$\left[D(\tilde{C}_*)\tilde{C}_{\tilde{x}}\right]_{\tilde{s}} + \int_0^{\bar{s}} \mathcal{J}[\tilde{C}] \exp\left[-\int_{\tilde{t}'}^{\bar{s}} \beta(\tilde{C}(\tilde{x},z))\,dz\right] d\tilde{t}'$$

$$+ \frac{[E(\tilde{C}_*)\beta(\tilde{C}_*)]_{\tilde{s}}\tilde{\sigma}(\tilde{s}(\tilde{t}),\tilde{t})}{\tilde{s}'(\tilde{t})} - \frac{E(\tilde{C}_*^+)\left[\eta\tilde{C}_* + \nu\tilde{C}_{\tilde{t}}\right]_{\tilde{s}}}{\tilde{s}'(\tilde{t})} = \tilde{a}\tilde{s}'(\tilde{t}). \tag{3.14}$$

Now using the first of equations (3.5a) and its *total* derivative with respect to t, we have

$$\left[\left(D(\tilde{C}_*) + \nu E(\tilde{C}_*^+)\right)\tilde{C}_{\tilde{x}}\right]_{\tilde{s}} + \int_0^{\bar{s}} \mathcal{J}[\tilde{C}] \exp\left[-\int_{\tilde{t}'}^{\bar{s}} \beta(\tilde{C}(\tilde{x},z))\,dz\right] d\tilde{t}'$$

$$+ \frac{[E(\tilde{C}_*)\beta(\tilde{C}_*)]_{\tilde{s}}\tilde{\sigma}(\tilde{s}(\tilde{t}),\tilde{t})}{\tilde{s}'(\tilde{t})} = \tilde{a}\tilde{s}'(\tilde{t}). \tag{3.15}$$

Hence we see that this particular form for f dictates a simple relationship between the viscoelastic flux contribution and the concentration flux contribution.

The term $\beta(\tilde{C})$ is worthy of special attention. It is the inverse of the *relaxation time*, which roughly corresponds to the amount of time one part of the polymer takes to respond to changes in concentration in neighboring parts. In the polymer-penetrant systems in which we are interested, $\beta(\tilde{C})$ changes greatly as the polymer goes from the *glassy* state to the *rubbery* state. Hence, its dependence on $\tilde{C}$ will be important and non-negligible. However, experiments have shown that variations in the relaxation time *within* phases seem to contribute little to the overall behavior.

Therefore, we average the relaxation time in each phase and use its overall value there. Thus we have

$$\beta(\tilde{C}) = \begin{cases} \beta_g, & 0 \le \tilde{C} \le \tilde{C}_*, \\ \beta_r, & \tilde{C} > \tilde{C}_*. \end{cases} \tag{3.16}$$

Under these assumptions, our flux condition (3.15) becomes

$$\left[\left(D(\tilde{C}_*) + \nu E(\tilde{C}_*^+)\right)\tilde{C}_{\tilde{x}}\right]_{\tilde{s}} + \int_0^{\bar{s}} \left[E(\tilde{C}_*)\right]_{\tilde{s}} \left[f_{\tilde{x}}\left(\tilde{C}(\tilde{x},\tilde{t}'), \tilde{C}_{\tilde{t}}(\tilde{x},\tilde{t}')\right)\right] e^{-\beta_g(\bar{s}-\tilde{t}')}\, d\tilde{t}'$$

$$+ \frac{[E(\tilde{C}_*)\beta(\tilde{C}_*)]_{\tilde{s}}\tilde{\sigma}(\tilde{s}(\tilde{t}),\tilde{t})}{\tilde{s}'(\tilde{t})} = \tilde{a}\tilde{s}'(\tilde{t}). \tag{3.17}$$

We note that changes in $E(\tilde{C})$ also do not contribute significantly to the behavior of the system. Hence, we approximate $E(\tilde{C})$ by its average value in the entire polymer, which we denote by E, a positive constant. Doing so, equations (3.1a) and (3.17) become the following:

$$\tilde{C}_{\tilde{t}} = \left(D(\tilde{C})\tilde{C}_{\tilde{x}}\right)_{\tilde{x}} + E\tilde{\sigma}_{\tilde{x}\tilde{x}}, \tag{3.18}$$

$$\left[\left(D(\tilde{C}_*) + \nu E\right)\tilde{C}_{\tilde{x}}\right]_{\tilde{s}} + \frac{E(\beta_g - \beta_r)\tilde{\sigma}(\tilde{s}(\tilde{t}),\tilde{t})}{\tilde{s}'(\tilde{t})} = \tilde{a}\tilde{s}'(\tilde{t}). \tag{3.19}$$

Note that since $\beta_r > \beta_g$, we have a negative contribution to the left-hand side of (3.19) from the stress, as postulated before. Note also that the classical technique of seeking similarity solutions will not in general solve an equation of the form of (3.19).

In order to make the problem analytically tractable, we make one more simplifying assumption. As stated before, the diffusion coefficient often, though not always, increases dramatically as the polymer goes from the glassy to rubbery state.

However, changes *within* phases are less important. Hence, we perform the same averaging as we did with the relaxation time to obtain the following form for $D(\tilde{C})$:

$$D(\tilde{C}) = \begin{cases} D_g, & 0 \le \tilde{C} \le \tilde{C}_*, \\ D_r, & \tilde{C} > \tilde{C}_*. \end{cases} \tag{3.20}$$

More discussion of various physically appropriate forms for $D(\tilde{C})$, $E(\tilde{C})$, and $f(\tilde{C}, \tilde{C}_{\tilde{t}})$ can be found in Cohen and White [12]. Since we have chosen this simplistic form, equation (3.18) may be written

$$\tilde{C}_{\tilde{t}} = D(\tilde{C})\tilde{C}_{\tilde{x}\tilde{x}} + E\tilde{\sigma}_{\tilde{x}\tilde{x}}. \tag{3.21}$$

We wish to model the penetration of solute into an initially "dry" semi-infinite polymer where the concentration at the boundary is our known function $\tilde{C}_b(\tilde{t})$, the maximum of which is $\tilde{C}_c$. Mathematically, we set

$$\tilde{C}_i(\tilde{x}) \equiv 0. \tag{3.22}$$

In addition, on physical grounds we expect that as the experiment progresses, the polymer will become totally saturated. The mathematical condition, which we will impose only when warranted, is

$$\tilde{C}(\tilde{x}, \infty) = \tilde{C}_c. \tag{3.23}$$

We introduce dimensionless variables as follows:

$$x = \frac{\tilde{x}}{\tilde{x}_c}, \quad t = \tilde{t}\beta_c, \quad s(t) = \frac{\tilde{s}(\tilde{t})}{\tilde{x}_c}, \quad C(x,t) = \frac{\tilde{C}(\tilde{x},\tilde{t})}{\tilde{C}_c}, \tag{3.24a}$$

$$\sigma(x,t) = \frac{\tilde{\sigma}(\tilde{x},\tilde{t})}{\nu\tilde{C}_c}, \quad C_b(t) = \frac{\tilde{C}_b(\tilde{t})}{\tilde{C}_c}, \quad C_* = \frac{\tilde{C}_*}{\tilde{C}_c}, \quad \sigma_i(x) = \frac{\tilde{\sigma}_i(\tilde{x})}{\nu\tilde{C}_c}, \tag{3.24b}$$

where $\tilde{x}_c$ and β_c are now arbitrary, but will be chosen later as dictated by a particular physical situation. Then equations (3.21), (3.13), (3.19), (3.3b), (3.22), (3.4)-(3.6), and (3.23) reduce to

$$C_t = \frac{D(C)}{\tilde{x}_c^2 \beta_c} C_{xx} + \frac{\nu E}{\tilde{x}_c^2 \beta_c} \sigma_{xx}, \tag{3.25a}$$

$$\sigma_t + \frac{\beta(C)}{\beta_c} \sigma = \frac{\eta}{\nu \beta_c} C + C_t, \tag{3.25b}$$

$$\left[\left(D(C_*) + \nu E \right) C_x \right]_s + \frac{\nu E (\beta_g - \beta_r)}{\beta_c} \frac{\sigma\left(s(t), t\right)}{\dot{s}} = a \tilde{x}_c^2 \beta_c \dot{s}, \tag{3.26}$$

$$C(0,t) = C_b(t), \qquad C(x,0) = 0, \qquad \sigma(x,0) = \sigma_i(x), \tag{3.27}$$

$$C(s(t),t) = C_*, \quad C_t(s(t)) > 0, \qquad \sigma^r\left(s(t),t\right) = \sigma^g(s(t),t), \tag{3.28}$$

$$s(0) = 0, \tag{3.29}$$

$$C(x,\infty) = 1, \tag{3.30}$$

where the dot now indicates differentiation with respect to t.

Since $\beta(C)$ and $D(C)$ are constant on either side of the threshold level $C = C_*$, we may differentiate (3.25a) with respect to t, and (3.25b) twice with respect to x to yield

$$C_{tt} = \frac{D(C)}{\tilde{x}_c^2 \beta_c} C_{xxt} + \frac{\nu E}{\tilde{x}_c^2 \beta_c} \sigma_{xxt}, \tag{3.31a}$$

$$\sigma_{xxt} + \frac{\beta(C)}{\beta_c} \sigma_{xx} = \frac{\eta}{\nu \beta_c} C_{xx} + C_{xxt}. \tag{3.31b}$$

Combining equations (3.31), we have

$$C_{tt} = \frac{D(C) + \nu E}{\tilde{x}_c^2 \beta_c} C_{xxt} - \frac{\beta(C)}{\beta_c} C_t + \frac{\beta(C) D(C) + \eta E}{\tilde{x}_c^2 \beta_c^2} C_{xx}, \tag{3.32}$$

$$\sigma_{tt} = \frac{D(C) + \nu E}{\tilde{x}_c^2 \beta_c} \sigma_{xxt} - \frac{\beta(C)}{\beta_c} \sigma_t + \frac{\beta(C) D(C) + \eta E}{\tilde{x}_c^2 \beta_c^2} \sigma_{xx}. \tag{3.33}$$

We now wish to solve these equations by using perturbation expansions in a small paramter ϵ to show that these equations lead to constant front speed, sharp fronts, and other behavior characteristic of non-Fickian polymer-penetrant systems.

Part Two: The

Weakly Diffusive Case

Chapter IV: Governing Equations for the Weakly Diffusive Case

Experimentally it has been shown that polymers have a near-instantaneous relaxation time in the rubbery state, while in the glassy state these substances are characterized by finite relaxation times. Hence, we assume that $\beta_g/\beta_r = \epsilon$, where $0 < \epsilon \ll 1$. One way that constant front speed can manifest itself is in the *weakly diffusive* case. In this case, we assume that the diffusion coefficient is always small and does not vary noticeably with concentration, *i.e.*, $D_g = D_r = D_0\epsilon$. Note that such a choice of parameters implies that the effects of the contribution to the flux will dominate the contribution from Fickian diffusion in (3.31a); thus, we would expect to see non-Fickian behavior from this choice of parameters.

We wish to incorporate effects of both the glassy and rubbery phases in our nondimensionalizations; hence we normalize $\tilde{x}$ by our diffusive length scale in the glassy region, and $\tilde{t}$ by the relaxation time in the rubbery region. Summarizing, we have

$$D_g = D_r = D_0\epsilon, \qquad \tilde{x}_c = \sqrt{\frac{D_0\epsilon}{\beta_g}}, \qquad \beta_c = \beta_r, \qquad \frac{\beta_g}{\beta_r} = \epsilon.$$

Making these substitutions in equations (3.32) and (3.25b), we see that for $C \leq C_*$ we have

$$C^g_{tt} = \frac{\epsilon D_0 + \nu E}{D_0} C^g_{xxt} - \epsilon C^g_t + \epsilon\left(\epsilon + \frac{\eta E}{D_0\beta_g}\right) C^g_{xx}, \tag{4.1a}$$

We now construct series for C and σ in ϵ by assuming that $C = C^0 + o(1)$ and $\sigma = \sigma^0 + o(1)$. Doing so, we see that to leading order, equations (4.1) and (4.2) become

$$C_{tt}^{0g} = \gamma C_{xxt}^{0g}, \tag{4.7a}$$

$$\sigma_t^{0g} = C_t^{0g}, \tag{4.7b}$$

$$C_{tt}^{0r} = \gamma C_{xxt}^{0r} - C_t^{0r}, \tag{4.8a}$$

$$\sigma_t^{0r} + \sigma^{0r} = C_t^{0r}, \tag{4.8b}$$

where $\gamma = \nu E/D_0$.

Solving equation (4.7b) subject to (4.5), we see that

$$\sigma^{0g} = C^{0g}. \tag{4.9a}$$

Then we may use equation (3.28) to see that

$$\sigma(s(t), t) = C_*. \tag{4.9b}$$

Our flux condition (4.3) now becomes, to leading order,

$$\left[C_x^0\right]_s - \frac{C_*}{\dot{s}} = \frac{a\dot{s}}{\gamma}. \tag{4.10}$$

We use the integral method adopted by Boley [24]. In his paper, he extended the equations which held on either side of the front to the entire domain. Then by introducing *fictitious* boundary conditions which held in the extended part of each equation's domain, he was able to construct solutions to the moving boundary-value problem. Following that method, we introduce two new quantities T^g and T^r which

extend each of equations (4.7a) and (4.8a) to the full semi-infinite region. We then make sure that each of these solutions satisfies the correct boundary conditions as follows:

$$T^r_{tt} = \gamma T^r_{xxt} - T^r_t, \quad 0 < x < \infty; \tag{4.11a}$$

$$T^r \equiv C^{0r}, \quad 0 < x < s(t); \tag{4.11b}$$

$$T^r(0,t) = 1, \qquad T^r(x,0) = 1 - f^i(x), \qquad T^r(x,\infty) = 1; \tag{4.12}$$

$$T^r(s(t),t) = C_*; \tag{4.13}$$

$$T^g_{tt} = \gamma T^g_{xxt}, \quad 0 < x < \infty; \tag{4.14a}$$

$$T^g \equiv C^{0g}, \quad s(t) < x < \infty; \tag{4.14b}$$

$$T^g(0,t) = f^b(t), \qquad T^g(x,0) = 0; \tag{4.15}$$

$$T^g(s(t),t) = C_*; \tag{4.16}$$

$$T^g_x(s(t),t) - T^r_x(s(t),t) - \frac{C_*}{\dot{s}} = \frac{a\dot{s}}{\gamma}; \tag{4.17}$$

$$s(0) = 0. \tag{4.18}$$

The new quantities T^r and T^g are simply C^{0r} and C^{0g} extended to the full semi-infinite range. The unknowns $f^i(x)$ and $f^b(t)$ are fictitious initial and boundary conditions introduced in order to facilitate the solution of the problem.

Integrating equation (4.11a) using (4.12), we have

$$T^r_t = \gamma T^r_{xx} + (1 - T^r), \quad 0 < x < \infty. \tag{4.19}$$

Now writing $T^r = 1 - e^{-t}T^u$, we have

$$T^u_t = \gamma T^u_{xx}, \quad 0 < x < \infty; \tag{4.20a}$$

$$T^u(0,t) = 0, \qquad T^u(x,0) = f^i(x). \tag{4.20b}$$

We introduce the standard notion of a Laplace transform:

$$\hat{f}(p) = \int_0^\infty f(t)e^{-pt}\,dt, \qquad f(t) = \frac{1}{2\pi i}\int_B \hat{f}(p)e^{pt}\,dp,$$

where B is the Bromwich contour. Taking the Laplace transform of equations (4.20), we have

$$p\hat{T}^u - f^i(x) = \gamma \hat{T}^u_{xx}, \qquad \hat{T}^u(0,p) = 0. \tag{4.21}$$

The Green's function for this problem is

$$G(x|z) = -\sqrt{\frac{\gamma}{p}}\sinh(x_<\sqrt{p/\gamma})\exp\left(-x_>\sqrt{\frac{p}{\gamma}}\right),$$

so we have that

$$\hat{T}^u(x,p) = \frac{1}{2\sqrt{\gamma p}}\int_0^\infty f^i(z)\left[e^{-|x-z|\sqrt{p/\gamma}} - e^{-(z+x)\sqrt{p/\gamma}}\right]dz. \tag{4.22}$$

The inverse Laplace transform of (4.22) is

$$T^u(x,t) = \frac{1}{2\sqrt{\pi\gamma t}}\int_0^\infty f^i(z)\left\{\exp\left[-\frac{(x-z)^2}{4\gamma t}\right] - \exp\left[-\frac{(x+z)^2}{4\gamma t}\right]\right\}dz. \tag{4.23}$$

Therefore, we have

$$T^r(x,t) = 1 - \frac{e^{-t}}{2\sqrt{\pi\gamma t}}\int_0^\infty f^i(z)\left\{\exp\left[-\frac{(x-z)^2}{4\gamma t}\right] - \exp\left[-\frac{(x+z)^2}{4\gamma t}\right]\right\}dz. \tag{4.24}$$

From a cursory examination of (4.24), we can see that sharp fronts are possible. This is because for long time, the behavior away from the front is basically $1 - e^{-t}$, which will cause an extremely sharp front to form as the solution plunges from 1 to C_* in the neighborhood of the front.

Next we solve for T^g. Using our initial condition (4.15), we may integrate equation (4.14a) once with respect to t to obtain the following:

$$T^g_t = \gamma T^g_{xx}. \tag{4.25}$$

We once again use the Laplace transform on (4.25). Doing so and using equation (4.15) yields

$$p\hat{T}^g = \gamma \hat{T}^g_{xx}, \qquad \hat{T}^g(0,p) = \hat{f}^b(p),$$

$$\hat{T}^g(x,p) = \hat{f}^b(p) \exp\left(-x\sqrt{\frac{p}{\gamma}}\right),$$

$$T^g(x,t) = \frac{x}{2\sqrt{\pi\gamma}} \int_0^t \frac{f^b(z)}{(t-z)^{3/2}} \exp\left[-\frac{x^2}{4\gamma(t-z)}\right] dz. \tag{4.26}$$

Now we may substitute equations (4.24) and (4.26) into (4.13), (4.16), and (4.17) (omitting explicitly the dependence of s on t) to yield the following:

$$1 - \frac{e^{-t}}{2\sqrt{\pi\gamma t}} \int_0^\infty f^i(z) \left\{ \exp\left[-\frac{(s-z)^2}{4\gamma t}\right] - \exp\left[-\frac{(s+z)^2}{4\gamma t}\right] \right\} dz = C_*, \tag{4.27}$$

$$\frac{s}{2\sqrt{\pi\gamma}} \int_0^t \frac{f^b(z)}{(t-z)^{3/2}} \exp\left[-\frac{s^2}{4\gamma(t-z)}\right] dz = C_*, \tag{4.28}$$

$$\frac{1}{2\sqrt{\pi\gamma}}\int_0^t \frac{f^b(z)}{(t-z)^{3/2}}\left[1-\frac{s^2}{2\gamma(t-z)}\right]\exp\left[-\frac{s^2}{4\gamma(t-z)}\right]dz$$

$$-\frac{e^{-t}}{4\gamma t\sqrt{\pi\gamma t}}\int_0^\infty f^i(z)\left\{(s-z)\exp\left[-\frac{(s-z)^2}{4\gamma t}\right]-(s+z)\exp\left[-\frac{(s+z)^2}{4\gamma t}\right]\right\}dz$$

$$-\frac{C_*}{\dot{s}}=\frac{a\dot{s}}{\gamma}. \quad (4.29)$$

Equations (4.27)-(4.29) now constitute three equations for our three unknowns $s(t)$, $f^b(t)$, and $f^i(x)$. We now seek asymptotic solutions to these equations for small and large t.

Chapter V: Asymptotics

1. Small Time

We begin by looking at the solution for t near 0. We note that for small t the dominant contribution to the integrals in (4.27)-(4.29) is from z near $s(t)$ (hence near 0) and from t near 0. Thus, we make the following assumptions for the forms of our unknown quantities:

$$f^i(x) \sim f_0^i, \quad x \to 0; \qquad f^b(t) \sim f_0^b, \quad s(t) \sim 2s_0 t^n \sqrt{\gamma}, \quad t \to 0. \tag{5.1}$$

Here $n > 0$ by (4.18).

Making these substitutions in equation (4.27), we have the following:

$$1 - f_0^i e^{-t} \operatorname{erf} s_0 t^{n-1/2} = C_*. \tag{5.2}$$

Note that if $n > 1/2$, then equation (5.2) becomes $C_* = 1$, which we consider to be a vacuous case. So we know that $0 < n \leq 1/2$. Substituting (5.1) in (4.28), we have

$$f_0^b \operatorname{erfc} s_0 t^{n-1/2} = C_*. \tag{5.3}$$

Note that if $n < 1/2$, then equation (5.3) becomes $C_* = 0$, which we also consider to be a vacuous case. Hence, we conclude that $n = 1/2$.

At first glance this result, which is standard in classical Fickian diffusion, would seem to be at odds with our claim that we are modeling non-Fickian systems.

However, it has always been our contention that the term which causes the non-Fickian behavior is the viscoelastic memory integral term. For small time, this memory term has not fully developed, since the polymer has no long concentration history. [Note that taking $\sigma_i(x) \equiv 0$ is equivalent to letting $\tilde{t}_0 = 0$ in (2.3b).]

Using the fact that $n = 1/2$, equation (5.2) becomes

$$f_0^i = \frac{1 - C_*}{\operatorname{erf} s_0}, \tag{5.4}$$

and equation (5.3) becomes

$$f_0^b = \frac{C_*}{\operatorname{erfc} s_0}. \tag{5.5}$$

Using (5.1) and the fact that $n = 1/2$ in (4.29), we have

$$\frac{f_0^i - f_0^b}{\sqrt{\pi\gamma t}} e^{-s_0^2} = \frac{a s_0}{\sqrt{\gamma t}}. \tag{5.6}$$

Substituting equations (5.4) and (5.5) in (5.6), we have the following:

$$e^{-s_0^2} (\operatorname{erfc} s_0 - C_*) = a s_0 \operatorname{erfc} s_0 \operatorname{erf} s_0 \sqrt{\pi}. \tag{5.7}$$

Figure 5a shows a graph of equation (5.7). Note that as we increase a or C_*, the value of s_0 at the intersection point (*i.e.*, our velocity coefficient) decreases. This is perfectly consistent with our physical intuition of the problem. As a increases, the difference in the flux needed to move the front a preset distance increases, so we would expect the speed to slow. As C_* increases, the value of the concentration at which the transition takes place increases, thereby slowing the speed of its advance. This slowing takes place even in the limit $C_* \to 1$, where $s_0 \to 0$. This is also

consistent with our argument above, since in that case $n > 1/2$. We also note from Figure 5a why we chose $a > 0$, since in this region there is always a unique solution of (5.7).

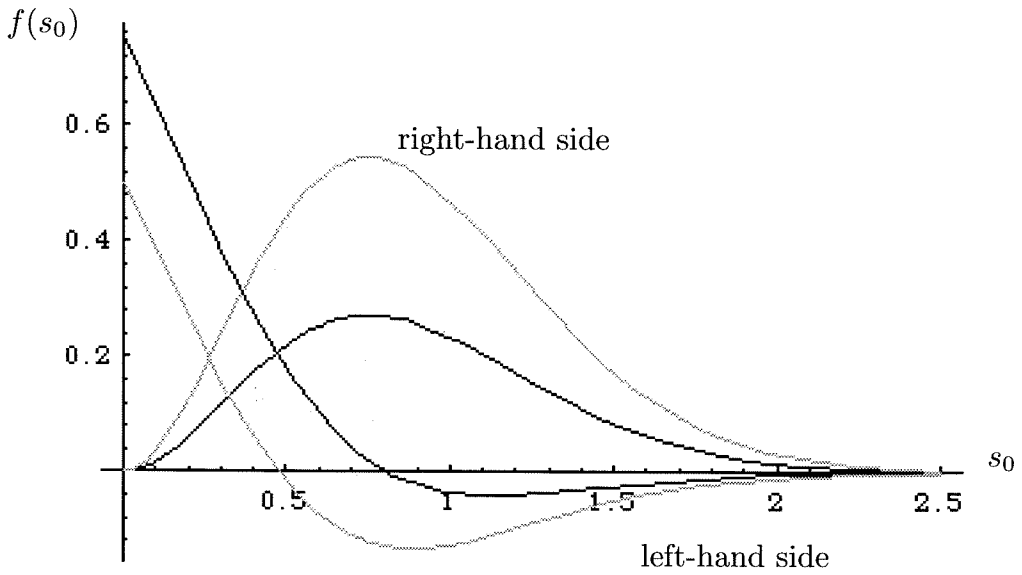

Figure 5a. Graphs of equation (5.7). Dark lines: $C_* = 1/4$, $a = 1$.

Light lines: $C_* = 1/2$, $a = 2$.

We may now complete our representations for small t.

$$s(t) \sim 2s_0\sqrt{\gamma t}, \quad t \to 0, \qquad e^{-s_0^2}(\operatorname{erfc} s_0 - C_*) = as_0 \operatorname{erfc} s_0 \operatorname{erf} s_0\sqrt{\pi}. \tag{5.8}$$

Using equation (5.5), we may conclude immediately from equation (4.26) that

$$C^{0g}(x,t) \sim \frac{C_*}{\operatorname{erfc} s_0} \operatorname{erfc}\left(\frac{x}{2\sqrt{\gamma t}}\right), \quad t \to 0. \tag{5.9}$$

Using equation (4.9a), we have the following:

$$\sigma^{0g}(x,t) \sim \frac{C_*}{\operatorname{erfc} s_0} \operatorname{erfc}\left(\frac{x}{2\sqrt{\gamma t}}\right), \quad t \to 0. \tag{5.10}$$

Using equation (5.4), we see from equation (4.24) that

$$C^{0r}(x,t) \sim 1 - \frac{1-C_*}{\operatorname{erf} s_0} e^{-t} \operatorname{erf}\left(\frac{x}{2\sqrt{\gamma t}}\right), \quad x \to 0. \tag{5.11}$$

Using equation (5.11) in (4.8b), we have that

$$e^t \sigma^{0r} = \frac{1-C_*}{\operatorname{erf} s_0}\left[x\sqrt{\frac{t}{\gamma\pi}}\exp\left(-\frac{x^2}{4\gamma t}\right) + \left(1-\frac{x^2}{2\gamma}\right)\operatorname{erfc}\left(\frac{x}{2\sqrt{\gamma t}}\right) + \operatorname{erf}\left(\frac{x}{2\sqrt{\gamma t}}\right)\right] + f(x),$$

where we use $f(x)$ to satisfy (4.9b). Our final expression is

$$\sigma^{0r}(x,t) = \frac{(1-C_*)e^{-t}}{\operatorname{erf} s_0}\left[x\sqrt{\frac{t}{\gamma\pi}}\exp\left(-\frac{x^2}{4\gamma t}\right) + \left(1-\frac{x^2}{2\gamma}\right)\operatorname{erfc}\left(\frac{x}{2\sqrt{\gamma t}}\right) + t\operatorname{erf}\left(\frac{x}{2\sqrt{\gamma t}}\right)\right] + \frac{(C_* - \operatorname{erfc} s_0)e^{-t}}{\operatorname{erf} s_0}, \quad x \to 0. \tag{5.12}$$

Note in equations (5.9)-(5.12) that the asymptotic variable for the expansion is the independent variable for the fictitious boundary condition. Hence, in equations (5.11) and (5.12) since $f^i(x)$ does not depend on t, this is a small x asymptotic expansion good for all t.

Figure 5b shows graphs of our concentration results (5.9) and (5.11) for a certain set of parameters [which satisfies (4.4)] and differing time values. The gap in the graphs of the different equations is due to the fact that our expansions are only good to leading order in t. The shape of the graphs can easily be seen to be of the general qualitative shape of a standard Fickian system as shown in figure 5c. This is consistent with the fact that the memory of the polymer has not fully developed at this point.

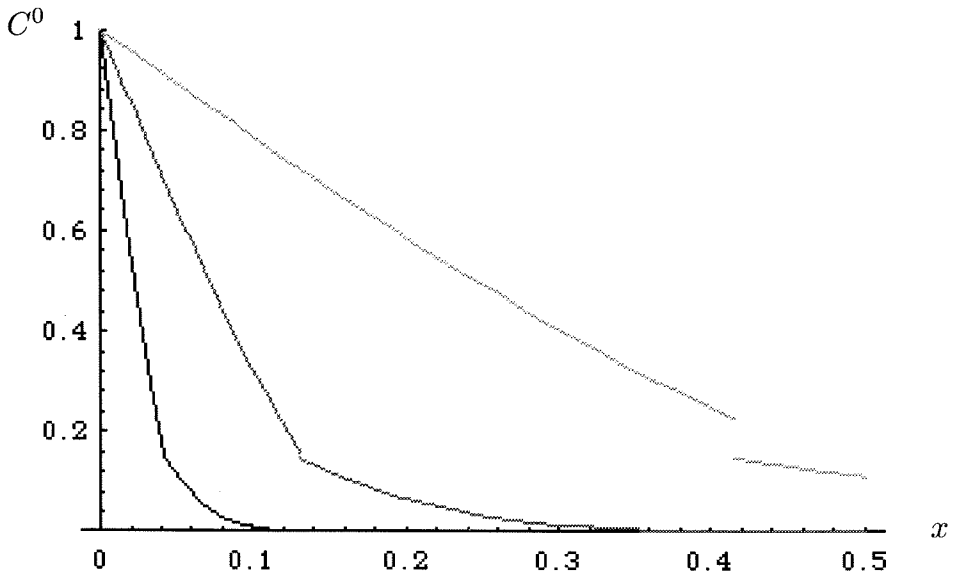

Figure 5b. Concentration profiles: $a = 0.5$, $C_* = 0.15$, $\gamma = 1$.

In decreasing order of darkness: $t = 0.001$, 0.01, 0.1.

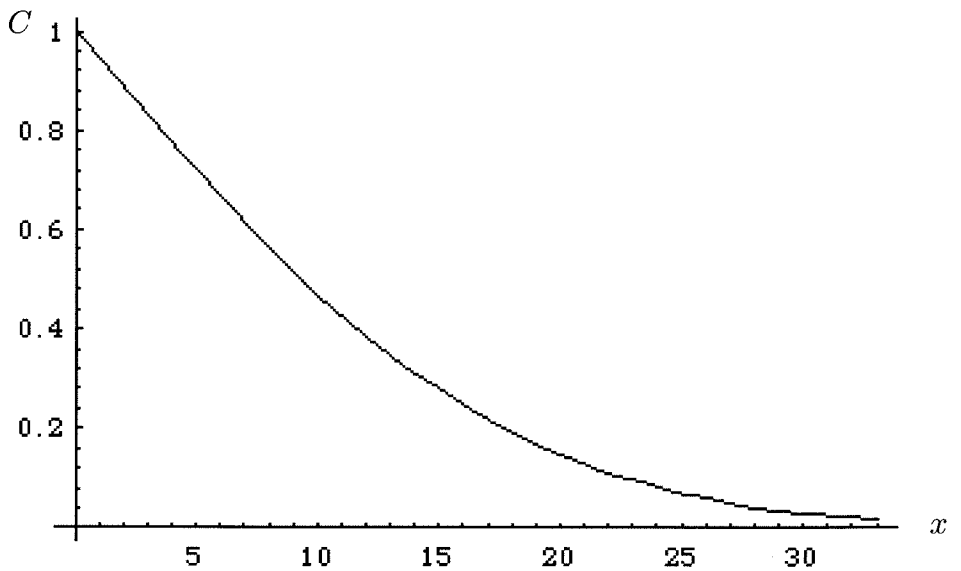

Figure 5c. Standard Fickian profile.

Figure 5d shows graphs of our stress results (5.10) and (5.12) for the same parameters and times. One thing to note is that the stress at the boundary is beginning to decay away. This trend will become more pronounced as the experiment progresses.

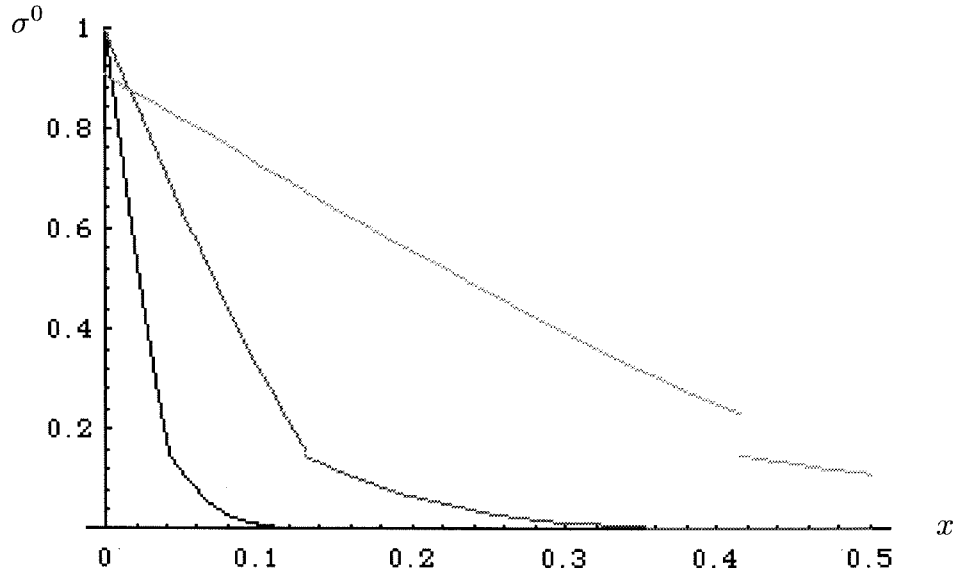

Figure 5d. Stress profiles: $a = 0.5$, $C_* = 0.15$, $\gamma = 1$.

In decreasing order of darkness: $t = 0.001$, 0.01, 0.1.

2. Large Time

Next we look at the solution for $t \to \infty$. We begin by examining the last two terms of equation (4.29). For any $s(t)$ not proportional to t, one of these terms will be growing for large t. We expect the derivatives of the concentration to be bounded for large t, so this large term would have nothing to balance it. Therefore, we conclude that $s(t) \sim 2s_\infty t\sqrt{\gamma}$ for large t.

This means that for large t, any solutions with error functions in them will die exponentially. Hence, a naïve assumption that $f^b(t)$ behaves like a constant for large t will be incorrect. In fact, what we need is a *growing* exponential. Thus we assume the following form for $f^b(t)$:

$$f^b(t) \sim f^b_\infty e^{A_b^2 t}, \quad t \to \infty. \tag{5.13}$$

Note that since $f^b(t)$ is a *fictitious* boundary condition, it does not make any difference that it is unbounded as $t \to \infty$ as long as T^g behaves properly for $x > s(t)$. Using (5.13), (4.26) becomes the following:

$$T^g(x,t) \sim \frac{f^b_\infty}{2} e^{A_b^2 t} \left[\exp\left(\frac{A_b x}{\sqrt{\gamma}}\right) \operatorname{erfc}\left(\frac{x}{2\sqrt{\gamma t}} + A_b\sqrt{t}\right) \right.$$
$$\left. + \exp\left(-\frac{A_b x}{\sqrt{\gamma}}\right) \operatorname{erfc}\left(\frac{x}{2\sqrt{\gamma t}} - A_b\sqrt{t}\right) \right]. \quad (5.14)$$

Now asymptotically expanding equation (5.14) for large t [using our assumption for $s(t)$] and putting the result in equation (4.28), we have

$$\frac{f^b_\infty}{2} \left\{ \frac{\exp\left(-s_\infty^2 t\right)}{(s_\infty + A_b)\sqrt{\pi t}} + \exp\left[(A_b^2 - 2A_b s_\infty)t\right] \operatorname{erfc}\left[(s_\infty - A_b)\sqrt{t}\right] \right\} = C_*,$$

from which we have

$$f^b_\infty = C_*, \qquad A_b = 2s_\infty. \quad (5.15)$$

Special care must also be taken with T^r. Once again, from examination of (4.24), we see that for $s(t) \propto t$ all terms arising from a bounded $f^i(x)$ are exponentially small. Therefore, we expect $f^i(x)$ to be exponentially large:

$$f^i(x) \sim f^i_\infty e^{A_i x}, \quad x \to \infty; \qquad A_i > 0. \quad (5.16)$$

Using (5.16) in equation (4.24), we have the following:

$$T^r(x,t) \sim 1 - \frac{f^i_\infty}{2} \exp\left[(A_i^2\gamma - 1)t\right] \times$$
$$\left[e^{A_i x} \operatorname{erfc}\left(-\frac{x}{2\sqrt{\gamma t}} - A_i\sqrt{\gamma t}\right) - e^{-A_i x} \operatorname{erfc}\left(\frac{x}{2\sqrt{\gamma t}} - A_i\sqrt{\gamma t}\right) \right]. \quad (5.17)$$

Upon substitution of equation (5.17) and our expression for $s(t)$, the leading orders of equation (4.27) become

$$\frac{f^i_\infty}{2}\exp\left[(A_i^2\gamma-1)t\right]\left\{e^{2A_i s_\infty t\sqrt{\gamma}}\operatorname{erfc}\left[-(s_\infty+A_i\sqrt{\gamma})\sqrt{t}\right]\right.$$
$$\left.-e^{-2A_i s_\infty t\sqrt{\gamma}}\operatorname{erfc}\left[(s_\infty-A_i\sqrt{\gamma})\sqrt{t}\right]\right\}=1-C_*. \quad (5.18)$$

Solving equation (5.18), we have

$$A_i=\frac{-s_\infty+\sqrt{s_\infty^2+1}}{\sqrt{\gamma}}, \qquad f^i_\infty=1-C_*. \quad (5.19)$$

Now we must solve for s_∞ by substituting our new results into equation (4.29). Before proceeding, we see that the only terms in the derivatives of (5.14) and (5.17) which are not exponentially decaying for $s(t)\propto t$ are the derivatives of the exponentials $e^{-A_b x}$ and $e^{A_i x}$. Keeping that argument in mind, we have the following for equation (4.29):

$$-\frac{C_*A_b}{2\sqrt{\gamma}}\exp\left(A_b^2t-\frac{A_bs}{\sqrt{\gamma}}\right)\operatorname{erfc}\left(\frac{s}{2\sqrt{\gamma t}}-A_b\sqrt{t}\right)$$
$$+\frac{A_i(1-C_*)}{2}\exp\left[(A_i^2\gamma-1)t+A_is\right]\operatorname{erfc}\left(-\frac{s}{2\sqrt{\gamma t}}-A_i\sqrt{\gamma t}\right)=\frac{a\dot{s}}{\gamma}+\frac{C_*}{\dot{s}}. \quad (5.20)$$

Substituting our expressions for A_i, A_b, and $s(t)$ and expanding for large t, we have

$$-\frac{2C_*s_\infty}{\sqrt{\gamma}}+\frac{(C_*-1)(s_\infty-\sqrt{s_\infty^2+1})}{\sqrt{\gamma}}=\frac{2as_\infty}{\sqrt{\gamma}}+\frac{C_*}{2s_\infty\sqrt{\gamma}}. \quad (5.21)$$

Rearranging terms, we have that s_∞ is one of

$$s_{\infty\pm}=\frac{1}{2}\left[\frac{1-2C_*a-3C_*\pm(1-C_*)\sqrt{1-4C_*-4C_*a}}{2(1+a)(C_*+a)}\right]^{1/2}. \quad (5.22)$$

Since $a > 0$ by (4.4), the requirement that

$$C_* \leq \frac{1}{4(1+a)} \tag{5.23}$$

guarantees that $s_{\infty\pm}$ are real.

Since we have two possible solutions, the natural next step is to check their stability. Thus, we introduce an $o(1)$ perturbation $\delta(t) \gg \epsilon$ into equation (4.17), which yields (to leading order in δ)

$$T_x^g\left(s(t),t\right) - T_x^r\left(s(t),t\right) + \delta[T_{xx}^g\left(s(t),t\right) - T_{xx}^r\left(s(t),t\right)] = \frac{C_*}{\dot{s}} + \frac{a\dot{s}}{\gamma} + \frac{\dot{\delta}}{\dot{s}}\left(\frac{a\dot{s}}{\gamma} - \frac{C_*}{\dot{s}}\right).$$

Using (4.13), (4.17), (4.19), (4.25), and our expression for $s(t)$, we have

$$\frac{\delta}{\gamma}\left[T_t^g\left(s(t),t\right) - T_t^r\left(s(t),t\right) + 1 - C_*\right] = \frac{\dot{\delta}}{2\gamma s_\infty}\left(2as_\infty - \frac{C_*}{2s_\infty}\right).$$

Using the total derivative of the first of equations (3.28) with respect to x, we have

$$\frac{\delta}{\gamma}\left(-\dot{s}[T_x]_s + 1 - C_*\right) = \frac{\dot{\delta}(4as_\infty^2 - C_*)}{4s_\infty^2}.$$

Using equation (4.17) and our expression for $s(t)$, we have

$$\delta(1 - 2C_* - 4as_\infty^2) = \frac{\dot{\delta}(4as_\infty^2 - C_*)}{4s_\infty^2}. \tag{5.24}$$

Since the other quantities are always positive, the criterion for stability is that the ratio of the two parenthesized quantities is negative. This will make δ decay exponentially as $t \to \infty$.

The parenthesized quantity on the left is zero when

$$a = \frac{1}{4C_*} - 1 - \frac{\lambda^2}{4C_*}, \text{ where } (C_* - 1)\lambda^2 + 2(1 - 3C_* + 2C_*^2)\lambda + 5C_* - 8C_*^2 - 1 = 0,$$

but the discriminant of the quadratic is negative, so the parenthesized quantity on the left is always of the same sign (namely positive). The parenthesized quantity on the right is always negative for $s_{\infty -}$, and it is positive for $s_{\infty +}$ when

$$C_* \leq \frac{1 - (1 + 2a - 2\sqrt{a^2 + a})^2}{4(1 + a)}, \tag{5.25}$$

which for $a > 0$ is stronger than (5.23). Thus, we have our compatibility condition (4.4).

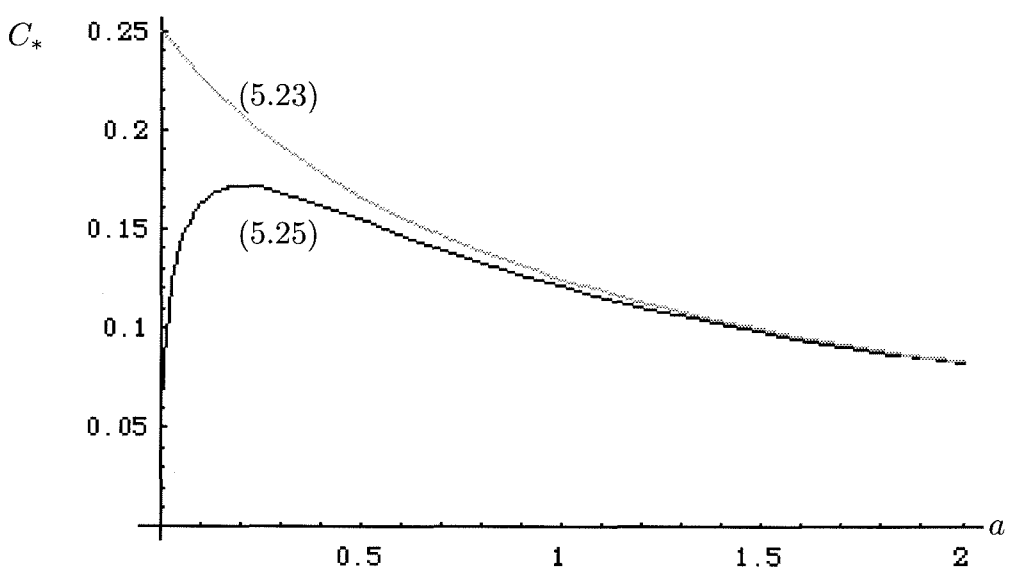

Figure 5e. Graphs of equations (5.23) and (5.25).

Note from Figure 5e that as $a \to \infty$, condition (5.25) approaches condition (5.23). We also note that as $a \to 0$ or $a \to \infty$, the range of validity for our solution is very thin. As $a \to \infty$, we see that the second term on the left-hand side of

equation (4.10) becomes negligible. Therefore, we would be left with a standard Stefan condition where the front would move with speed proportional to $t^{-1/2}$. As $a \to 0$, we see that equation (4.10) would allow solutions with fronts that moved at speeds faster than a constant.

We may now complete our representations for large t.

$$s(t) \sim 2s_\infty t\sqrt{\gamma}, \quad t \to \infty; \tag{5.26a}$$

$$s_\infty = \frac{1}{2}\left[\frac{1 - 2C_*a - 3C_* - (1 - C_*)\sqrt{1 - 4C_* - 4C_*a}}{2(1+a)(C_* + a)}\right]^{1/2}. \tag{5.26b}$$

Using equations (5.15) in (5.14), we immediately have

$$C^{0g}(x,t) \sim \frac{C_* e^{4s_\infty^2 t}}{2}\left[\exp\left(\frac{2s_\infty x}{\sqrt{\gamma}}\right)\operatorname{erfc}\left(\frac{x}{2\sqrt{\gamma t}} + 2s_\infty\sqrt{t}\right)\right.$$

$$\left. + \exp\left(-\frac{2s_\infty x}{\sqrt{\gamma}}\right)\operatorname{erfc}\left(\frac{x}{2\sqrt{\gamma t}} - 2s_\infty\sqrt{t}\right)\right], \quad t \to \infty, \tag{5.27}$$

and from equation (4.9a) we have

$$\sigma^{0g}(x,t) \sim \frac{C_* e^{4s_\infty^2 t}}{2}\left[\exp\left(\frac{2s_\infty x}{\sqrt{\gamma}}\right)\operatorname{erfc}\left(\frac{x}{2\sqrt{\gamma t}} + 2s_\infty\sqrt{t}\right)\right.$$

$$\left. + \exp\left(-\frac{2s_\infty x}{\sqrt{\gamma}}\right)\operatorname{erfc}\left(\frac{x}{2\sqrt{\gamma t}} - 2s_\infty\sqrt{t}\right)\right], \quad t \to \infty. \tag{5.28}$$

Using equations (5.19) in (5.17) we have

$$A_i = \frac{-s_\infty + \sqrt{s_\infty^2 + 1}}{\sqrt{\gamma}}, \tag{5.29}$$

$$C^{0r}(x,t) \sim 1 - \frac{1 - C_*}{2}\exp\left[(A_i^2\gamma - 1)t\right] \times$$

$$\left[e^{A_i x}\operatorname{erfc}\left(-\frac{x}{2\sqrt{\gamma t}} - A_i\sqrt{\gamma t}\right) - e^{-A_i x}\operatorname{erfc}\left(\frac{x}{2\sqrt{\gamma t}} - A_i\sqrt{\gamma t}\right)\right], \quad x \to \infty. \tag{5.30}$$

Now we continue by solving for σ^{0r} for large t. When taking the derivative of (5.30), we see that the dominant term is the following:

$$C_t^{0r} \sim -\frac{(1-C_*)(A_i^2\gamma - 1)}{2} \exp\left[(A_i^2\gamma - 1)t\right] e^{A_i x} \operatorname{erfc}\left(-\frac{x}{2\sqrt{\gamma t}} - A_i\sqrt{\gamma t}\right).$$

We may now take the error function to be approximately equal to 2, and plug into equation (4.8b) to obtain the following:

$$\sigma^{0r}(x,t) \sim -\frac{2(1-C_*)s_\infty}{s_\infty - \sqrt{s_\infty^2+1}} \exp\left[-(s_\infty - \sqrt{s_\infty^2+1})\left(\frac{x}{\sqrt{\gamma}} - 2s_\infty t\right)\right] + f(x)e^{-t},$$

where $f(x)$ is chosen to satisfy (4.9b). This yields

$$\sigma^{0r}(x,t) \sim \frac{2(1-C_*)s_\infty}{\sqrt{s_\infty^2+1} - s_\infty} \exp\left[-(s_\infty - \sqrt{s_\infty^2+1})\left(\frac{x}{\sqrt{\gamma}} - 2s_\infty t\right)\right]$$

$$+ \left[C_* - \frac{2(1-C_*)s_\infty}{\sqrt{s_\infty^2+1} - s_\infty}\right] \exp\left(\frac{x}{2s_\infty\sqrt{\gamma}} - t\right), \quad x \to \infty. \quad (5.31)$$

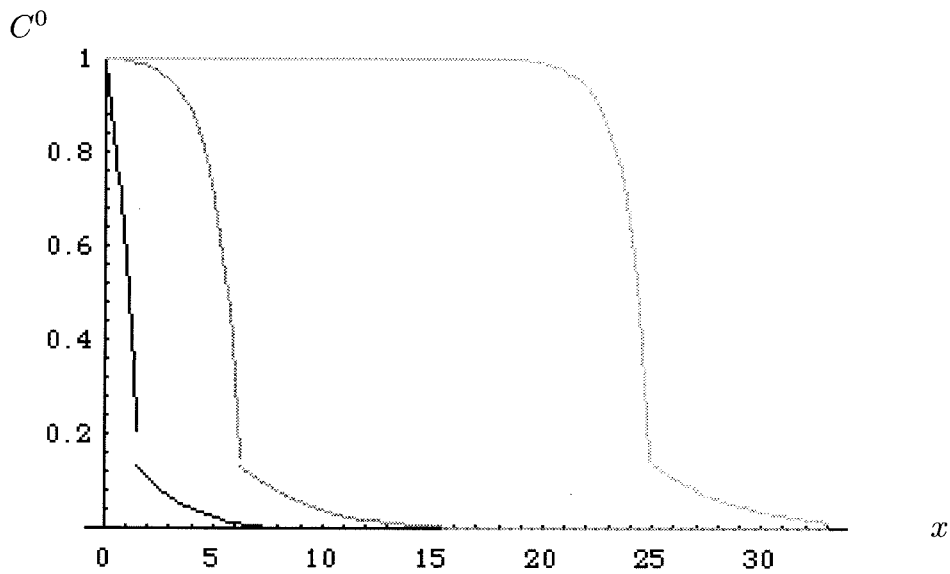

Figure 5f. Concentration profiles: $a = 0.5$, $C_* = 0.15$, $\gamma = 1$.

In decreasing order of darkness: $t = 6$, 24, 96.

Figure 5f shows graphs of our concentration results (5.27) and (5.30) for the same set of parameters as before. Since (5.30) satisfies our boundary condition $C(0,t) = 1$, we have used it as the plot for the entire domain $0 < x < s(t)$. The only difference between (5.30) and the more reliable (5.11) to leading orders as $x \to 0$ and $t \to \infty$ is the coefficient of e^{-t}; hence for the purposes of graphical interpretation the two are indistinguishable. Once again, the gaps in the graphs are due to the fact that we are graphing asymptotic solutions, not exact solutions. Note that as $t \to \infty$, our front is sharper than the standard Fickian behavior shown in Figure 5c. Our profile, where the concentration is almost identically 1 behind the front before plunging sharply downward at the front, has been seen in numerical simulations of Case II transport [25] and experimentally in polymer-penetrant systems [9].

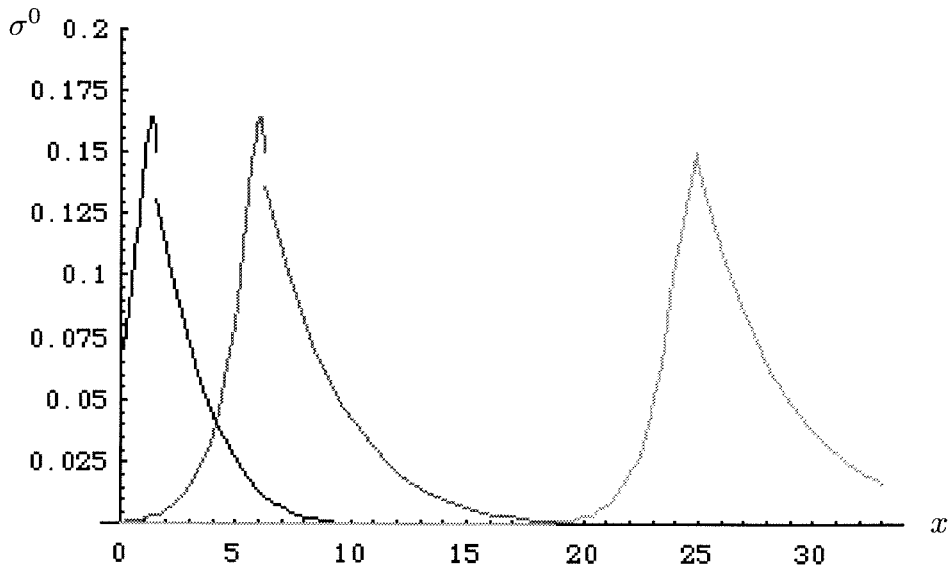

Figure 5g. Stress profiles: $a = 0.5$, $C_* = 0.15$, $\gamma = 1$.

In decreasing order of darkness: $t = 6$, 24, 96.

Figure 5g shows graphs of our stress results (5.28) and (5.31) for the same parameters and times. An argument similar to the one outlined above can be made for plotting (5.31) for $x \to 0$ rather than (5.12). As expected, our stress now has a

maximum slightly behind the front (the position of which can be ascertained from the gap). Recall that in Chapter III we stated that we wished to model a case where the stress had a peak *at* the phase transition. However, in that chapter we also postulated that such a profile would probably imply that $a < 0$, which is not true in the weakly diffusive case. In Chapter VIII we will consider a case where $a < 0$ and the stress has its maximum at the phase transition.

Lastly, note that in the region where the concentration of the penetrant is nearly 1, the stress in the polymer is nearly 0; that is, the polymer is fully relaxed.

Chapter VI: Remarks

The results in Chapter V clearly demonstrate that in polymer-penetrant systems where the diffusion coefficient is small, non-Fickian behavior ensues. The addition of the non-negligible nonlinear viscoelastic stress term to the chemical potential introduces memory effects which greatly change the character of the solution. Though the moving boundary-value problem which results is no longer solvable in closed form, thankfully Boley's method yields analytical results.

Since the system of integro-differential equations which results cannot be solved in closed form, an asymptotic approach is expedient. For any $a > 0$, a solution was found which moved with speed proportional to $t^{-1/2}$, as expected from a diffusive system. This is indicative of the fact that as $t \to 0$, the effect of memory is not yet important, since our definition of the stress implies that the time history begins at $t = 0$.

However, as time progresses, the effect of memory becomes more and more important. This memory effect, which makes its presence felt in the second term on the left-hand side of (4.10), eventually forces the front to move with constant speed, a phenomenon not seen in Fickian systems with bounded initial and boundary conditions. In addition, as time grows ever larger, our equations lead to solutions where an increasing portion of the rubbery polymer is fully saturated. Lastly, the width of the region in which the solution decays from 1 to C_* is much narrower than in Fickian systems. This behavior successfully models some of the phenomena seen in polymer-penetrant systems [9], [25].

Obviously, (4.4) is a restrictive class of parameters. However, this does not mean that there do not exist solutions when C_* does not satisfy (5.25). What can we say about such systems when a is positive? Well, our discussion in the first paragraph of Chapter V.2 still holds; that is, the front must move with constant speed in order to satisfy (4.29). However, our solution (5.26) is based on the assumption that the next order in the asymptotic expansion with respect to t is $O(1)$. If the next term is larger than $O(1)$, then our expansions for T^g and T^r would be exponentially decaying or increasing. Therefore, it is possible that solutions do exist for our problem which move with constant speed with a correction that is greater than $O(1)$. These solutions cannot be obtained by using such simplistic expressions as the simple exponentials in (5.13) and (5.16) for our fictitious boundary conditions. However, to leading order the front would still move with constant speed.

In the next part of this thesis we will consider a problem which involves the use of singular perturbation techniques. The solution profiles for these cases will share some similarities with the solutions found here, but in other ways will be quite different.

Part Three: The

Heavily Stressed Case

Chapter VII: The Heavily Stressed Case: Preliminaries

1. Governing Equations

We now wish to model polymer systems where the stress is very large compared to other quantities in the problem. Since the polymer still has a rubbery and glassy phase, we retain the same nondimensionalizations and relationships between relaxation times as in Chapter III. We once again assume that the variation in the diffusion coefficient is minimal, so we expect $D_g = D_r = D$. However, now we let $D = O(1)$. In such a polymer-dissolution system, we expect the effects of the stress to be important, so we let $\eta = \eta_0 \epsilon^{-2}$. It will be shown that these choices of orders of magnitude for our parameters lead to solutions which mimic the desired behavior. Summarizing, we have the following:

$$D_g = D_r = D, \qquad \tilde{x}_c = \sqrt{\frac{D}{\beta_g}}, \qquad \beta_c = \beta_r, \qquad \frac{\beta_g}{\beta_r} = \epsilon, \qquad \eta = \eta_0 \epsilon^{-2}.$$

Making these substitutions in equations (3.32) and (3.25b), we see that for $C \leq C_*$ we have the following equations:

$$C^g_{tt} = \alpha \epsilon C^g_{xxt} - \epsilon C^g_t + \left(\epsilon^2 + \frac{\eta_0 E}{\beta_g D}\right) C^g_{xx}, \tag{7.1a}$$

$$\sigma^g_t + \epsilon \sigma^g = \frac{\eta_0 \epsilon^{-1}}{\nu \beta_g} C^g + C^g_t, \tag{7.1b}$$

while for $C > C_*$ we have

$$C^r_{tt} = \alpha\epsilon C^r_{xxt} - C^r_t + \left(\epsilon + \frac{\eta_0 E}{\beta_g D}\right) C^r_{xx}, \tag{7.2a}$$

$$\sigma^r_t + \sigma^r = \frac{\eta_0 \epsilon^{-1}}{\nu\beta_g} C^r + C^r_t, \tag{7.2b}$$

where $\gamma = \nu E/D$ and $\alpha = 1 + \gamma$. In addition, equation (3.26) becomes

$$[(D + \nu E)C_x]_s + \nu E(\epsilon - 1)\frac{\sigma\,(s(t), t)}{\dot{s}} = \frac{aD}{\epsilon}\dot{s}, \tag{7.3}$$

and equation (3.25a) becomes

$$C_t = \epsilon C_{xx} + \gamma\epsilon\sigma_{xx}. \tag{7.4}$$

We postulate the following expansions for C and σ in ϵ:

$$C = C^0 + o(1), \quad \sigma = \epsilon^{-1}\sigma^0 + o(\epsilon^{-1}).$$

Note that these forms, which are dictated by our choice of parameters, indicate that the effects of the stress will dominate those of Fickian diffusion in (7.4). Therefore, we expect to see non-Fickian behavior in this system. Inserting these expressions into equations (7.1)-(7.4) and retaining terms to leading order, we have the following:

$$C^{0g}_{tt} = \kappa^2 C^{0g}_{xx}, \tag{7.5a}$$

$$\sigma^{0g}_t = \frac{\kappa^2}{\gamma} C^{0g}, \tag{7.5b}$$

$$C^{0r}_{tt} = \kappa^2 C^{0r}_{xx} - C^{0r}_t, \tag{7.6a}$$

$$\sigma_t^{0r} + \sigma^{0r} = \frac{\kappa^2}{\gamma} C^{0r}, \tag{7.6b}$$

$$\alpha\epsilon \left[C_x^0\right]_s - \gamma \frac{\sigma^0\left(s(t),t\right)}{\dot{s}} = a\dot{s}, \tag{7.7}$$

$$C_t^0 = \gamma \sigma_{xx}^0, \tag{7.8}$$

where $\kappa^2 = \eta_0 E/\beta_g D$.

If there is no boundary layer in the concentration to balance the stress term (which will always be positive) in equation (7.7), we see that $a < 0$. Therefore, a cannot be considered as directly analogous to a latent heat. This result may seem odd at first, but recall that we have now defined our total flux to include the gradient of the stress. Hence, even though the jump in the *concentration* flux may be positive at the front, the jump in the *total* flux may not be. Even if a boundary layer does exist, it is plausible to assume that there will indeed be cases where $a < 0$. Indeed, these are precisely the cases we will examine in this part of the thesis.

2. Using the Integral Method

From further examination of (7.7) it is clear that the method of similarity variables will also not work for this problem. Once again, we will need to use Boley's integral method. We begin by stating that it will not be necessary to use Boley's method to solve for the concentration or the stress in the glassy region. The truth of this statement will be demonstrated later. Therefore, we need only introduce a new quantity T^c which extends equation (7.6a) to the fully semi-infinite region.

Note that (7.6a) is a hyperbolic equation, and thus we will need to have a fictitious condition for $T_t^c(x,0)$. Due to the form of (7.7), we will also need to know the stress in the rubbery region to solve our system of equations. To solve for the stress, we note that since (3.32) and (3.33) are identical, equation (7.6a) holds for σ^{0r} as well. Then we use Boley's method with the new quantity T^σ. We denote our unknown Dirichlet conditions by the following:

$$T^c(x,0) = C_u(x), \qquad T^\sigma(x,0) = \sigma_u(x). \tag{7.9}$$

From equations (7.6b) and (7.8), we have the Neumann boundary conditions:

$$T_t^\sigma(x,0) = \frac{\kappa^2}{\gamma} C_u(x) - \sigma_u(x), \qquad T_t^c(x,0) = \gamma \sigma_u''(x). \tag{7.10}$$

We may also solve for the stress at the boundary using equation (7.6b):

$$\sigma^{0r}(0,t) = \sigma_u(0)e^{-t} + \frac{\kappa^2}{\gamma}\int_0^t C_b(z)e^{-(t-z)}\,dz. \tag{7.11}$$

Here we have imposed continuity for reasons which will differ from experiment to experiment; the reasons will be discussed in later sections.

We now extend our equations to the entire semi-infinite region, which yields the following:

$$T_{tt}^c = \kappa^2 T_{xx}^c - T_t^c, \quad 0 < x < \infty; \tag{7.12a}$$

$$T^c \equiv C^{0r}, \quad 0 < x < s(t); \tag{7.12b}$$

$$T^c(0,t) = C_b(t); \tag{7.13}$$

$$T_{tt}^\sigma = \kappa^2 T_{xx}^\sigma - T_t^\sigma, \quad 0 < x < \infty; \tag{7.14a}$$

$$T^{\sigma} \equiv \sigma^{0r}, \quad 0 < x < s(t); \tag{7.14b}$$

$$T^{\sigma}(0,t) = \sigma^{0r}(0,t); \tag{7.15}$$

$$s(0) = 0. \tag{7.16}$$

Note that we have not included any front conditions in our equations. This is because the front conditions will differ depending on whether there are boundary layers in our solution or not. These possibilities will be explored in later chapters. For now, we wish to solve only for our solution fields.

The solution of equations (7.9), (7.10), (7.12), and (7.13) can be written as $T^{c} = T^{ck} + T^{cu} + T^{cd}$, where each solution solves only one of the boundary conditions. Here T^{ck} is the part of the solution which solves only the boundary condition at $x = 0$:

$$T^{ck}_{tt} = \kappa^2 T^{ck}_{xx} - T^{ck}_{t}, \quad 0 < x < \infty; \tag{7.17}$$

$$T^{ck}(0,t) = C_b(t) - C_u(0), \qquad T^{ck}(x,0) = 0, \qquad T^{ck}_{t}(x,0) = 0. \tag{7.18}$$

Equations (7.17) and (7.18) describe the *telegraph equation*, the solution of which is given in Carrier, Krook, and Pearson [26], equation (6-64):

$$T^{ck}(x,t) = H(\kappa t - x)\left\{ \frac{x}{2} \int_{x/\kappa}^{t} e^{-z/2}[C_b(t-z) - C_u(0)] \frac{I_1(\sqrt{\kappa^2 z^2 - x^2}/2\kappa)}{\sqrt{\kappa^2 z^2 - x^2}}\, dz \right.$$

$$\left. + [C_b(t - x/\kappa) - C_u(0)]e^{-x/2\kappa} \right\}, \tag{7.19}$$

where I_1 is the first modified Bessel function. Note that equation (7.19), with $\kappa = 1$, is a correction to Cox [14], equation (3.25).

T^{cu} is the part of the solution arising from the Dirichlet initial condition, so it solves the operator in (7.17) and

$$T^{cu}(0,t) = C_u(0), \qquad T^{cu}(x,0) = C_u(x), \qquad T^{cu}_t(x,0) = 0. \tag{7.20}$$

We begin by applying the Laplace transform to equation (7.17) subject to (7.20):

$$(p^2+p)\hat{T}^{cu} - (p+1)C_u(x) = \kappa^2 \hat{T}^{cu}_{xx}, \qquad \hat{T}^{cu}(0,p) = \frac{C_u(0)}{p}. \tag{7.21}$$

Equation (7.21) is in exactly the form of equation (4.21), so we may immediately write the solution as

$$\hat{T}^{cu}(x,p) = \frac{C_u(0)e^{-x\sqrt{p(p+1)}/\kappa}}{p} + \frac{1}{2\kappa}\sqrt{\frac{p+1}{p}}\int_0^\infty C_u(z)\left[e^{-|x-z|\sqrt{p(p+1)}/\kappa} - e^{-(x+z)\sqrt{p(p+1)}/\kappa}\right] dz.$$

Inverting the Laplace transform, we have

$$T^{cu}(x,t) = C_u(x) + \kappa\int_0^t \left[C'_u(x+\kappa z) - C'_u(|x-\kappa z|)\right] g_u(z,t)\, dz, \text{ where} \tag{7.22a}$$

$$g_u(z,t) = \left[\frac{e^{-z/2}}{2} + \frac{z}{4}\int_z^t e^{-y/2}\frac{I_1(\sqrt{y^2-z^2}/2)}{\sqrt{y^2-z^2}}\, dy\right] H(t-z). \tag{7.22b}$$

Finally, T^{cd} is the part of the solution arising from the Neumann initial condition, so it solves the operator in (7.17) and

$$T^{cd}(0,t) = 0, \qquad T^{cd}(x,0) = 0, \qquad T^{cd}_t(x,0) = \gamma\sigma''_u(x). \tag{7.23}$$

Once again applying a Laplace transform to (7.17) subject to (7.23), we have

$$(p^2+p)\hat{T}^{cd} - \gamma\sigma_u''(x) = \kappa^2\hat{T}^{cd}_{xx}, \qquad \hat{T}^{cd}(0,p) = 0. \tag{7.24}$$

Equation (7.24) is also in the form of (4.21), so we may write

$$\hat{T}^{cd}(x,p) = \frac{1}{2\kappa\sqrt{p(p+1)}} \int_0^\infty \gamma\sigma_u''(x) \left[e^{-|x-z|\sqrt{p(p+1)}/\kappa} - e^{-(x+z)\sqrt{p(p+1)}/\kappa} \right] dz.$$

Inverting the Laplace transform, we have

$$T^{cd}(x,t) = \begin{cases} \dfrac{\gamma e^{-t/2}}{2\kappa} \displaystyle\int_{x-\kappa t}^{x+\kappa t} \sigma_u''(z) g_d(x-z,t)\, dz, & x > \kappa t; \\ \dfrac{\gamma e^{-t/2}}{2\kappa} \left[\displaystyle\int_0^{x+\kappa t} \sigma_u''(z) g_d(x-z,t)\, dz \right. & \\ \qquad \left. - \displaystyle\int_0^{\kappa t - x} \sigma_u''(z) g_d(x+z,t)\, dz \right], & x < \kappa t, \text{ where} \end{cases} \tag{7.25a}$$

$$g_d(y,t) = I_0(\sqrt{\kappa^2 t^2 - y^2}/2\kappa). \tag{7.25b}$$

Note that with the exception of T^{ck} all our solutions are continuous across the line $x = \kappa t$.

Similarly, the solution of equations (7.9)-(7.11), (7.14), and (7.15) is $T^\sigma = T^{\sigma k} H(\kappa t - x) + T^{\sigma u} + T^{\sigma d}$, where

$$T^{\sigma k}(x,t) = \frac{x}{2} \int_{x/\kappa}^t e^{-z/2} [T^\sigma(0,t-z) - \sigma_u(0)] \frac{I_1(\sqrt{\kappa^2 z^2 - x^2}/2\kappa)}{\sqrt{\kappa^2 z^2 - x^2}}\, dz$$

$$+ [T^\sigma(0,t-x/\kappa) - \sigma_u(0)] e^{-x/2\kappa}; \tag{7.26}$$

$$T^{\sigma u}(x,t) = \sigma_u(x) + \kappa \int_0^t [\sigma_u'(x+\kappa z) - \sigma_u'(|x-\kappa z|)]\, g_u(z,t)\, dz; \tag{7.27}$$

$$T^{\sigma d}(x,t) = \begin{cases} \dfrac{e^{-t/2}}{2\kappa} \displaystyle\int_{x-\kappa t}^{x+\kappa t} \left[\frac{\kappa^2}{\gamma} C_u(z) - \sigma_u(z)\right] g_d(x-z,t)\,dz, & x > \kappa t; \\ \dfrac{e^{-t/2}}{2\kappa} \left\{ \displaystyle\int_0^{x+\kappa t} \left[\frac{\kappa^2}{\gamma} C_u(z) - \sigma_u(z)\right] g_d(x-z,t)\,dz \right. & \\ \qquad \left. - \displaystyle\int_0^{\kappa t - x} \left[\frac{\kappa^2}{\gamma} C_u(z) - \sigma_u(z)\right] g_d(x+z,t)\,dz \right\}, & x < \kappa t. \end{cases} \tag{7.28}$$

Now that we have the representations for our solutions, in the next two chapters we will select particular boundary conditions and parameter ranges for two specific problems.

Chapter VIII: The Dissolving Polymer

1. Governing Equations

We now wish to model a polymer entanglement network dissolving in the presence of a solvent. Here C is the concentration of the solvent. Imagine an experiment in which a polymer matrix is exposed to a infinite well of diluent. Though the concentration of the diluent may be 1 at the edge of the polymer matrix, it is clear that at the *instant* that we introduce the polymer into the solvent, the concentration can be no greater than C_*, which is now defined as that concentration at which the entanglement network dissolves. We would expect that the maximal concentration of the diluent at the boundary will be achieved only in the mathematical limit $t \to \infty$. This motivates our boundary condition

$$C(0^+, t) = C_b(t) = 1 - (1 - C_*)e^{-rt}, \tag{8.1}$$

where r is a constant.

We also choose to model this experiment by the *state-dependent* case, where $\tilde{t}_0 = 0$. This reflects the case where some other physical parameter, such as temperature, density, or pressure, affects whether the polymer has a memory. Here we postulate the memory "turns on" when the polymer is first plunged into the diluent. In this case, the stress must be 0 initially *by definition*, so we have

$$\sigma_i(x) \equiv 0, \qquad \sigma_u(x) \equiv 0. \tag{8.2}$$

Equations (8.1) and (8.2) imply that

$$\sigma^{0r}(0,t) = \frac{\kappa^2}{\gamma}\left[1 - e^{-t} + \frac{1-C_*}{1-r}(e^{-t} - e^{-rt})\right]. \tag{8.3}$$

Here we have assumed that $r \neq 1$. A solution still exists for $r = 1$, but the algebra is messier. We have assumed continuity of the stress, which follows trivially from the fact that $\tilde{t}_0 = 0$. In this section we will derive the interesting result that r is actually determined by the material properties of the matrix. Thus, there is actually a *self-regulating mass uptake* at the boundary.

In this problem, we expect that the dominant mechanism by which the front moves is the release of stress accumulated in the entanglement network. As the polymer dissolves, the stress is reduced, which forces the front forward. Hence, we expect $[\sigma_x]_s < 0$; in fact, we expect $[\sigma_x]_s$ to be so negative that $a < 0$. In addition, for reasons that will become later we wish to restrict a to the following range:

$$-1 \leq a \leq -C_*. \tag{8.4}$$

We begin by examining equation (7.5a). Since this is a hyperbolic equation and our initial condition is $C^{0g}(x,0) = C_t^{0g}(x,0) = 0$, we see that for $x > \kappa t$ the solution is exactly 0, unless there is a boundary layer in that region. It will be shown that our choice of a in (8.4) precludes a boundary layer in this region. The case of a boundary layer for $x > \kappa t$ will be covered in Chapter IX. Hence, we expect there to be a discontinuity around the line $x = \kappa t$. For a first guess, we assume that $C(\kappa t^-, t) > C_*$. This means that our glass-rubber interface lies in the boundary layer around $x = \kappa t$. Thus, we introduce the following scalings:

$$\zeta = \frac{x - s(t)}{\epsilon^m}, \quad \tau = t, \quad \frac{\partial}{\partial x} = \epsilon^{-m}\frac{\partial}{\partial \zeta}, \quad \frac{\partial}{\partial t} = \frac{\partial}{\partial \tau} - \dot{s}\epsilon^{-m}\frac{\partial}{\partial \zeta}, \tag{8.5a}$$

$$C^g(x,t) = C^{0+}(\zeta,\tau) + o(1), \quad \sigma^g(x,t) = \sigma^{0+}(\zeta,\tau) + o(1), \tag{8.5b}$$

where the dot now indicates differentiation with respect to τ. Then equations (7.1) become the following, to leading orders:

$$-2\dot{s}\epsilon^{-m}C^{0+}_{\zeta\tau} + \epsilon^{-2m}\dot{s}^2 C^{0+}_{\zeta\zeta} = -\alpha\dot{s}\epsilon^{1-3m}C^{0+}_{\zeta\zeta\zeta} + \epsilon^{-2m}(\kappa^2+\epsilon)C^{0+}_{\zeta\zeta}, \tag{8.6a}$$

$$-\dot{s}\epsilon^{-m}\sigma^{0+}_{\zeta} + \epsilon\sigma^{0+} = \frac{\eta_0\epsilon^{-1}}{\nu\beta_g}C^{0+} - \kappa\epsilon^{-m}C^{0+}_{\zeta}. \tag{8.6b}$$

We note that if $\dot{s} = \kappa$, then the ϵ^{-2m} terms cancel, leaving the dominant balance as $m = 1/2$. However, from equations (8.5a) and (8.6b) we see that both C^{0+}_x and σ^{0+} are $O(\epsilon^{-1/2})$, which means that there is nothing to balance the right-hand side of equation (7.3). Hence we conclude that our scaling is wrong.

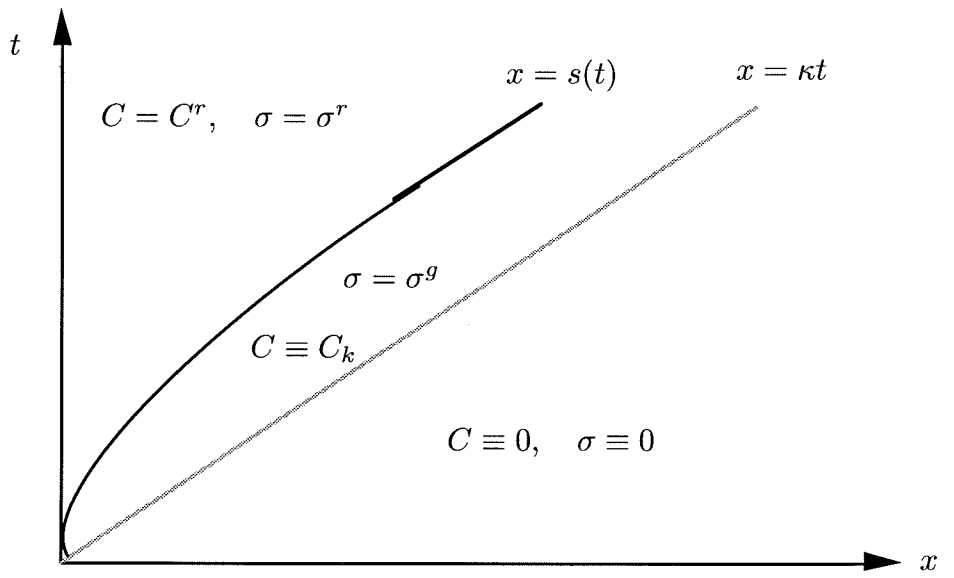

Figure 8a. Regions of validity for different outer representations.

Now we have already determined that there must be a discontinuity at $x = \kappa t$. Therefore, we will call the line $x = \kappa t$ the *primary front*, the word primary referring to the fact that it is the first signal to reach a certain point. We define the

secondary front $x = s(t)$ to be the curve where the network is completely dissolved. Mathematically, the secondary front is given by (3.28). It is clear that $s(t) < \kappa t$ for all t. We see from equation (7.5a) that characteristics carry some constant value $C = C_k$ forward with speed κ, so there must exist a "mushy region" $s(t) < x < \kappa t$ where $C \equiv C_k$. This is illustrated in figure 8a.

In order to determine C_k, we see if there can be a boundary layer in C^{0g} around our secondary front. Since $\dot{s} \neq \kappa$, we see that the $O(\epsilon^{-2m})$ terms do not cancel in (8.6a) and that $m = 1$. Therefore, we have

$$\dot{s}^2 C^{0+}_{\zeta\zeta} = -\alpha \dot{s} C^{0+}_{\zeta\zeta\zeta} + \kappa^2 C^{0+}_{\zeta\zeta},$$

the solution of which is

$$C^{0+}(\zeta, \tau) = f_0(\tau) + f_1(\tau)\zeta + f_2(\tau) \exp\left[\frac{(\kappa^2 - \dot{s}^2)\zeta}{\alpha \dot{s}}\right]. \tag{8.7}$$

However, since $\dot{s} < \kappa$, we see that in the matching region $\zeta \to \infty$, equation (8.7) becomes transcendentally large. Thus there is no layer in C^{0g} and $C_k = C_*$.

Our next step is to retain the smoothing internal layer around $x = \kappa t$, since equation (7.1a) cannot support a discontinuity there. Hence, we use equation (8.6a) with our choice of $m = 1/2$:

$$-2C^{0+}_{\zeta\tau} = -\alpha C^{0+}_{\zeta\zeta\zeta} \tag{8.8a}$$

with the initial condition

$$C^{0+}(\zeta, 0) = C_* H(-\zeta). \tag{8.8b}$$

Equation (8.8a) is simply the heat equation on an unbounded interval, the solution of which is, subject to (8.8b),

$$C^{0+}(\zeta,\tau) = \frac{C_*}{2}\operatorname{erfc}\left(\frac{\zeta}{\sqrt{2\alpha\tau}}\right). \tag{8.9}$$

Next we solve for σ. Using equation (7.5b) in the region where $x > \kappa t$, and recalling our new initial condition (8.2), we see that $\sigma^g \equiv 0$ there as well. In the mushy region, we may immediately solve (7.5b) to yield

$$\sigma^{0g}(x,t) = \frac{\kappa^2 C_*}{\gamma}\left(t - \frac{x}{\kappa}\right). \tag{8.10}$$

Hence, in order for σ^{0g} stay bounded (which is what we expect both on physical and mathematical grounds), we see that

$$s(t) \sim \kappa t - s_\infty + s_1(t) \text{ as } t \to \infty, \tag{8.11}$$

where $s_\infty \geq 0$ and $s_1(t) \to 0$ as $t \to \infty$. Using equation (8.10) evaluated at our secondary front, we see that equation (7.7) becomes

$$\alpha\epsilon\left[C_x\right]_s - \frac{\kappa^2 C_*}{\dot{s}}\left[t - \frac{s(t)}{\kappa}\right] = a\dot{s}. \tag{8.12}$$

Next we consider the possibility of a layer in C^{0r} around our secondary front. Performing the same analysis as that prior to (8.7), we see that if we let $C^r(x,t) = C^{0-}(\zeta,\tau) + o(1)$, equation (8.7) is a representation for C^{0-} which is bounded in the matching region $\zeta \to -\infty$. Matching and using (3.28), we have

$$C^{0-}(\zeta,\tau) = C^{0r}(s(\tau),\tau) + \left[C_* - C^{0r}(s(\tau),\tau)\right]\exp\left[\frac{(\kappa^2 - \dot{s}^2)\zeta}{\alpha\dot{s}}\right]. \tag{8.13}$$

Now let $\sigma^r(x,t) = \epsilon^{-1}\sigma^{0-}(\zeta,\tau) + o(\epsilon^{-1})$. Note $\sigma^{0-}(s(t),t) \neq 0$ since we are matching to equation (8.10). Using our scalings (8.5a) with $m = 1$ in (7.2b), we have

$$-\dot{s}\epsilon^{-1}\sigma_\zeta^{0-} + \sigma^{0-} = \frac{\kappa^2}{\gamma}C^{0-} - \kappa C_\zeta^{0-}.$$

Thus there is no boundary layer in σ^{0r} and one of our front conditions for Boley's method is

$$T^\sigma(s(t),t) = \frac{\kappa^2 C_*}{\gamma}\left[t - \frac{s(t)}{\kappa}\right]. \tag{8.14}$$

In addition, we must solve *one* of the following two sets of conditions. If there is no boundary layer in C^{0r}, equation (8.12) becomes

$$\kappa^2 C_*\left[t - \frac{s(t)}{\kappa}\right] = |a|\dot{s}^2. \tag{8.15a}$$

In addition, we have from (3.28) that

$$T^c(s(t),t) = C_*. \tag{8.15b}$$

However, if we do have a boundary layer, equation (8.12) becomes

$$-\alpha C_\zeta^{0-} - \kappa^2 C_*\left[t - \frac{s(t)}{\kappa}\right] = a\dot{s}.$$

Using equation (8.13), we have

$$\left[C^{0r}(s(t),t) - C_*\right](\kappa^2 - \dot{s}^2) - \kappa^2 C_*\left[t - \frac{s(t)}{\kappa}\right] = a\dot{s}^2. \tag{8.16}$$

Note there is no condition analogous to (8.15b).

Now we have completed enumerating our front conditions. In the next section, we will perform asymptotic analyses for small and large time to obtain solution profiles.

2. Large Time Asymptotics

Now we perform asymptotic estimates for large t. In order to complete our solution, it will be necessary to do large-time asymptotics for the following integral, the form for which is inspired by (7.28):

$$F(t) = \int_0^{s+\kappa t} f(z) I_0(\sqrt{\kappa^2 t^2 - (s-z)^2}/2\kappa)\, dz, \tag{8.17}$$

where $s = \kappa t - s_\infty$ and s_∞ is a constant. This form for $s(t)$ is motivated by equation (8.11). From AMS 55 [27], $I_n(z)$ is $O(1)$ for moderate values of z, but diverges for $z \to \infty$ large as

$$I_n(z) \sim \frac{e^z}{\sqrt{2\pi z}} \left(1 - \frac{4n^2 - 1}{8z}\right). \tag{8.18}$$

Hence the dominant contribution to $F(t)$ comes from the neighborhood of $z = s$. In this region, the argument of the Bessel function is $O(t)$. Outside this neighborhood, the argument of the Bessel function is $O(t^{1/2})$. Therefore, we may approximate $F(t)$ by the following:

$$F(t) \sim \kappa \sqrt{\frac{t}{\pi}} \int_{1-\delta}^{1+\delta} \frac{f(\kappa t y)}{(2y - y^2)^{1/4}} \exp\left[\frac{t}{2}\sqrt{2y - y^2}\right] dz, \tag{8.19}$$

where $y = z/\kappa t$ and we have neglected the terms with s_∞ in them.

We now wish to use Laplace's method on (8.19). From Bender and Orszag [28] (6.4.35), we have a general expression for a Laplace integral:

$$\int_{A_-}^{A_+} f(y)e^{t\phi(y)}\,dz \sim \sqrt{\frac{2\pi}{-t\phi''(c)}}e^{t\phi(c)}\left\{f(c)+\frac{1}{t}\left[-\frac{f''(c)}{2\phi''(c)}+\frac{f(c)\phi^{(4)}(c)}{8[\phi''(c)]^2}\right.\right.$$

$$\left.\left.+\frac{f'(c)\phi^{(3)}(c)}{2[\phi''(c)]^2}-\frac{5[\phi^{(3)}(c)]^2 f(c)}{24[\phi''(c)]^3}\right]\right\}, \quad t\to\infty, \tag{8.20}$$

where $\phi'(c)=0$. Using Laplace's method on (8.19) to leading order, we have

$$F(t) \sim 2\kappa f(\kappa t)e^{t/2}. \tag{8.21}$$

We note that since $\sigma_u(x)\equiv 0$, $T^{\sigma u}\equiv 0$. We also note that $T^{\sigma k}$ is exponentially decaying. Therefore, the dominant contribution to the stress is from (7.28). Using our form for $\sigma_u(x)$, we then have

$$T^{\sigma}(s(t),t) \sim \frac{e^{-t/2}}{2\kappa}\left\{2\kappa\left[\frac{\kappa^2}{\gamma}C_u(\kappa t)\right]e^{t/2}\right\}. \tag{8.22}$$

Using (8.22) and our assumption for $s(t)$ in (8.14), we have

$$\frac{\kappa^2}{\gamma}C_u(\kappa t) \sim \frac{\kappa^2 C_*}{\gamma}\left[t-\frac{\kappa t - s_\infty}{\kappa}\right]. \tag{8.23}$$

In order to construct our solutions for long time, we postulate the following expansion:

$$C_u(x) \sim C_\infty + o(1), \quad x\to\infty. \tag{8.24}$$

Using equation (8.24) in (8.23), we have

$$\frac{\kappa^2}{\gamma}C_\infty \sim \frac{\kappa C_* s_\infty}{\gamma},$$

$$C_\infty \sim \frac{C_* s_\infty}{\kappa}, \qquad \sigma^{0r}(s(t),t) \sim \frac{\kappa C_* s_\infty}{\gamma}. \tag{8.25}$$

Next we examine the concentration for large time. We note that in this case, $T^{cd} \equiv 0$ and T^{ck} is exponentially decaying. Therefore, we have

$$T^c(s,t) \sim C_u(\kappa t).$$

Using (8.25), we have

$$T^c(s,t) \sim \frac{C_* s_\infty}{\kappa}. \tag{8.26}$$

If there is no boundary layer, then we immediately have from (8.15b) that $s_\infty = \kappa$. However, with no boundary layer, we also must satisfy equation (8.15a), which becomes

$$-\frac{\kappa C_* s_\infty}{\kappa} = a\kappa.$$

Since $s_\infty = \kappa$, we have $C_* = |a|$. However, each of these parameters is supposed to be independent. Hence, we conclude that there must be a boundary layer unless we are in a very special case.

If we have a boundary layer, then we use equation (8.16), which becomes

$$-C_* \left(1 - \frac{s_\infty}{\kappa}\right)(\kappa^2 - \dot{s}^2) - \kappa C_* s_\infty = a\kappa^2,$$

$$s_\infty = \frac{|a|\kappa}{C_*}, \qquad C^{0r}(s(t),t) \sim |a|. \tag{8.27}$$

Then we see that from $C_* \leq C^{0r} \leq 1$ we have our compatibility condition (8.4). Physically, we see that if the absolute jump in flux needed to move the front is too small, the front will try to move faster than κt, but cannot since the boundary layer

solution does not hold. In addition, we see that if the absolute jump in the flux needed is larger than the saturation concentration (in some appropriate nondimensionalization), the front cannot move at all. We interpret this as a deficiency in our model which reflects a physical phenomenon, in the same way that the fact that the Fickian model is unstable for negative diffusion coefficients is indicative of the fact that negative diffusion coefficients are not physically reasonable.

Summarizing our results, we have the following:

$$C^{0g}(x,t) = \frac{C_*}{2}\operatorname{erfc}\left(\frac{x-\kappa t}{\sqrt{2\alpha\epsilon t}}\right), \tag{8.28a}$$

$$\sigma^{0g}(x,t) = \frac{\kappa^2 C_*}{\gamma}\left(t - \frac{x}{\kappa}\right) H(\kappa t - x), \tag{8.28b}$$

$$C^{0r}(x,t) = T^c(x,t) + [C_* - T^c(s(t),t)]\exp\left\{\frac{(\kappa^2 - \dot{s}^2)[x-s(t)]}{\alpha\epsilon\dot{s}}\right\}, \tag{8.28c}$$

$$t \to \infty, \quad 0 \ll x < \kappa t$$

$$s(t) \sim \kappa t - \frac{|a|\kappa}{C_*}, \tag{8.29a}$$

$$T^c(x,t) \sim |a| + \left[1 - (1-C_*)e^{-r(t-x/\kappa)}\right] e^{-x/2\kappa}$$

$$+ \frac{x}{2}\int_{x/\kappa}^{t} e^{-z/2}\left[1 - (1-C_*)e^{-r(t-z)}\right] \frac{I_1(\sqrt{\kappa^2 z^2 - x^2}/2\kappa)}{\sqrt{\kappa^2 z^2 - x^2}}\, dz, \tag{8.29b}$$

$$\sigma^{0r}(x,t) \sim \frac{x}{2}\int_{x/\kappa}^{t} e^{-z/2} T^\sigma(0,t-z) \frac{I_1(\sqrt{\kappa^2 z^2 - x^2}/2\kappa)}{\sqrt{\kappa^2 z^2 - x^2}}\, dz + T^\sigma(0,t-x/\kappa)e^{-x/2\kappa}$$

$$+ \frac{\kappa|a|e^{-t/2}}{2\gamma}\int_{-\kappa t}^{\kappa t} g_d(z,t)\, dz. \tag{8.29c}$$

Figure 8b shows our large-time asymptotic expansion of C for a selected set of parameter values which satisfies (8.4). Though not quite so pronounced for $t = 6$, we see the three-stage concentration profile we predicted. The concentration profile starts out at 0, rises quickly to C_* at the primary front, remains at C_* in the mushy region, which for large time is of constant finite width, rises quickly to $|a|$ at $s(t)$, and then slowly rises for $x < s(t)$. Since these concentration profiles are only good for $x \to \infty$, we see that they rise above 1. We would then expect the true concentration profile to depart from our long-time asymptotics and converge to 1 at $x = 0$.

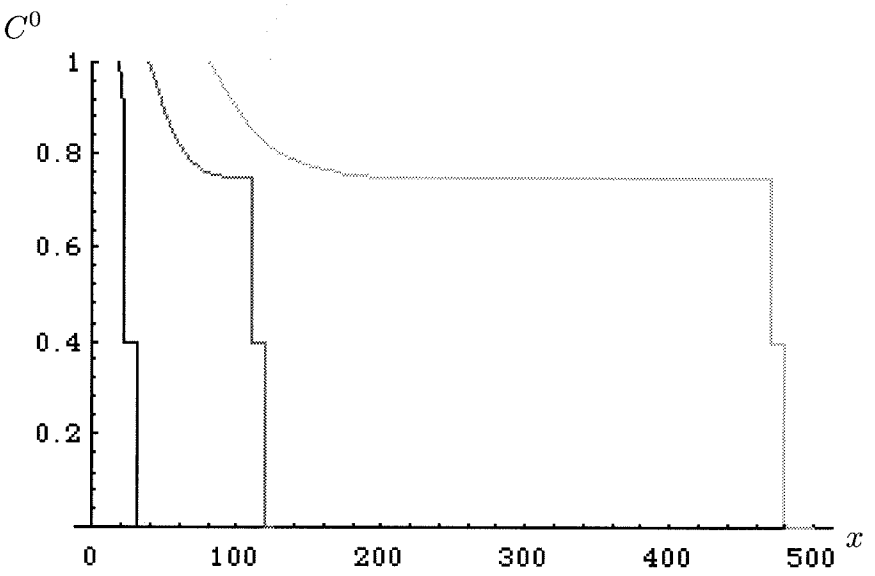

Figure 8b. Concentration profiles: $a = -0.75$, $C_* = 0.4$, $\gamma = 2$, $\alpha = 3$, $\epsilon = 0.0001$, $\kappa = 5$. In decreasing order of darkness: $t = 6$, 24, 96.

Figure 8c shows our large-time asymptotic expansion of σ for the same parameters and times. The gap for $t = 6$ is due to the fact that we are graphing analytical asymptotic expansions. Once again, we see that the asymptotic expansions do not hold for x near 0; straight lines have been drawn to indicate the value of $\sigma^0(0, t)$ for the times indicated. Note the steep rise of σ over the relatively small scale of

the mushy region. It may seem as if there is a discontinuity in σ_x at the primary front, but this is not the case. Since there exists a boundary layer in C across the primary front, there exists a boundary layer in σ_x^0 as well. Thus, though the derivative changes rapidly, there is no discontinuity. Note also that in this case there is no peak in σ, but that the rise in σ is much slower once the polymer entaglement network has begun to dissolve. It also difficult to ascertain the position of the secondary front from this graph. That is because σ_x^0 is nearly identical on both sides of that front.

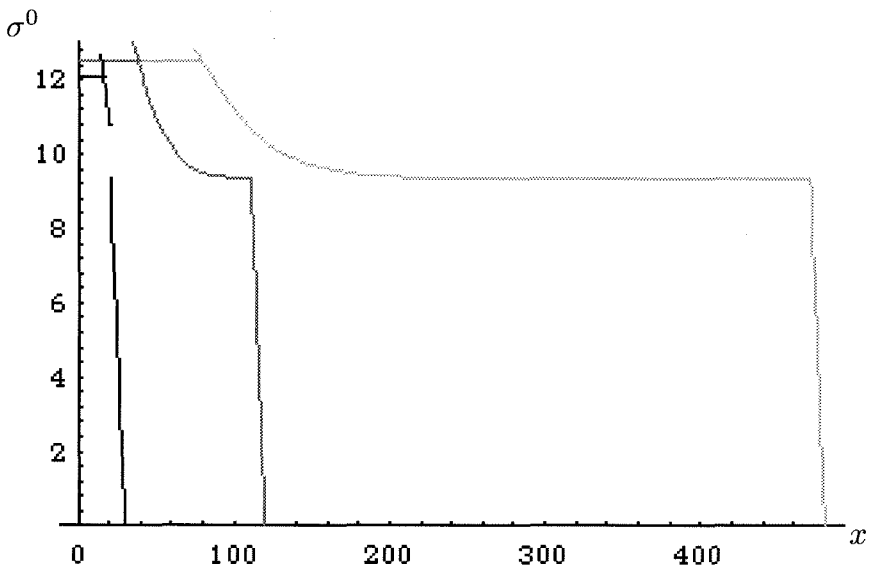

Figure 8c. Stress profiles: $a = -0.75$, $C_* = 0.4$, $\gamma = 2$, $\alpha = 3$, $\epsilon = 0.0001$, $\kappa = 5$. In decreasing order of darkness: $t = 6$, 24, 96.

3. Small Time Asymptotics

Now we construct our asymptotic solutions for small t. We postulate the fol-

lowing expression for our ficititious initial condition as $x \to 0$:

$$C_u(x) \sim C_0 + C_1 x + \frac{C_2 x^2}{2} + \cdots. \tag{8.29}$$

We then perform small-time asymptotics on equations (7.26) and (7.28) (recalling that $T^{\sigma u} \equiv 0$), keeping only those terms that are $O(1)$, $O(t)$, $O(x)$, $O(t^2)$, $O(xt)$, and $O(t^3)$. Note that by keeping only these terms we are making an implicit assumption that $s(t) = o(t^{3/2})$. We will verify this assumption shortly.

Since the value of the bracketed quantity in the integral in $T^{\sigma k}$ near 0 is 0, $T^{\sigma k}$ doesn't contribute since its terms are all $o(xt)$. To expand $T^{\sigma d}$, we first construct a Taylor series in x. For some arbitrary function $f(z)$, we have

$$F_\pm(x,t) \equiv \int_0^{\kappa t \pm x} f(z) g_d(x \mp z, t)\, dz,$$

$$F_\pm(x,t) \sim \int_0^{\kappa t} f(z) g_d(z,t) \pm x \left[f(\kappa t) I_0(0) + \int_0^{\kappa t} f(z) \frac{z I_1(\sqrt{\kappa^2 - z^2}/2\kappa)}{2\kappa\sqrt{\kappa^2 - z^2}}\, dz \right].$$

Using our expressions for $C_u(x)$ and $\sigma_u(x)$, we have

$$F_+(x,t) - F_-(x,t) \sim 2x \left\{ C_0 + \kappa t C_1 + t \left[\frac{t C_u(\kappa t)}{2} \lim_{z \to \kappa t} \frac{I_1(\sqrt{\kappa^2 - z^2}/2\kappa)}{\sqrt{\kappa^2 - z^2}} \right]_{t=0} \right\}$$

$$\sim 2xC_0 + 2\kappa x t C_1.$$

Therefore, we have

$$T^{\sigma d} \sim \frac{\kappa x}{\gamma} C_0 + \frac{\kappa x t}{\gamma} \left(\kappa C_1 - \frac{C_0}{2} \right). \tag{8.30}$$

We expand (8.3) for small t and x to yield

$$T^{\sigma}(0,t-x/\kappa) \sim \frac{C_*\kappa^2}{\gamma}\left(t-\frac{x}{\kappa}\right)+\frac{\kappa^2 t}{\gamma}[(1-C_*)(1+r)-1]\left(\frac{t}{2}-\frac{x}{\kappa}\right)$$

$$+\frac{\kappa^2[(1-C_*)(1+r+r^2)-1]t^3}{6\gamma},$$

$$T^{\sigma}(0,t-x/\kappa)e^{-x/2\kappa} \sim \frac{C_*\kappa^2}{\gamma}\left(t-\frac{x}{\kappa}\right)+\frac{\kappa^2 t^2[r(1-C_*)-C_*]}{2\gamma}$$

$$-\frac{\kappa x t}{\gamma}\left[r(1-C_*)-\frac{C_*}{2}\right]-\frac{\kappa^2[r(1-C_*)(1+r)-C_*]t^3}{6\gamma}. \tag{8.31}$$

Using (8.30) and (8.31) in (8.14), we have the following:

$$\frac{\kappa^2 C_*}{\gamma}\left(t-\frac{s}{\kappa}\right)=\frac{C_*\kappa^2}{\gamma}\left(t-\frac{s}{\kappa}\right)-st\left[r(1-C_*)+\frac{C_0-C_*}{2}-\kappa C_1\right]$$

$$+\frac{\kappa t^2[r(1-C_*)-C_*]}{2}-\frac{\kappa[r(1-C_*)(1+r)-C_*]t^3}{6}+sC_0. \tag{8.32}$$

It is clear that the first terms on each side cancel.

We now expand our concentration field for small time. In this expansion, we keep only those terms which are $O(1)$, $O(t)$, $O(x)$, and $O(t^2)$. (Note that our assumption about $s(t)$ is now slightly weaker.) We know that the integral in $T^{ck} = o(xt)$. It can be shown that the integral in T^{cu} is $O(xt)$, and we know that $T^{cd} \equiv 0$, so we are only left with expanding

$$\left[1-C_u(0)-(1-C_*)e^{-r(t-x/\kappa)}\right]e^{-x/2\kappa}$$

$$\sim C_*-C_0+rt(1-C_*)-\frac{x}{\kappa}\left[r(1-C_*)+\frac{C_*-C_0}{2}\right]-\frac{(1-C_*)r^2t^2}{2}.$$

Once we add on $C_u(x)$, our final expression is

$$T^c(x,t) \sim C_* + tr(1-C_*) + \frac{x}{\kappa}\left[\kappa C_1 - r(1-C_*) + \frac{C_0 - C_*}{2}\right] - \frac{r^2t^2}{2}(1-C_*). \quad (8.33)$$

Now we use equation (8.33) in our boundary condition (8.16). Letting $s = s_0 t^n$, we have (to leading orders)

$$\left\{tr(1-C_*) + \frac{s_0 t^n}{\kappa}\left[\kappa C_1 - r(1-C_*) + \frac{C_0 - C_*}{2}\right] - \frac{r^2t^2(1-C_*)}{2}\right\} \times$$
$$(\kappa^2 - n^2 s_0^2 t^{2n-2}) - \kappa^2 C_* \left[t - \frac{s_0 t^n}{\kappa}\right] = an^2 s_0^2 t^{2n-2}. \quad (8.34)$$

Now we must strike a balance among the $O(t)$, $O(t^n)$, and $O(t^{2n-2})$ terms. The first obvious balance is $n = 3/2$, which balances the right-hand side with the $O(t)$ terms. However, note how this assumption will affect (8.32). In order to balance the t^2 term therein, we would have to introduce an $x^{4/3}$ term in our expression for $C_u(x)$. However, we expect our functional forms will be everywhere twice differentiable, which $x^{4/3}$ is not. Therefore we conclude that $n \neq 3/2$.

Thus, the $O(t)$ terms must balance one another. This can only happen if

$$r(1-C_*) = C_*. \quad (8.35)$$

What does this mathematical constraint mean physically? It says that in order for our dissolution front to propagate, the concentration at the interface between the polymer and the reservoir must be regulated *by the polymer network itself.* Thus r in some sense represents the internal dissolution rate of the polymer and could be related to the strength of the entanglement network.

Using (8.35), the next orders in (8.34) become the following:

$$s_0\kappa t^n\left[\kappa C_1 - C_* + \frac{C_0 - C_*}{2}\right] - \frac{\kappa^2 C_*^2 t^2}{2(1-C_*)} + \kappa C_* s_0 t^n = an^2 s_0^2 t^{2n-2}. \tag{8.36}$$

from which we have that $n = 2$. Therefore, our supposition above that $s(t) = o(t^{3/2})$ is correct. Using (8.35) in (8.32), we have

$$st\left(\kappa C_1 - \frac{C_0 + C_*}{2}\right) - \frac{\kappa r C_* t^3}{6} + sC_0 = 0.$$

So we may conclude that $C_0 = 0$, and we have

$$s_0\left(\kappa C_1 - \frac{C_*}{2}\right) - \frac{\kappa C_*^2}{6(1-C_*)} = 0. \tag{8.37}$$

Using the fact that $C_0 = 0$ and $n = 2$ in (8.36), we have

$$s_0\kappa\left(\kappa C_1 - \frac{3C_*}{2}\right) + s_0\kappa C_* - \frac{\kappa^2 C_*^2}{2(1-C_*)} = 4as_0^2. \tag{8.38}$$

Using (8.37) in (8.38), we have that

$$s_0 = \frac{\kappa C_*}{2\sqrt{3|a|(1-C_*)}}. \tag{8.39}$$

Using (8.39) in (8.37), we have

$$C_1 = \frac{C_*}{\kappa}\left[\frac{1}{2} + \sqrt{\frac{|a|}{3(1-C_*)}}\right]. \tag{8.40}$$

Note that (8.40) gives us that C_1 is positive, as we expect. This means that our fictitious initial condition starts off with zero and a positive slope, so it is reasonable to conclude that it remains positive.

Summarizing our results, we have the following:

$$t \to 0$$

$$s(t) \sim \frac{\kappa C_* t^2}{2\sqrt{3|a|(1-C_*)}}, \qquad r = \frac{C_*}{1-C_*}, \tag{8.41a}$$

$$T^c(x,t) \sim \frac{C_* x}{\kappa}\left[\frac{1}{2} + \sqrt{\frac{|a|}{3(1-C_*)}}\right] + \left[1-(1-C_*)e^{-r(t-x/\kappa)}\right] e^{-x/2\kappa}$$

$$+ \frac{x}{2}\int_{x/\kappa}^{t} e^{-z/2}\left[1-(1-C_*)e^{-r(t-z)}\right] \frac{I_1(\sqrt{\kappa^2 z^2 - x^2}/2\kappa)}{\sqrt{\kappa^2 z^2 - x^2}}\, dz, \tag{8.41b}$$

$$\sigma^{0r}(x,t) \sim \frac{x}{2}\int_{x/\kappa}^{t} e^{-z/2} T^\sigma(0,t-z) \frac{I_1(\sqrt{\kappa^2 z^2 - x^2}/2\kappa)}{\sqrt{\kappa^2 z^2 - x^2}}\, dz + T^\sigma(0,t-x/\kappa)e^{-x/2\kappa}$$

$$+ \frac{C_* e^{-t/2}}{2\gamma}\left[\frac{1}{2} + \sqrt{\frac{|a|}{3(1-C_*)}}\right] \times$$

$$\left[\int_0^{x+\kappa t} z g_d(x-z,t)\, dz - \int_0^{\kappa t - x} z g_d(x+z,t)\, dz\right]. \tag{8.41c}$$

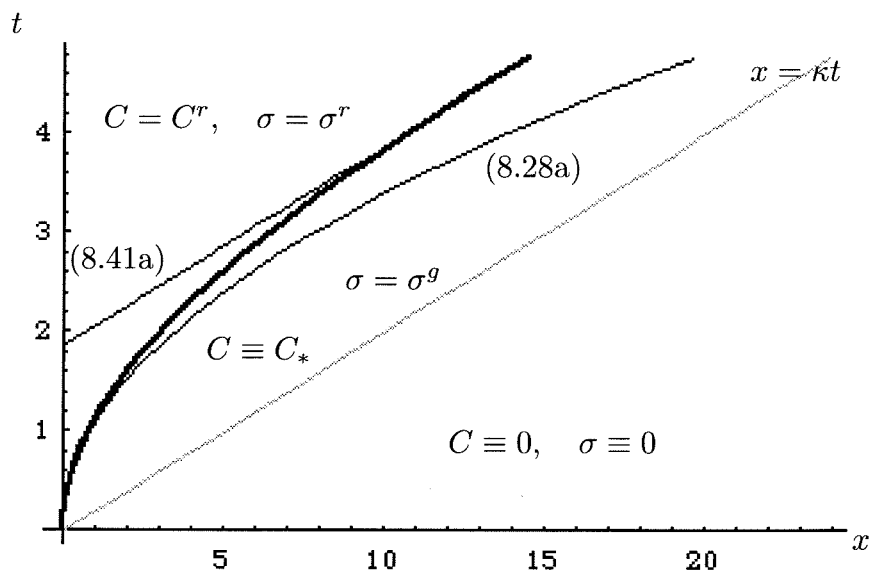

Figure 8d. Front diagram with superimposed asymptotic expansions.

$a = -0.75$, $C_* = 0.4$, $\gamma = 2$, $\alpha = 3$, $\epsilon = 0.0001$, $\kappa = 5$.

Figure 8d shows a plot of our superimposed asymptotic expansions for the listed set of parameter values. The grey line is the primary front. The narrow lines are the graphs of our actual asymptoic expansions (8.28a) and (8.41a), while the thicker line is simply a sketch of the way the actual front would interpolate between these two expansions. Note that there are several important results here from an experimental point of view. By simply performing the experiment heretofore outlined, one can determine κ (from the front speed), C_* (from the concentration in the mushy region), and a (from the width of the mushy region).

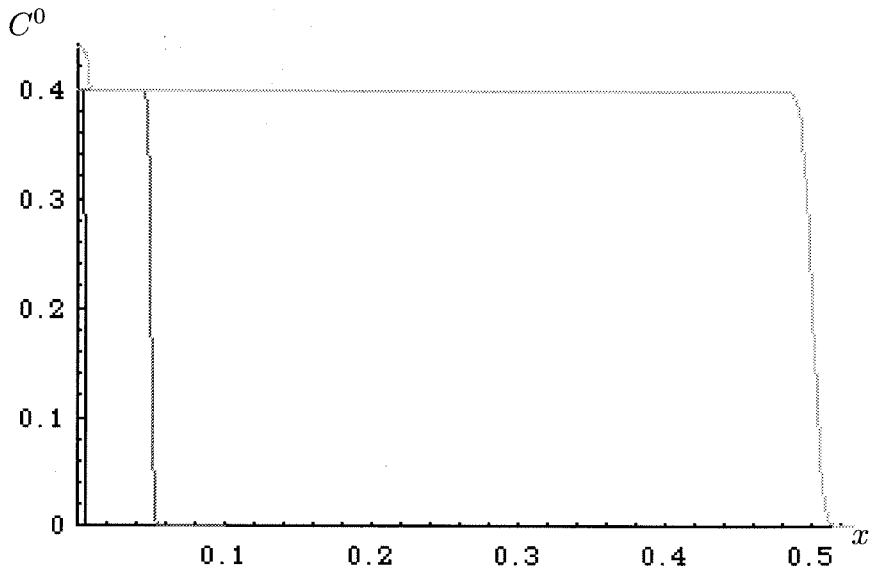

Figure 8e. Concentration profiles: $a = -0.75$, $C_* = 0.4$, $\gamma = 2$, $\alpha = 3$, $\epsilon = 0.0001$, $\kappa = 5$. In decreasing order of darkness: $t = 0.001$, 0.01, 0.1.

Figure 8e shows a graph of C for smal times. Note that we have made sure that $\epsilon = o(t)$ for all graphed values. While difficult to ascertain from the graph for $t = 0.001$, it is clear from the other graphs that we have once again reproduced our three-stage process. The concentration starts out at 0, then rises quickly to C_* at the primary front. C remains at C_* in the mushy region (which for t small is a much larger relative area), and then slowly rises for $x < s(t)$.

Figure 8f shows a graph of σ for the same times and parameter values. The graph for $t = 0.001$ can only be ascertained as an extra pixel in the lower left-hand corner of the graph; the stress is that small for small time. Note that we have linear growth in the mushy region, which now encompasses nearly the entire graph. Note that it is once again difficult to ascertain the position of the secondary front from these graphs because of the small discontinuity in σ_x.

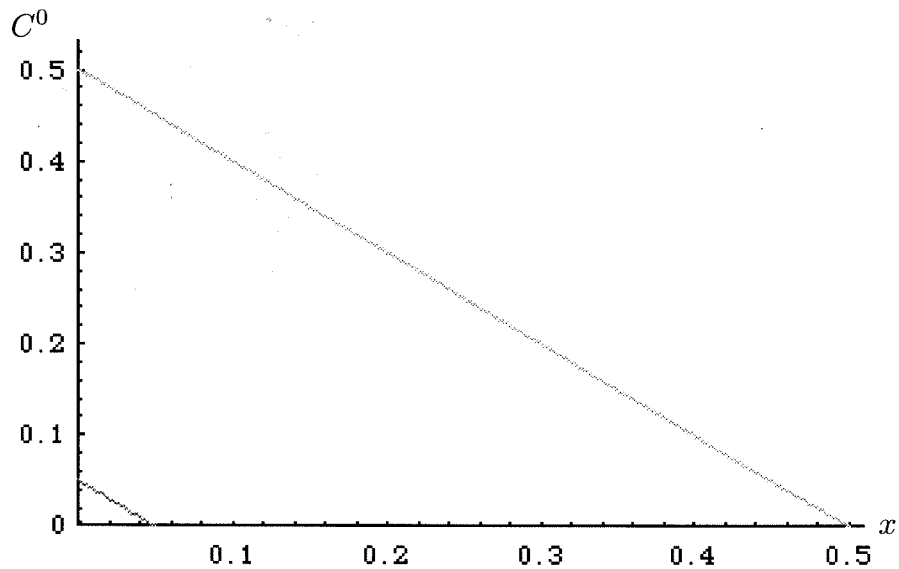

Figure 8f. Stress profiles: $a = -0.75$, $C_* = 0.4$, $\gamma = 2$, $\alpha = 3$, $\epsilon = 0.0001$, $\kappa = 5$. In decreasing order of darkness: $t = 0.001$, 0.01, 0.1.

Chapter IX: Can Our Front Move Faster Than a Subcharacteristic?

1. The Unstressed Case

We now wish to examine the case of penetration of some liquid or gaseous substance into a polymer. Here we consider the case where the memory is state-independent, that is where $\tilde{t}_0 = -\infty$. This corresponds to the case where the polymer always has a memory. The mathematical manifestation of this physical property is the fact that $\sigma_u(x) \not\equiv 0$. In addition, we want to examine the case omitted in chapter VIII, namely that of a boundary layer in the glassy region. For this case we need another set of parameter values for a, namely

$$-C_* < a \leq 0. \tag{9.1}$$

The expression for C^{0+} in such a boundary layer is given by (8.7). We note that for our solution to be bounded, $s(t) > \kappa t$. Hence, there can be no corresponding boundary layer in C^{0r} around $s(t)$ in this case. Since we know that our outer solution is $C^{0g} \equiv 0$ for $x > \kappa t$, we have a boundary condition which gives our solution as

$$C^{0+} = C_* \exp\left[\frac{(\kappa^2 - \dot{s}^2)\zeta}{\alpha \dot{s}}\right]. \tag{9.2}$$

Is a layer possible in σ^g? No, since in that case equation (7.1b) becomes (to

leading order)

$$-\dot{s}\epsilon^{-1}\sigma_\zeta^+ = \frac{\kappa^2\epsilon^{-1}}{\gamma}C^+ - \kappa\epsilon^{-1}C_\zeta^+.$$

This shows that $\sigma^+ = O(1)$, which implies that

$$\sigma^{0r}(s(t),t) = 0. \tag{9.3}$$

In addition, since σ^{0r} does not contribute to our matching in equation (7.7), we have

$$\alpha C_\zeta^{0+} = a\dot{s},$$

$$s(t) = \kappa t\sqrt{\frac{C_*}{C_*+a}}. \tag{9.4}$$

Note from equation (9.4) why our compatibility condition (9.1) becomes important. Note also that equation (9.4) is good *for all time.*

We note that we must use our boundary condition (8.15b) since there can be no boundary layer in C^{0r} for $x > \kappa t$. Now in this region, we see that T^{ck} does not contribute when we try to match our solutions together. Therefore, any solution which we construct will necessarily be *independent of* $C_b(t)$.

Now we perform our asymptotic analysis for small t and x. We assume the following forms:

$$\sigma_u(x) \sim \sigma_0 + \sigma_1 x + \frac{\sigma_2 x^2}{2}, \qquad C_u(x) \sim C_0 + C_1 x, \qquad x \to 0. \tag{9.5}$$

We begin by expanding T^{cd}, which is now nonzero:

$$T^{cd}(x,t) \sim \gamma\sigma_2 t + \gamma\sigma_3 xt - \frac{\gamma t^2}{2}\sigma_2. \tag{9.6}$$

T^{ck} does not contribute (since $x > \kappa t$), so we may combine (9.6) with our previous expansion for T^{cu} to obtain an expression for (8.15b) to $O(t)$, recalling that $O(s)$ is now also $O(t)$:

$$C_* = C_0 + C_1 s + \gamma\sigma_2 t.$$

Using (9.4), we have

$$C_0 = C_*, \qquad C_1\kappa\sqrt{\frac{C_*}{C_* + a}} = -\gamma\sigma_2. \tag{9.7}$$

Next we turn to the stress. Once again $T^{\sigma k}$ does not contribute, and our asymptotic expansion of $T^{\sigma u}$ is

$$T^{\sigma u}(x,t) \sim \sigma_0 + \sigma_1 s + \frac{\sigma_2 s^2}{2} + \kappa\sigma_2 t^2. \tag{9.8}$$

By using an analogous form of (9.6) to expand $T^{\sigma d}$ to higher orders, we rewrite (9.3) to $O(t^2)$:

$$0 = \sigma_0 + \sigma_1 s + \frac{\sigma_2 s^2}{2} + \kappa^2\sigma_2 t^2 + t\left(\frac{\kappa^2}{\gamma}C_0 - \sigma_0\right) + \left(\frac{\kappa^2}{\gamma}C_1 - \sigma_1\right) st - \frac{t^2}{2}\left(\frac{\kappa^2}{\gamma}C_0 - \sigma_0\right). \tag{9.9}$$

Using equation (9.7), we have

$$\sigma_0 = 0, \qquad \sigma_1 s + \frac{\sigma_2 s^2}{2} + \kappa^2\sigma_2 t^2 + \frac{\kappa^2 C_* t}{\gamma} + \left(\frac{\kappa^2}{\gamma}C_1 - \sigma_1\right) st - \frac{\kappa^2 C_* t^2}{2\gamma} = 0. \tag{9.10}$$

Using equation (9.4), we have the following, matching the $O(t)$ terms:

$$\sigma_1 = -\frac{\kappa\sqrt{C_*(C_* + a)}}{\gamma}. \tag{9.11}$$

Using equations (9.4), (9.7), and (9.11) in (9.10), we have, matching the $O(t^2)$ terms:

$$\frac{\sigma_2}{2}\left[1+\frac{C_*}{C_*+a}\right]+\frac{\kappa C_1}{\gamma}\sqrt{\frac{C_*}{C_*+a}}+\frac{C_*}{2\gamma}=0. \tag{9.12}$$

Combining equations (9.7) and (9.12), we can solve for σ_2 and C_1, yielding

$$\sigma_2=\frac{C_*(C_*+a)}{a\gamma}, \qquad C_1=\frac{|C_*+a|^{3/2}\sqrt{C_*}}{|a|\kappa}. \tag{9.13}$$

However, note that $C_1 > 0$. Though this solution is mathematically valid for our *fictitious* problem, it is not a solution of our *full* problem since it says that for some $x < s(t)$ (that is, in our rubbery region), $C^{0r} < C_*$, which is a violation of the definition of the rubbery polymer.

The only other assumption we have made about our solution is in our compatibility condition (9.1). However, we see that if $a < -C_*$, $s(t)$ is imaginary. If $a > 0$, $s(t) < \kappa t$. Therefore, if the stress is initially zero, there does not exist a solution where the front moves faster than the subcharacteristic $x = \kappa t$.

2. The Prestressed Case

In order to continue to find a solution of the form we seek, we now consider a polymer-penetrant system which has an initial stress distribution. This is perfectly reasonable in certain polymer-penetrant systems, where polymers may have stresses imposed upon them even before any penetrant is introduced. Such systems arise in pharmaceutical delivery applications when substances are imbedded in the polymer matrix above their natural solubility limit [6]. For simplicity, we consider the case

where the polymer is uniformly stressed:

$$\sigma_i(x) \equiv \sigma_*. \tag{9.14}$$

We no longer require (9.1) to hold.

What happens in this case? Well, equation (9.2) still holds, and there is still no boundary layer in σ^g, so equation (9.3) is now replaced by

$$\sigma^{0r}(s(t),t) \equiv \sigma_*. \tag{9.15}$$

Thus our choice of the asterisk subscript is appropriate, since σ_* is also the transition value of the stress. Equation (7.7) then becomes

$$\alpha C_\zeta^{0+} - \frac{\gamma\sigma_*}{\dot{s}} = a\dot{s},$$

$$s(t) = t\sqrt{\frac{\kappa^2 C_* - \gamma\sigma_*}{C_* + a}}. \tag{9.16}$$

Note from equation (9.16) that we have the restrictions on our parameters that the argument of the square root be larger than κ^2. Note once again that our expression for the front (9.16) is good *for all time.*

This time we perform our asymptotics for large t and x. We begin by assuming that both $C_u(x)$ and $\sigma_u(x)$ are bounded as $x \to \infty$. When we make that assumption, we see that all of the derivatives in our integrals vanish as $x \to \infty$, so equations (8.15b) and (9.15) become, to leading order,

$$C_* = C_u(s), \tag{9.17a}$$

$$\sigma_* = \sigma_u(s) + \frac{e^{-t/2}}{2\kappa}\int_{s-\kappa t}^{s+\kappa t}\left[\frac{\kappa^2}{\gamma}C_u(z) - \sigma_u(z)\right] g_d(s-z,t)\,dz. \tag{9.17b}$$

Now since $s(t)$ is still in the range of integration of $T^{\sigma d}$, we may use equation (8.21), so (9.17b) becomes

$$\sigma_* \sim \sigma_u(s) + \frac{\kappa^2}{\gamma} C_u(s) - \sigma_u(s), \tag{9.18}$$

$$\gamma\sigma_* \sim \kappa^2 C_*,$$

which contradicts our assumption that σ_* is a free parameter. In addition, (9.16) implies that $s(t) \sim 0$.

All is not lost, however; we have some options. Since they are fictitious conditions, we may allow one or both of $C_u(x)$ and $\sigma_u(x)$ to become unbounded as $x \to \infty$. We begin by letting only $\sigma_u(x)$ grow without bound. How will this help us? Well, the correct form of (9.18) is

$$\sigma_* \sim \sigma_u(s) + \left[1 + O\left(\frac{1}{t}\right)\right]\left[\frac{\kappa^2}{\gamma} C_u(s) - \sigma_u(s)\right],$$

where the error comes from our Laplace's method asymptotics of (8.17). Therefore, the simplest way to introduce a nonvanishing contribution is to let

$$C_u(x) \sim C_\infty, \qquad \sigma_u(x) \sim \sigma_\infty x, \qquad x \to \infty.$$

We immediately note that (9.17a) still holds, so we have

$$C_\infty = C_*. \tag{9.19}$$

Since $\sigma_u'(x)$ is constant and the integral in $T^{\sigma u}$ does not contribute, equation (9.17b) becomes, neglecting terms which are vanishing,

$$\sigma_* \sim \sigma_u(s) + \frac{\kappa^2}{\gamma} C_\infty - \frac{e^{-t/2}\sigma_\infty}{2\kappa} \int_{s-\kappa t}^{s+\kappa t} z I_0(\sqrt{\kappa^2 t^2 - (s-z)^2}/2\kappa)\, dz.$$

We may now exploit the fact that we have a representation for $s(t)$ by writing $s(t) = s_\infty \kappa t$. We use both terms in (8.18) to yield the following:

$$\sigma_* \sim \sigma_\infty s + \frac{\kappa^2}{\gamma} C_*$$

$$- \frac{e^{-t/2}\sigma_\infty \kappa t^{3/2}}{2\sqrt{\pi}} \int_{s_\infty - \delta}^{s_\infty + \delta} \frac{y \exp(t\sqrt{1-(s_\infty - y)^2}/2)}{[1-(s_\infty - y)^2]^{1/4}} \left\{ 1 + \frac{1}{4t\sqrt{1-(s_\infty - y)^2}} \right\} dy.$$

It is trivial to see that the stationary point is $y = s_\infty$. We know that the leading order term arising from the first braced term will cancel $\sigma_\infty s$. We then use the full expression for Laplace's method given by (8.20) to yield our final answer. It is clear that we need the second-order term for Laplace's method only for the first braced term. We denote the kernel for the first braced quantity f_1 and the kernel for the second braced term f_2.

In order to use (8.20), we construct a glossary of functions. It is clear that $\phi(y)$ is even about the point s_∞, so $\phi^{(3)}(s_\infty) = 0$. The rest of the terms needed are as follows:

$$f_1(y) = \frac{y}{[1-(s_\infty - y)^2]^{1/4}}, \qquad f_1(s_\infty) = s_\infty;$$

$$f_1''(y) = \frac{3y - 2s_\infty}{2(1-(s_\infty - y)^2)^{5/4}} + \frac{5y(s_\infty - y)^2}{4(1-(s_\infty - y)^2)^{9/4}}, \qquad f_1''(s_\infty) = \frac{s_\infty}{2};$$

$$f_2(y) = \frac{y}{4t[1-(s_\infty - y)^2]^{3/4}}, \qquad f_2(s_\infty) = \frac{s_\infty}{4t};$$

$$\phi''(y) = -\frac{1}{2(1-(s_\infty - y)^2)^{3/2}}, \qquad \phi''(s_\infty) = -\frac{1}{2};$$

$$\phi^{(4)}(y) = -\frac{3[1+4(s_\infty - y)^2]}{2(1-(s_\infty - y)^2)^{7/2}}, \qquad \phi^{(4)}(s_\infty) = -\frac{3}{2}.$$

Using those terms, we have

$$\sigma_* \sim \sigma_\infty s_\infty \kappa t + \frac{\kappa^2}{\gamma} C_* - \frac{e^{-t/2}\sigma_\infty \kappa t^{3/2}}{2\sqrt{\pi}} \sqrt{\frac{4\pi}{t}} e^{t/2} \left(s_\infty - \frac{s_\infty}{4t} + \frac{s_\infty}{4t} \right)$$

$$\sim \frac{\kappa^2}{\gamma} C_*$$

as before.

Therefore, the constant terms which we hoped would arise from the next order in Laplace's method exactly cancel. Our next guess might to be let $\sigma_u(x) \sim \sigma_\infty x^2$. This would have the advantage that T^{cd} would now contribute a constant term to (9.17a), thus making C_∞ a free parameter. Unfortunately, the terms arising in the second order of the Laplace's method asymptotics of $T^{\sigma d}$ [which are now $O(t)$] do not cancel, even with the terms arising from $T^{\sigma u}$. Therefore, a quadratically unbounded $\sigma_u(x)$ leaves an unbounded stress field, and similarly for other forms for $\sigma_u(x)$ we might try.

Our next guess then would be to make $C_u(x)$ unbounded. Unfortunately, in order for equation (9.17a) to remain true, $\sigma_u(x)$ would have to behave like $x^2 C_u(x)$, which would then introduce other non-cancelling unbounded terms in (9.17b). Note that our assumption of a uniform initial stress field has no bearing on the situation, since this conflict would arise unless $\gamma \sigma_i(x) \to \kappa^2 C_*$ as $x \to \infty$.

Once again, note that nowhere in our analysis did we use a specific form for $C_b(t)$, and we have used no other assumptions. Therefore, it seems clear that our system of equations (7.1)-(7.4) does not allow solutions which move faster than the subcharacteristic $x = \kappa t$.

Chapter X: Remarks

The results in Chapter VIII clearly demonstrate that when the stress is large enough to dominate other quantities in the system, non-Fickian behavior ensues. Rather than a regular perturbation problem as in Part Two, here we are faced with a singular perturbation problem with two boundary layers. The first arises from the hyperbolicity of the outer expansion partial differential equations (7.5a) and (7.6a). These hyperbolic equations can propagate discontinuities which the full equations (7.1a) and (7.2a) cannot; hence, a boundary layer ensues. This "primary front" tracks the first "signal" of the solvent in the polymer network, and is therefore analogous to the penetration front in a more standard polymer-penetrant system. Behind it, there is a "mushy region" of finite width where the polymer changes from glass to rubber as it dissolves. The second boundary layer at our front $s(t)$ arises due to the form of our front condition (7.7); a sharp concentration gradient is needed to balance the effects of the stress. Each of these behaviors is unobtainable with a standard Fickian model. However, the results in Chapter VIII do seem to replicate experiments involving dissolving polymers, notably toluene or chlorobenzene dissolving poly-methyl-methocrylate or polystyrene [29].

In Part Three we chose $a < 0$; therefore, in cases where the stress is important, a cannot be directly related to the latent heat in a Stefan problem. However, note that $[C_x]_s > 0$. The jump in the standard Fickian flux was positive, as found in a standard Stefan problem; it was the non-Fickian stress contribution to the flux which forced $a < 0$.

We also found another unusual result: the *self-regulating mass uptake* of the dissolving polymer. Perhaps related to the strength of the entanglement network, this uptake reflects the internal dissolution rate of the polymer. However, note that when we derived an expression for r, we did so having assumed the form of $C(0^+, t)$ as in (8.1). Though (8.1) is certainly a reasonable first approximation to the actual kinetics at the boundary, certainly other forms could be postulated. Linear and quadratic uptake models at the boundary would also lead to undetermined constants for which one could solve in a similar fashion to that outlined in Chapter VIII.

Chapter IX is more than just an exercise in futility; it illustrates a very systematic attempt to try to get equations (7.1)-(7.4) to yield solutions which move faster than the subcharacteristics of the outer problem. Such an exercise, though doomed to failure by the nature of the aforementioned equations, illustrates the pitfalls encountered when trying to solve this very complicated set of equations for various parameter ranges. In some sense we could have predicted that no solutions could be found, since from elementary perturbation theory we know it is rare for an $O(1)$ disturbance to occur ahead of a subcharacteristic [30]. However, it was worth trying since with such an unusual front condition as (7.7) it is difficult to tell what sort of solutions may occur.

In the next section we will consider the case where the diffusion coefficient is a piecewise constant function of the concentration (or the phase). Such an analysis will lead to solutions which are in many ways similar to the results in previous sections, but which differ in several key respects.

Part Four: Varying the Diffusion Coefficient

Chapter XI: Varying the Diffusion Coefficient: Preliminaries

In Chapter III, we mentioned that in some polymer penetrant systems, the effect of a varying diffusion coefficient is pronounced. Now we will examine such a case by abandoning the assumption used in previous chapters that $D_g = D_r$. We retain (3.20), but note that in certain polymer-penetrant systems, the diffusion coeficient in the rubbery region is much greater than that of the glassy region. This motivates the choice $D_r = D_0\epsilon^{-1}$. We still expect the effects of stress to be important, so we let $\eta = \eta_0\epsilon^{-1}$. It will be shown that these choices for the relative magnitudes of our parameters will lead to solutions which replicate the desired behavior. Also in contrast to the previous chapters, we use the relaxation time in the glassy region, which is on the order of seconds, as our characteristic time rather than the much shorter relaxation time in the rubbery region. We normalize length by a mixture of the two scales. Summarizing, we have the following:

$$\tilde{x}_c = \sqrt{\frac{D_r}{\beta_g}}, \qquad \beta_c = \beta_g, \qquad D_r = D_0\epsilon^{-1}, \qquad \eta = \eta_0\epsilon^{-1}.$$

Making these substitutions in (3.32) and (3.25b), we see that for $C \leq C_*$ we have the following equations:

$$C^g_{tt} = \epsilon\alpha_g C^g_{xxt} - C^g_t + \left(\frac{\epsilon D_g}{D_0} + \kappa^2\right) C^g_{xx}, \tag{11.1a}$$

$$\sigma_t^g + \sigma^g = \frac{\kappa^2}{\gamma\epsilon} C^g + C_t^g, \tag{11.1b}$$

where $\kappa^2 = \eta_0 E/\beta_g D_0$, $\gamma = \nu E/D_0$, and $\alpha_g = D_g/D_0 + \gamma$. Similarly, we see that in the rubbery region we have

$$C_{tt}^r = (1+\epsilon\gamma)\, C_{xxt}^r - \epsilon^{-1} C_t^r + (\epsilon^{-1} + \kappa^2) C_{xx}^r, \tag{11.2a}$$

$$\epsilon\sigma_t^r + \sigma^r = \frac{\kappa^2}{\gamma} C^r + \epsilon C_t^r. \tag{11.2b}$$

In addition, equation (3.26) becomes

$$\alpha_g \epsilon C_x^g\,(s(t),t) - C_x^r\,(s(t),t) - \frac{\gamma\sigma\,(s(t),t)}{\dot{s}} = a\dot{s}. \tag{11.3}$$

Upon examination of equations (11.1b) and (11.2b), we postulate the following expansions for C and σ in ϵ:

$$C = C^0 + o(1), \qquad \sigma^r = \sigma^{1r} + o(1), \qquad \sigma^g = \sigma^{0g}\epsilon^{-1} + O(1).$$

We note immediately from the above that either $\sigma^{0g}(s(t),t) = 0$ or we have a maximum in the stress at the front as sketched in Figure 3c. Inserting our expansions into (11.1a), (11.2a), and (11.3) and retaining terms to leading order, we have the following:

$$C_{tt}^{0g} = -C_t^{0g} + \kappa^2 C_{xx}^{0g}, \tag{11.4}$$

$$C_t^{0r} = C_{xx}^{0r}, \tag{11.5}$$

$$\alpha_g \epsilon C_x^{0g}\,(s(t),t) - C_x^{0r}\,(s(t),t) - \frac{\gamma\sigma^{0g}\,(s(t),t)}{\epsilon\dot{s}} = a\dot{s}. \tag{11.6}$$

From equation (11.5a) we see that there are three separate cases to consider: $\dot{s} = \kappa$, $\dot{s} < \kappa$, and $\dot{s} > \kappa$. We restrict ourselves to the case where $\dot{s} \leq \kappa$. In order to consider such cases, we need to introduce boundary layer variables as follows:

$$\zeta = \frac{x - s(\tau)}{\epsilon^m}, \qquad \tau = t, \qquad \frac{\partial}{\partial x} = \epsilon^{-m}\frac{\partial}{\partial \zeta}, \tag{11.7a}$$

$$\frac{\partial}{\partial t} = \frac{\partial}{\partial \tau} - \dot{s}\epsilon^{-m}\frac{\partial}{\partial \zeta}, \qquad C^g(x,t) \sim C^{0+}(\zeta,\tau) + o(1). \tag{11.7b}$$

Substituting equations (11.7) in equation (11.1a), we have the following (to leading orders):

$$-2\dot{s}\epsilon^{-m}C^{0+}_{\zeta\tau} + \epsilon^{-2m}\dot{s}^2 C^{0+}_{\zeta\zeta} = -\epsilon^{1-3m}\alpha_g \dot{s} C^{0+}_{\zeta\zeta\zeta} + \epsilon^{-m}\dot{s}C^{0+}_{\zeta} + \epsilon^{-2m}\kappa^2 C^{0+}_{\zeta\zeta}. \tag{11.8}$$

First we consider the case where $\dot{s} = \kappa$. In this case, the two $C^{0+}_{\zeta\zeta}$ terms cancel, and the balance is $m = 1/2$. However, we note that with this scaling equation (11.1b) becomes to leading order, with $\sigma^g = \sigma^+$:

$$-\epsilon^{-1/2}\kappa\sigma^+_{\zeta} + \sigma^+ = \frac{\kappa^2}{\gamma\epsilon}C^+ - \kappa\epsilon^{-1/2}C^{0+}_{\zeta}. \tag{11.9a}$$

For a balance in equation (11.9a), we have that $\sigma^+ = O(\epsilon^{-1/2})$. However, equation (11.2b) becomes to leading order, with $\sigma^r \sim \epsilon^{-1/2}\sigma^{0-}$ in order to match with σ^+:

$$-\kappa\sigma^{0r}_{\zeta} + \epsilon^{-1/2}\sigma^{0r} = \frac{\kappa^2}{\gamma}C^r - \epsilon^{1/2}\kappa C^r_{\zeta}. \tag{11.9b}$$

Note that there is no balance in equation (11.9b). So we conclude that our assumption is wrong.

Therefore, we see that $m = 1$ and (11.8) becomes

$$\alpha_g \dot{s} C^{0+}_{\zeta\zeta\zeta} + (\dot{s}^2 - \kappa^2) C^{0+}_{\zeta\zeta} = 0.$$

However, we see that for $s < \kappa t$ there is no bounded solution as $\zeta \to \infty$, which is the matching region for the glassy polymer. Thus, there is no layer in the concentration in the glassy region. Since (11.1a) also holds for σ^g, we see that there is no layer in the stress, either. So in order to match $\sigma^r = O(1)$ to $\sigma^g = O(\epsilon^{-1})$, we need a boundary layer in the rubbery region around $x = s(t)$. Introducing the scalings in (11.7) with $\sigma^r(x,t) \sim \epsilon^{-1}\sigma^{0-}(\zeta,\tau)$ and $m = 1$ into (11.2b), we have (to leading order)

$$-\epsilon^{-1}\dot{s}\sigma^{0-}_{\zeta} + \epsilon^{-1}\sigma^{0-} = \frac{\kappa^2}{\gamma} C^r - \dot{s} C^r_{\zeta}.$$

Using the fact that $\sigma^r = O(1)$, we note that $\sigma^{0-}(-\infty,\tau) = 0$. Therefore, the solution becomes

$$\sigma^{0-}(\zeta,\tau) = \sigma^{0g}(s(\tau),\tau) e^{\zeta/\dot{s}}, \tag{11.10}$$

which decays as $\zeta \to -\infty$, as required.

Substituting our scalings (11.7) in (11.2a) in order to find the boundary-layer equation for $C^r(x,t) \sim C^{0-}(\zeta,\tau)$, we have

$$0 = -\dot{s} C^{0-}_{\zeta\zeta\zeta} + C^{0-}_{\zeta\zeta},$$

the solution of which is, subject to our boundary condition (3.28),

$$C^{0-}(\zeta,\tau) = C^{0r}(s(\tau),\tau) + \left[C_* - C^{0r}(s(\tau),\tau)\right] e^{\zeta/\dot{s}}. \tag{11.11}$$

Note that in this case that (11.6) becomes, to leading order,

$$\frac{C^{0r}(s(t),t) - C_*}{\dot{s}} - \frac{\gamma\sigma^{0g}(s(t),t)}{\dot{s}} = 0, \tag{11.12}$$

which does not explicity involve a. Therefore, in this case we see that the feature which controls the dynamics is a balance between the two contributions to the flux.

Chapter XII: Calculations

1. The Integral Method

Now that we have constructed the necessary boundary conditions for our problem, we will once again have to use Boley's integral method and fictitious boundary or initial conditions to complete the problem. However, since we have only equation (11.12) to solve in the rubbery region, we note that we have too many unknowns if we use Boley's method there. Fortunately, we note that the boundary layer in this problem can play the role of "adjusting" the rubbery concentration instead of the fictitious initial condition in Boley's method. Therefore, we consider the case where the fictitious initial condition is the actual initial condition for the problem: that is,

$$C^{0r}(x,0) = C_i(x) \equiv 0. \tag{12.1}$$

Note that in some sense the two approaches are equivalent. If we were not using a perturbation method and were tackling the full equations directly, some fictitious initial condition $C^{0r}(x,0)$ could be constructed which would replicate the boundary-layer behavior of our problem.

For reasons that will become clear later, we consider the case where

$$C_*(1+\kappa^2) < 1. \tag{12.2}$$

In Chapter X we pointed out that there are various types of boundary conditions

which we could impose at $x = 0$, including a linear profile which ramps the concentration up to 1. We use that approach here:

$$C_b(t) = \begin{cases} C_* + (1 - C_*)t/r, & 0 < t < r; \\ 1, & t \geqslant r; \end{cases} \qquad \frac{(1 - C_*)\sqrt{\pi}}{\kappa C_*(\kappa\sqrt{\pi} + 1)} < r < \frac{1 - C_*}{C_*\kappa^2}. \tag{12.3}$$

The restrictions on r will also become clear later.

Once again we use Boley's method for our problem by introducing fictitious variables T^r and T^g. Therefore, equations (11.5), (12.3), (12.1), (11.4), (3.27), (3.28), and (11.12) become

$$T^r_t = T^r_{xx}, \quad 0 < x < \infty; \tag{12.4}$$

$$T^r \equiv C^{0r}, \quad 0 < x < s(t);$$

$$T^r(x, 0) = 0, \qquad T^r(0, t) = \begin{cases} C_* + (1 - C_*)t/r, & 0 < t < r; \\ 1, & t > r; \end{cases} \tag{12.5}$$

$$T^g_{tt} = \kappa^2 T^g_{xx} - T^g_t, \quad 0 < x < \infty; \tag{12.6}$$

$$T^g \equiv C^{0g}, \quad s(t) < x < \infty;$$

$$T^g(0, t) = f_b(t), \qquad T^g(x, 0) = 0, \qquad T^g_t(x, 0) = 0; \tag{12.7}$$

$$T^g(s(t), t) = C_*; \tag{12.8}$$

$$T^r(s(t), t) - \gamma\sigma^{0g}(s(t), t) = C_*; \tag{12.9}$$

$$s(0) = 0. \tag{12.10}$$

From the form of equation (12.9) we see that in order to solve our problem we will need to calculate σ^{0g}. We once again take the case of an unstressed polymer

by setting $\tilde{t}_0 = 0$, which implies that $\sigma_i(x) \equiv 0$. An easy way to solve for σ^{0g} is to note that equation (12.6) also holds for σ^{0g}. Our initial conditions are the same, so $\sigma^{0g}(0,t)$ may be calculated from (11.1b):

$$\sigma^{0g}(0,t) = \frac{\kappa^2 e^{-t}}{\gamma} \int_0^t f_b(z) e^z \, dz. \tag{12.11}$$

Note in equation (12.11) we have enforced continuity of stress at $(x,t) = (0,0)$ because $\tilde{t}_0 = 0$.

The solution of equations (12.4)-(12.5) is given by (4.26). We begin by substituting our expression for $T^r(0,t)$ in the case where $t < r$:

$$T^r(x,t) = \left[\frac{(2t+x^2)(1-C_*)}{2r} + C_*\right] \operatorname{erfc}\left(\frac{x}{2\sqrt{t}}\right) - \frac{(1-C_*)x}{r}\sqrt{\frac{t}{\pi}} \exp\left(-\frac{x^2}{4t}\right). \tag{12.12}$$

We may solve similarly for the case where $t > r$:

$$T^r(x,t) = \operatorname{erfc}\left(\frac{x}{2\sqrt{t}}\right) + (1-C_*)\left(1 - \frac{x^2+2t}{2r}\right)\left[\operatorname{erf}\left(\frac{x}{2\sqrt{t}}\right) - \operatorname{erf}\left(\frac{x}{2\sqrt{t-r}}\right)\right]$$
$$- \frac{(1-C_*)x}{r\sqrt{\pi}}\left\{\sqrt{t}\exp\left(-\frac{x^2}{4t}\right) - \sqrt{t-r}\exp\left[-\frac{x^2}{4(t-r)}\right]\right\}. \tag{12.13}$$

The solution of equations (12.6)-(12.7) is given by (7.19). Since our region of interest is where $s < \kappa t$, we may omit the Heaviside function and equation (12.8) becomes

$$\frac{s}{2}\int_{s/\kappa}^t e^{-z/2} f_b(t-z) \frac{I_1(\sqrt{\kappa^2 z^2 - s^2}/2\kappa)}{\sqrt{\kappa^2 z^2 - s^2}} \, dz + f_b(t - s/\kappa) e^{-s/2\kappa} = C_*. \tag{12.14}$$

However, note from (7.19) that there is a discontinuity around $x = \kappa t$ which our full equation (11.1a) cannot propagate. Therefore, we then let $\dot{s} = \kappa$ and $m = 1/2$

in (11.8), which then becomes, to leading order,

$$-2\kappa C^{0+}_{\zeta\tau} = -\alpha_g \kappa C^{0+}_{\zeta\zeta\zeta} + \kappa C^{0+}_{\zeta}.$$

Letting $C^{0+} = e^{-\tau/2} T^{+}$ and integrating once with respect to ζ, we have

$$-2T^{+}_{\tau} = -\alpha_g T^{+}_{\zeta\zeta}. \tag{12.15}$$

Our initial condition is found from (12.14) to be

$$T^{+}(\zeta, 0) = f_b(0) H(-\zeta). \tag{12.16}$$

Solving (12.15) subject to (12.16) yields

$$C^{0+}(\zeta, \tau) = \frac{f_b(0) e^{-\tau/2}}{2} \operatorname{erfc}\left(\frac{\zeta}{\sqrt{2\alpha_g \tau}}\right). \tag{12.17}$$

2. Small Time Asymptotics

We begin by performing small time asymptotics. We postulate the following expansions of our unknown functions:

$$f_b(t) \sim f_0, \qquad s(t) \sim s_0 t^n, \qquad n \geq 1, \tag{12.18}$$

where our restriction on n comes from the case we are considering. Substituting (12.18) into (12.14), we have

$$\frac{f_0 s_0 t^n}{2} \int_{s/\kappa}^{t} e^{-z/2} \frac{I_1(\sqrt{\kappa^2 z^2 - s^2}/2\kappa)}{\sqrt{\kappa^2 z^2 - s^2}}\, dz + f_0 \left(1 - \frac{s_0 t^n}{2\kappa}\right) \sim C_*.$$

We see immediately from the leading-order balance that

$$f_0 = C_*. \tag{12.19}$$

Now we may immediately solve for σ^{0g}, which is also valid only for $x < \kappa t$:

$$\sigma^{0g}(x,t) = \frac{x}{2}\int_{x/\kappa}^{t} e^{-z/2}\sigma^{0g}(0,t-z)\frac{I_1(\sqrt{\kappa^2 z^2 - x^2}/2\kappa)}{\sqrt{\kappa^2 z^2 - x^2}}\,dz + \sigma^{0g}(0,t-x/\kappa)e^{-x/2\kappa}. \tag{12.20}$$

Using (12.19) and (12.11) in (12.20), we have

$$\sigma^{0g}(s(t),t) \sim \frac{\kappa^2 C_*}{\gamma}\left(t - \frac{s_0 t^n}{\kappa}\right). \tag{12.21}$$

Using (12.21) and the leading orders of (12.12) in (12.9), we have

$$C_* - \frac{C_* s_0 t^{n-1/2}}{\sqrt{\pi}} + \frac{t(1-C_*)}{r} - \gamma\left(\frac{\kappa^2 C_*}{\gamma}\right)\left(t - \frac{s_0 t^n}{\kappa}\right) = C_*. \tag{12.22}$$

Matching the leading order of (12.22) gives

$$-\frac{C_* s_0 t^{n-1/2}}{\sqrt{\pi}} + \frac{t(1-C_*)}{r} - \kappa^2 C_* t + \kappa C_* s_0 t^n = 0. \tag{12.23}$$

Upon examination of (12.23), we see that the dominant balance is $n = 3/2$, which yields

$$s_0 = \left(\frac{1-C_*}{C_* r} - \kappa^2\right)\sqrt{\pi}. \tag{12.24}$$

Note from equation (12.24) that in order to have $0 < s_0 < \kappa$ as required, then the compatibility condition in (12.3) must be true.

Summarizing our results, we have the following, where we recall (11.10) and (11.11):

$$C^{0r}(x,t) \sim T^r(x,t) + [C_* - T^r(s(t),t)] \exp\left[\frac{x-s(t)}{\epsilon \dot{s}}\right], \tag{12.25a}$$

$$T^r(x,t) = \begin{cases} \left(\dfrac{2t+x^2}{2r} + C_*\right) \operatorname{erfc}\left(\dfrac{x}{2\sqrt{t}}\right) - \dfrac{(1-C_*)x}{r}\sqrt{\dfrac{t}{\pi}} \exp\left(-\dfrac{x^2}{4t}\right), & t < r; \\ \operatorname{erfc}\left(\dfrac{x}{2\sqrt{t}}\right) \\ \quad +(1-C_*)\left(1 - \dfrac{x^2+2t}{2r}\right)\left[\operatorname{erf}\left(\dfrac{x}{2\sqrt{t}}\right) - \operatorname{erf}\left(\dfrac{x}{2\sqrt{t-r}}\right)\right] \\ \quad -\dfrac{(1-C_*)x}{r\sqrt{\pi}}\left\{\sqrt{t}\exp\left(-\dfrac{x^2}{4t}\right) - \sqrt{t-r}\exp\left[-\dfrac{x^2}{4(t-r)}\right]\right\}, & t > r; \end{cases} \tag{12.25b}$$

$$\sigma^{0-}(x,t) = \sigma^{0g}(s(t),t) \exp\left[\frac{x-s(t)}{\dot{s}}\right], \tag{12.25c}$$

$$t \to 0$$

$$s(t) \sim \left(\frac{1-C_*}{C_* r} - \kappa^2\right) t^{3/2}\sqrt{\pi}, \tag{12.26}$$

$$x < \kappa t$$

$$C^{0g}(x,t) \sim C_* \left[\frac{x}{2}\int_{x/\kappa}^{t} e^{-z/2} \frac{I_1(\sqrt{\kappa^2 z^2 - x^2}/2\kappa)}{\sqrt{\kappa^2 z^2 - x^2}}\, dz + e^{-x/2\kappa}\right] - \frac{C_* e^{-t/2}}{2} \operatorname{erfc}\left(\frac{\kappa t - x}{\sqrt{2\alpha_g \epsilon t}}\right), \tag{12.27a}$$

$$\sigma^{0g}(x,t) \sim \frac{C_*\kappa^2}{\gamma}\left[\frac{x}{2}\int_{x/\kappa}^{t} e^{-z/2}[1-e^{-(t-z)}]\frac{I_1(\sqrt{\kappa^2 z^2 - x^2}/2\kappa)}{\sqrt{\kappa^2 z^2 - x^2}}\,dz\right.$$

$$\left.+[1-e^{-(t-x/\kappa)}]e^{-x/2\kappa}\right], \quad (12.27b)$$

$$x > \kappa t$$

$$C^{0g}(x,t) \sim \frac{C_* e^{-t/2}}{2}\,\mathrm{erfc}\left(\frac{x-\kappa t}{\sqrt{2\alpha_g \epsilon t}}\right). \quad (12.28)$$

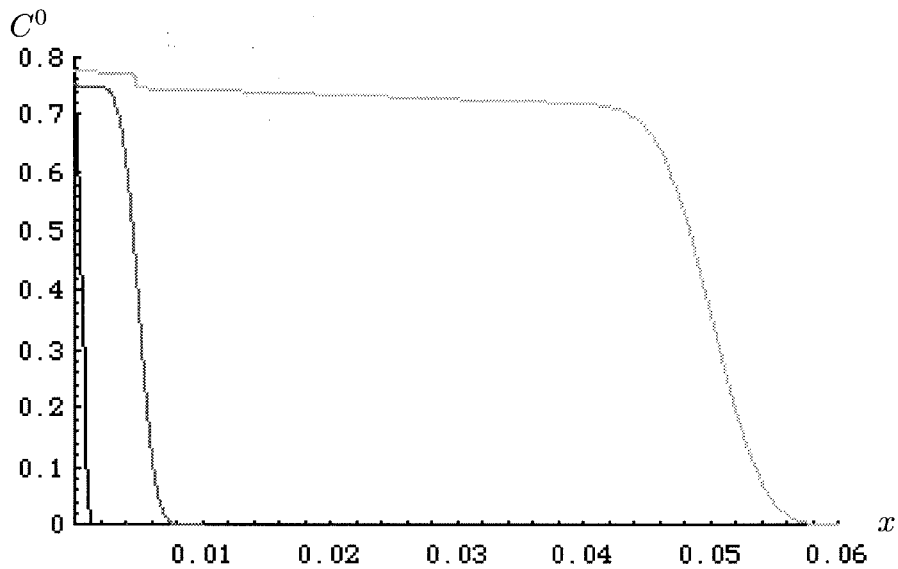

Figure 12a. Concentration profiles: $C_* = 0.75$, $r = 1$, $\gamma = 0.5$, $\alpha_g = 1$, $\epsilon = 0.0001$, $\kappa = 0.5$. In decreasing order of darkness: $t = 0.001$, 0.01, 0.1.

Figure 12a shows graphs of our concentration field expansions for small times [though they are large enough that $\epsilon = o(t)$] and for parameters which satisfy (12.2) and (12.3). Note that we once again see a three-stage profile. The concentration starts at 0, then rises through the boundary layer around $x = \kappa t$. The boundary layer doesn't seem that sharp since our x scale is so small. Then there is a relatively flat region in the glassy polymer until the second boundary layer brings

the concentration from the transition value C_* to the rubbery region described by (12.25b).

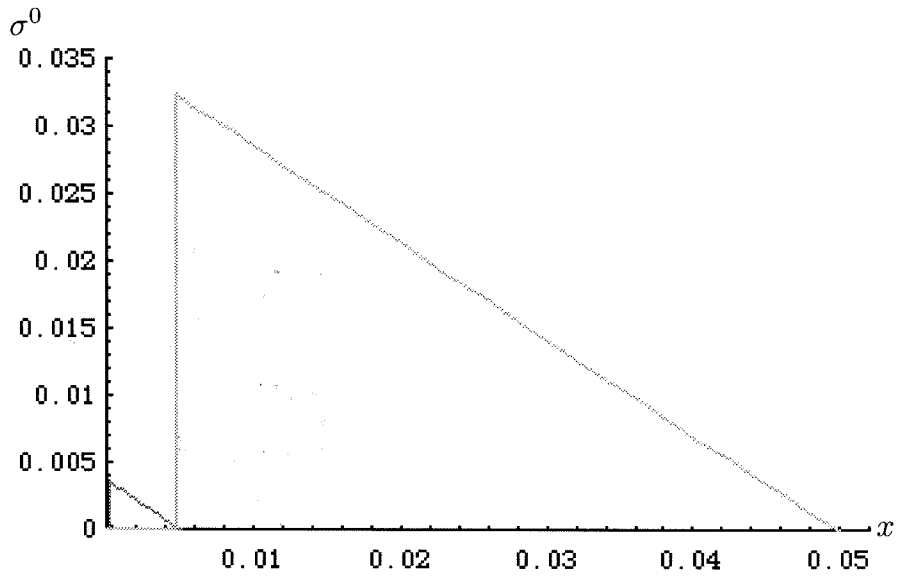

Figure 12b. Stress profiles: $C_* = 0.75$, $r = 1$, $\gamma = 0.5$, $\alpha_g = 1$, $\epsilon = 0.0001$, $\kappa = 0.5$. In decreasing order of darkness: $t = 0.001$, 0.01, 0.1.

Figure 12b shows graphs of our stress field for the same parameters and times as before. The case where $t = 0.001$ appears only as an extra pixel near $(0, 0)$. Note that in this case we truly do have a maximum at $x = s(t)$ as promised in Chapter III. Therefore, the stress which builds up in the polymer as the penetrant builds up in the glassy region is nearly totally released when the polymer enters the rubbery state. Note also that there is no discontinuity at $x = \kappa t$ since $\sigma^{0g}(0, 0) = 0$.

3. Large Time Asymptotics

Next we perform large-time asymptotics. We begin by noting that for long

time, equation (12.6) behaves like

$$\kappa^2 T^g_{xx} = T^g_t + o(1), \tag{12.29}$$

and equation (11.2b) behaves like

$$\sigma^{0g} = \frac{\kappa^2}{\gamma} C^{0g}. \tag{12.30}$$

Hence, using equation (12.30) evaluated at the front, equation (12.9) becomes

$$T^r(s(t), t) = C_*(1 + \kappa^2). \tag{12.31}$$

From our condition that $C \leq 1$, we see that (12.2) must hold. Then using equation (12.13) in (12.31), we see that

$$\operatorname{erfc}\left(\frac{x}{2\sqrt{t}}\right) + (1 - C_*)\left(1 - \frac{x^2 + 2t}{2r}\right)\left[\operatorname{erf}\left(\frac{x}{2\sqrt{t}}\right) - \operatorname{erf}\left(\frac{x}{2\sqrt{t-r}}\right)\right]$$
$$- \frac{(1 - C_*)x}{r\sqrt{\pi}}\left\{\sqrt{t}\exp\left(-\frac{x^2}{4t}\right) - \sqrt{t-r}\exp\left[-\frac{x^2}{4(t-r)}\right]\right\} = C_*(1 + \kappa^2).$$

The only way to get an $O(1)$ balance is if $s(t) \sim 2s_\infty\sqrt{t}$. In this case, when we asymptotically expand for large time, only the first term contributes to leading order, so we have

$$\operatorname{erfc} s_\infty = C_*(1 + \kappa^2). \tag{12.32}$$

Now we wish to expand our rubbery solution. From the form of (12.29), we see that (4.26) is now a long-time asymptotic solution in the rubbery region. We see that the dominant contribution to (4.26) for $x \propto \sqrt{t}$ and t large is from the neighborhood of $z = t$. Therefore, we postulate the following expansion:

$$f_b(t) \sim f_\infty + o(1), \quad t \to \infty.$$

Substituting our expression into (4.26), we immediately see that

$$T^g \sim f_\infty \operatorname{erfc}\left(\frac{x}{2\kappa\sqrt{t}}\right). \tag{12.33}$$

Using (12.33) in (12.8), we have that

$$f_\infty = \frac{C_*}{\operatorname{erfc}(s_\infty/\kappa)}. \tag{12.34}$$

Summarizing our results, we have the following:

$$t \to \infty$$

$$s(t) \sim 2s_\infty\sqrt{t}, \qquad \operatorname{erfc} s_\infty = C_*(1+\kappa^2), \tag{12.35}$$

$$x < \kappa t$$

$$C^{0g}(x,t) \sim \frac{C_*}{\operatorname{erfc}(s_\infty/\kappa)}\left[\frac{x}{2}\int_{x/\kappa}^{t} e^{-z/2}\frac{I_1(\sqrt{\kappa^2z^2-x^2}/2\kappa)}{\sqrt{\kappa^2z^2-x^2}}\,dz + e^{-x/2\kappa}\right]$$

$$- \frac{C_* e^{-t/2}}{2\operatorname{erfc}(s_\infty/\kappa)}\operatorname{erfc}\left(\frac{\kappa t - x}{\sqrt{2\alpha_g\epsilon t}}\right), \tag{12.36a}$$

$$\sigma^{0g}(x,t) \sim \frac{C_*\kappa^2}{\gamma\operatorname{erfc}(s_\infty/\kappa)}\left[\frac{x}{2}\int_{x/\kappa}^{t} e^{-z/2}\frac{I_1(\sqrt{\kappa^2z^2-x^2}/2\kappa)}{\sqrt{\kappa^2z^2-x^2}}\,dz + e^{-x/2\kappa}\right], \tag{12.36b}$$

$$x > \kappa t$$

$$C^{0g}(x,t) \sim \frac{C_* e^{-t/2}}{2\operatorname{erfc}(s_\infty/\kappa)}\operatorname{erfc}\left(\frac{\kappa t - x}{\sqrt{2\alpha_g\epsilon t}}\right). \tag{12.37}$$

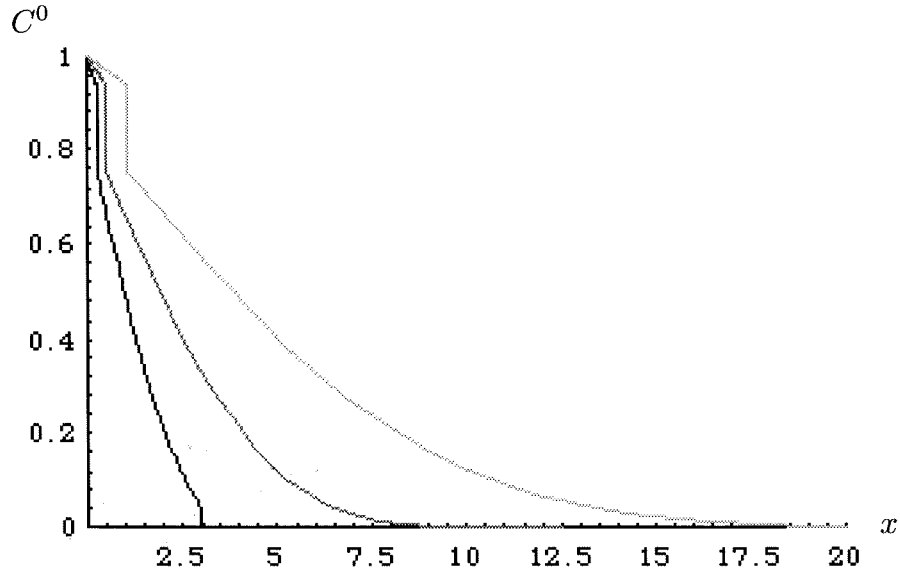

Figure 12c. Concentration profiles: $C_* = 0.75$, $r = 1$, $\gamma = 0.5$, $\alpha_g = 1$, $\epsilon = 0.0001$, $\kappa = 0.5$. In decreasing order of darkness: $t = 6$, 24, 96.

Figure 12c shows graphs of our long-time concentration field expansions for the same parameters as before. The three-stage behavior is not as pronounced in this model since $C^{0g}(\kappa t, t)$ is exponentially decaying. The clearest picture of the sharp front at $x = \kappa t$ is shown for $t = 6$. The glassy region has a nearly Fickian profile, as does the rubbery region, but they are still separated by the sharp boundary layer at $x = s(t)$.

Figure 12d shows graphs of our long-time stress field expansions for the same parameters as before. Note the gap that arises for $t = 6$. This is due to the fact that figure 12d is a graph of (12.36b), which is not uniformly valid up to the front $x = \kappa t$. However, the error behaves like $e^{-t/2}$, and thus becomes negligible for the larger values of t. Once again note the slow Fickian rise of the stress, which reaches its maximum at $x = s(t)$ before plunging quickly down to 0.

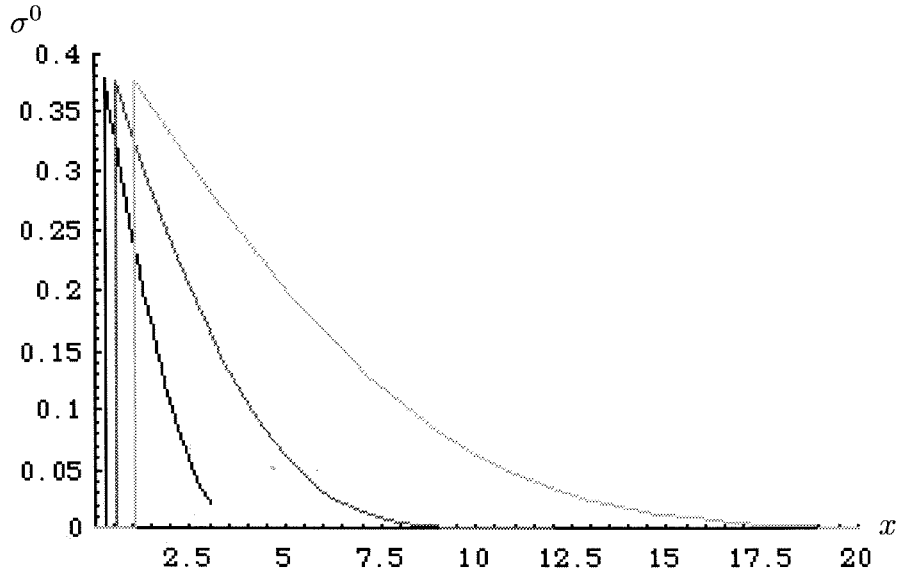

Figure 12d. Stress profiles: $C_* = 0.75$, $r = 1$, $\gamma = 0.5$, $\alpha_g = 1$, $\epsilon = 0.0001$, $\kappa = 0.5$. In decreasing order of darkness: $t = 6$, 24, 96.

Chapter XIII: Remarks

When discussions about non-Fickian polymer-penetrant systems take place, the subject of the molecular diffusion coefficient naturally arises. It is known that in some systems the diffusion coefficient greatly increases as the polymer changes from the glassy to the rubbery state. What is only surmised is the degree to which such a change influences the qualitative structure of the solution. The results in Part Four shed new light upon this subject.

In Chapter XI, we derived results for a case where the diffusion coefficient varied from $O(1)$ to very large. Some of the salient features of the solutions derived in previous parts were reproduced. The moving boundary condition which resulted was still not solvable by similarity variables, and Boley's method had to be used. The moving boundary condition still involved matching two different operators at the front, rather than the same operator with different coefficients. The solution for the concentration exhibited two fronts, as in the heavily stressed case. There was a leading subcharacteristic front $x = \kappa t$, as well as our true front $x = s(t)$.

However, upon comparison of the results of this part with the results of other parts, there are substantial differences. The parameter a did not play a role here to leading order; hence the flux used up in the phase transition is not a dominant effect. The dominant balance is between the concentration and stress contributions to the flux.

Since $D(C)$ had vastly different values on either side of the front, this caused a large difference in the size of the flux from the glassy and rubbery regions. This

discrepancy manifested itself by making the stress in the glassy region an order of magnitude larger than the stress in the rubbery region. This produced the first results in this dissertation where the stress had its maximum *exactly* at the secondary front. However, this behavior is directly dependent on our choice of $D(C)$ as piecewise constant. If $D(C)$ were made to depend smoothly on C throughout all phases of the polymer, the flux contributions would be of roughly the same size at the moving front. Regardless, other models which do not incorporate a phase transition but do have a rapidly increasing diffusion coefficient still have steep fronts [25].

Therefore, upon examination of these results, it seems that while introducing a varying diffusion coefficient does affect some aspects of our solutions, other aspects remain the same. Thus, it would behoove each individual investigator to examine both cases carefully, weighing the qualitative changes induced by a changing diffusion coefficient against the additional computational work involved.

Part Five: Conclusions

Chapter XIV: Conclusions

New materials and their large number of widely varied applications have revolutionized several scientific fields. This has led the engineering community to seek coherent mathematical models in order better to control the design of such materials. The standard Fickian diffusion model is insufficient to explain the phenomena observed, including sharp fronts moving with constant speed and fronts where the concentration flux behind the front is less than that ahead of the front.

By postulating the extremely general model (1.1) for the flux in these polymer-penetrant systems, we are able to model the most salient nonstandard feature of many classes of polymer-penetrant systems: a non-local "memory" effect which induces a viscoelastic stress. This effect varies between the polymer phases, as can the diffusion coefficient. The moving boundary-value problem which ensues is not solvable by similarity solutions. Hence, we rely upon an integral method developed by Boley [24] which gives solutions which are not in closed form. In order to use such a method, we simplified our model, using experimental data as a guide, to determine the dominant physical processes in the systems we wished to study. By using a perturbation expansion in a suitable small parameter, we were able to obtain asymptotic estimates for the motion of the front and the functional form of our solution profiles.

We note that even after making several simplifying assumptions, our resulting equations (3.25)-(3.30) are extremely versatile. By making the effects of σ small enough, we can reproduce Fickian diffusion. Hints of this can be found in the

small-time asymptotics of the weakly diffusive case. In addition, we were able to construct three different types of solutions by adjusting the relative size of our *constant* parameters.

In the weakly diffusive case, we solved a complicated regular perturbation problem. The moving boundary problem is unusual in two respects. First, rather than matching the same operator with two different *coefficients*, as in the standard Stefan problem [10], our problem involved matching two different *operators*—a problem we have yet to find in the literature. Second, the moving boundary problem was not solvable by standard similarity variable techniques; the full partial differential equations had to be solved. By using asymptotic techniques, we were able to construct small- and long-time solutions. For small time, the effects of the memory had not fully manifested themselves. However, as time passed, the effects of memory grew stronger, distorting the solution profile from the standard Fickian type into one which is much sharper and which has a phase transition front that moves with constant speed.

In the heavily stressed case, some of the difficulties of dealing with even the simplest of nonlinear equations manifested themselves. We could not obtain solutions with certain kinds of behavior, for the problem would not allow it. We obtained two feasible solutions in certain parameter regimes, and were forced to use stability analysis in order to determine which was stable. In the cases where we did find results, the departure from Fickian behavior is astounding. Two "waves" of concentration wash through the polymer. The first, moving with constant speed, provides the first strong signal of diluent to the polymer. The second, moving initially like t^2 but eventually converging to a fixed distance behind the primary front, heralds the beginning of the dissolution of the entanglement matrix. This result, which

matches well with other numerical simulations and experiments [29], provides great confidence in our model's ability to replicate the behavior in non-Fickian systems correctly.

When the diffusion coefficient is allowed to vary with concentration, the resulting solutions replicate several additional features of polymer-penetrant systems. The singular perturbation problem which resulted led to sharp fronts moving with constant speed, which we have come to expect. However, now the stress has its maximum exactly at the phase transition: something we had not seen in previous simpler models. Such a system did not allow fronts which moved with speed greater than the subcharacteristc speed. In addition, it was only in this section where $D(C)$ varied did we get vastly different sizes of the ingoing and outgoing concentration fluxes. This behavior forced the leading order balance at the front to be between the concentration and stress contributions to the flux, rather than a balance involving the front evolution term, which contains a.

In each of these three cases, we chose to use analytical and asymptotic methods rather than numerical ones. Obviously no choice is without disadvantages. We sacrificed computed profiles for all x and t and avoided the challenges which a numerical implementation of our problem would entail. In addition, attacking the problem analytically necessitated making many simplifying assumptions. However, the analytical problem is certainly not without challenges, and by remaining true to the analytics, we now have solutions with explicit dependence on various physical and state parameters. These results are worth the sacrifice, for they provide chemical engineers a way to check these results in the laboratory. If these results are shown to have broad-based merit, then chemical engineers, who can now custom-design a polymer with specific properties, can estimate the form of penetration fronts in

such polymers.

Chapter XV: Areas for Further Resarch

As is the case with most dissertations, this work raises as many questions as it answers. There are certainly many areas in which the work in this paper could be expanded, and there a number of applications which this thesis has not even attempted to model.

Of course, one of the easiest ways to extend the work of this thesis would be to eliminate some of our simplifications outlined in Chapter III. Some of the constant parameters could be chosen to vary in a piecewise constant or more complicated manner as a function of $\tilde{C}$. Throughout this dissertation we solved problems in a semi-infinite medium. This is convenient from an analytical point of view, and simplifies the mathematical problems caused by swelling in the polymer. However, there are a variety of interesting problems on finite domains that need to be solved. By placing the problem on a finite domain, the effects of swelling could be measured. In addition, the penetration of substances through thin polymer films is one on which chemical engineers would like to see numerical results. This problem also raises the spectre of multidimensional analysis. Though there are some numerical results on multidimensional problems [18], there is still much room for multidimensional analytical work. Perturbation methods could easily be used if one of the dimensions is much greater than the other, as is the case with thin films.

There are several scientists currently working on numerical analysis of math-

ematical models of polymer-penetrant systems. Though some follow the general mode of reasoning outlined here [21], [25], others choose to begin with more comprehensive equations of thermodynamics and directly implement them on the computer [29]. Certainly the work herein could be numerically analyzed in a variety of ways.

Most generally, suitable forms based on experimental data could be chosen for $D(\tilde{C})$, $E(\tilde{C})$, $\beta(\tilde{C})$, and $f(\tilde{C}, \tilde{C}_{\tilde{t}})$, allowing equations (2.5) to be implemented on the computer. In this case, one must take great care that the algorithm used could handle the sharp fronts present in such systems. Other sets of equations that could be discretized include (4.1)-(4.3) or (7.1)-(7.3). Once again, an adaptive grid scheme should be used when discretizing. Another way to approach the problem numerically would be to solve the integral equations arising from the use of Boley's method [for instance, (4.27)-(4.29)] approximately on the computer. This would yield solutions for our fictitious boundary conditions and our front position for the entire ranges of their arguments. Such an implementation would require the use of integral equation solvers, rather than partial differential equation solvers. Certainly each of the methods above would yield a difficult problem in numerical analysis and significant results from a practical point of view.

A facet of this problem which we discussed only briefly was that of the dependence of memory on state as signified by our choice of $\tilde{t}_0$. In Part Two, it made no difference; we never had to explicitly choose $\tilde{t}_0$. In other cases, it did make a difference. There are certain polymers which fall into each category: state-dependent and -independent. A more thorough study comparing and contrasting the relative properties of the two types of substances would be welcome.

Lastly, there is the problem of our general expansion (1.1). We have confidence

in this model for the flux because it is so general. However, our choices for the terms in the flux expansion were motivated by the types of polymer-penetrant systems we wished to study. Thus, for different types of polymers different forms of the flux and chemical potential would have to be chosen. Hence, even though there are several significant results in this dissertation, we have only scratched the surface of the mathematical problems involved in modeling polymer-penetrant systems.

References

[1] E. Martuscelli and C. Marchetta, eds., *New polymeric materials: Reactive Processing and Physical Properties*, Proceedings of International Seminar, 9-13 June 1987, Naples, Italy, VNU Science Press, Utrecht, The Netherlands, 1987.

[2] S.R. Shimabukuro, *Stress Assisted Diffusion in Polymers*, Ph.D. thesis, California Institute of Technology, 1991.

[3] P.J. Tarche, *Polymers for Controlled Drug Deliveries*, CRC Press, 1991.

[4] T.J. Roseman and S.Z. Mansdorf, eds. *Controlled Release Delivery Systems*, Marcel Dekker, New York, 1983.

[5] R. Langer, *New methods of drug deliveries*, Science, 249 (1990), pp. 1527–1534.

[6] D.R. Paul and F.W. Harris, eds., *Controlled Release Polymeric Formulations*, ACS Symposium Series 33, American Chemical Society, Washington, 1976.

[7] L.F. Thompson, C.G. Wilson, and M.J. Bowden, *Introduction to Microlithography*, ACS Symposium Series 219, American Chemical Society, Washington, 1983.

[8] J.S. Vrentas, C.M. Jorzelski, and J.L. Duda, *A Deborah number for diffusion in polymer-solvent systems*, AIChE J., 21 (1975), pp. 894–901.

[9] N. Thomas and A.H. Windle, *A theory of Case II diffusion*, Polymer, (1982), pp. 529–542.

[10] J. Crank, *Free and Moving Boundary Problems*, Oxford University Press, New York, 1984.

[11] D.A. Edwards and D.S. Cohen, *An unusual moving boundary condition arising*

in anomalous diffusion problems, SIAM J. Appl. Math., submitted.

[12] D.S. Cohen and A.B. White, Jr., *Sharp fronts due to diffusion and viscoelastic relaxation in polymers*, SIAM J. Appl. Math., 51 (1991), pp. 472–483.

[13] _____, *Sharp fronts due to diffusion and stress at the glass transition in polymers*, Los Alamos Technical Report 88-2081, June 1988; J. Polymer Sci., Part B: Polymer Physics, 27 (1989), pp. 1731–1747.

[14] R.W. Cox, *A Model for Stress-driven Diffusion in Polymers*, Ph.D. thesis, California Institute of Technology, 1988.

[15] R.W. Cox and D.S. Cohen, *A mathematical model for stress-driven diffusion in polymers*, J. Polymer Science B: Polymer Physics, 27 (1989), pp. 589–602.

[16] C.K. Hayes, *Diffusion and Stress Driven Flow in Polymers*, Ph.D. thesis, California Institute of Technology, 1990.

[17] C.K. Hayes and D.S. Cohen, *The evolution of steep fronts in non-Fickian polymer-penetrant systems*, J. Polymer Sci., Part B: Polymer Physics, 30 (1992), pp. 145–161.

[18] D.S. Cohen, A.B. White, Jr., and T.P. Witelski, *Shock Formation in a Viscoelastic Diffusive System*, SIAM J. Appl. Math., submitted.

[19] J. Crank, *The Mathematics of Diffusion*, 2nd edition, Oxford University Press, New York, 1976.

[20] N. Thomas and A.H. Windle, *Transport of methanol in poly-(methyl-methocrylate)*, Polymer, 19 (1978), pp. 255–265.

[21] C.J. Durning, *Differential sorption in viscoelastic-fluids*, J. Polymer Sci., Polymer Phys. Ed., 23 (1985), pp. 1831–1855.

[22] J. Slattery, *Momentum, Energy, and Mass Tranfer in Continua*, 2nd ed.,

McGraw-Hill, New York, 1972.

[23] W.G. Knauss and V.H. Kenner, *On the hygrothermomechanical characterization of polyvinyl acetate*, J. Appl. Phys., 51 (1980), pp. 5131–5136.

[24] B.A. Boley, *A method of heat conduction analysis of melting and solidification problems*, J. Math. Phys, 40 (1961), pp. 300–313.

[25] T.Z. Fu and C.J. Durning, *Numerical simulation of case II transport*, AIChE J. 39 (1993), pp. 1030–1044.

[26] G.F. Carrier, M. Krook, and C.E. Pearson, *Functions of a Complex Variable: Theory and Technique*, Hod Books, Ithaca, 1983.

[27] M. Abramowitz and I.E. Stegun, eds., *Handbook of Mathematical Functions*, Applied Mathematics Series 55, National Bureau of Standards, Washington, 1972.

[28] C.M. Bender and S.A. Orszag, *Advanced Mathematical Methods for Scientists and Engineers*, International Series in Pure and Applied Mathematics, McGraw-Hill, San Francisco, 1978.

[29] J.C. Wu, Quantum Chemical Process Research Center, private communication, March 11, 1994.

[30] J. Kevorkian and J.D. Cole, *Perturbation Methods in Applied Mathematics*, Applied Mathematical Sciences 34, Springer-Verlag, New York, 1981.